The Dissertation Committee for Dean Kirson Certifies that this is the approved version of the following dissertation:

The Relationship Between Glycine Receptor Agonist Efficacy and Allosteric Modulation

Committee:

S. John Mihic, Supervisor

R. Adron Harris

Richard W. Aldrich

Carlton K. Erickson

Jonathan T. Pierce-Shimomura

The Relationship Between Glycine Receptor Agonist Efficacy and Allosteric Modulation

by

Dean Kirson, B.S.

Dissertation

Presented to the Faculty of the Graduate School of

The University of Texas at Austin

in Partial Fulfillment

of the Requirements

for the Degree of

Doctor of Philosophy

The University of Texas at Austin

May 2014

Dedication

This dissertation is dedicated to all the people who helped me throughout my time in graduate school, and especially to the memory of Jascha Pohl, whose friendship will be sorely missed.

Acknowledgements

Many people helped me throughout my time in graduate school, and I would like to express my gratitude here for those that went above and beyond in helping me. First, I would like to thank my advisor, S. John Mihic for all he has done for me. A person in graduate school could not ask for a better advisor, mentor, and example of how to be a scientist and teacher. Even before I was in John's lab, he served as the graduate advisor for the Neuroscience program and he was always approachable and helpful in this role. When my graduate school experience was not all I thought it would be, he gave me a second chance, allowing me to join his lab where he has provided the best guidance and help even now through helping me in the next step after graduating. Somehow he always maintained a positive attitude and fostered a constructive and collaborative environment. We have a saying that the worst thing about being in John's lab is that when you leave you'll never have a boss as great as John, and it's a very true statement.

I would also like to thank the members of my dissertation committee for all their advice and guidance. Adron Harris was always available for help with research questions as his knowledge of alcohol research is encyclopedic. Additionally, the Waggoner Center for Alcohol and Addiction Research, of which Dr. Harris is the director, provided funding for my research in the Bruce/Jones Fellowship, a wide variety of addiction research to learn about, and a weekly meeting that was one of the only consistently productive seminars/journal clubs in graduate school. Rick Aldrich is the expert in channel biophysics, and he was always available for discussions that aided my understanding of receptor functioning as well as discussions about film and television which were much needed breaks from reality. He also hosted one of the only other consistently informative

journal clubs in graduate school. Jon Pierce-Shimomura always had thought provoking questions, which helped to guide my research, as well as advice in future endeavors beyond graduate school. Carlton Erickson has been a great resource in advice on writing and pushing me to interpret my research into what clinical implications it may have for drug abuse and addiction.

Many other past and present graduate students aided me in completing my research. First, Brian Welsh has been a great friend, and was instrumental in my joining the Mihic lab. Both he and his undergrad at the time, Hunter Allen, trained me in basic oocyte electrophysiology, giving me my start in the lab, and Brian initiated me into the world of single channel electrophysiology. Megan Tipps and Jelena Todorovic both helped me to refine my research techniques, and aided in me in designing my own research. Jelena in particular has been a great friend, helping me in all of my endeavors inside and outside the lab. I would also like to thank Garrett Cornelison and Ashley Philpo, who were very helpful in obtaining some of the data in this dissertation.

Lastly, the friendships you form in graduate school are instrumental in traversing the trials and tribulations of graduate school. I have been fortunate to form many friendships with other graduate students and post-docs past and present, too many to name here, though a few must be mentioned. Deena Walker has been one of my best friends in graduate school as a sounding board for both scientific discussion and personal problems. Jascha Pohl was my other best friend in graduate school who helped to serve in these same roles. Additionally, he and I explored the depths of culinary offerings Austin has to offer. I would also like to thank my family for anything they were able to do to help me during this time. Lastly, I have to acknowledge and thank my wonderful

and adorable dog Coffee. She is my continuous source of love and stress relief, and has been my constant companion throughout graduate school.

The Relationship Between Glycine Receptor Agonist Efficacy and Allosteric Modulation

Dean Kirson, Ph.D.

The University of Texas at Austin, 2014

Supervisor: S. John Mihic

The glycine receptor (GlyR) is a ligand-gated ion channel member of the cys-loop receptor superfamily, responsible for inhibitory neurotransmission in the brain and spinal cord. Both glycine and the partial agonist taurine act as endogenous ligands of the GlyR. Taurine-activated GlyR may have a role in the rewarding effects of drugs of abuse, such as ethanol. As a partial agonist, taurine has a decreased efficacy relative to glycine, resulting in a decreased maximum response. We investigated the effects of ethanol, anesthetics, inhalants, and zinc to determine if these allosteric modulators could increase the efficacy of the taurine-activated GlyR. Whole cell recordings of wild type GlyR revealed that each of the allosteric modulators potentiated currents generated by saturating concentrations of taurine but not glycine, implying an increase in efficacy. Zinc is found at GlyR-potentiating concentrations throughout the nervous system, so we examined the combinatorial effects of these allosteric modulators with zinc to mimic *in vivo* conditions. Whole cell recordings revealed that zinc potentiation of saturating taurine-generated currents decreased further potentiation by another allosteric modulator, indicating no synergistic effects on efficacy. We next investigated the actions of ethanol and isoflurane on the taurine-activated GlyR at the single channel level, finding that both

allosteric modulators stabilized the channel open state, increasing the efficacy of the taurine-activated GlyR. We previously identified a mutation in the ligand-binding domain of the GlyR (D97R) that produces spontaneously activating channels, on which taurine has increased efficacy. We identified a residue, R131, as a possible binding partner of D97 in forming an electrostatic interaction that holds the channel in the closed state. We found that disruption of this interaction results in greatly increased taurine efficacy, indicating that efficacy for partial agonists may be determined by agonist ability to break this bond early in the activation process following binding. Thus we find differential mechanisms of allosteric modulation and efficacy determinations for the GlyR when activated by taurine vs. glycine.

Table of Contents

List of Tables

List of Figures

List of Abbreviations

5-HT_3R	serotonin type 3 receptor
a	amplitude, likelihood
AChBP	acetylcholine binding protein
ANOVA	analysis of variance
β-ABA	β-aminobutyric acid
β-AIBA	β-aminoisobutyric acid
CMV	cytomegalovirus
CNS	central nervous system
E	efficacy
EC	effective concentration
ELIC	*Erwinia chrysanthemi* ligand-gated ion channel
EtOH	ethanol
g	conductance
GABA	γ-aminobutyric acid
$GABA_AR$	γ-aminobutyric acid type A receptor
GLIC	*Gloeobacter violaceus* ligand-gated ion channel
GluCl	*Caenorhabditis elegans* glutamate-gated chloride channel α
Gly	glycine
GlyR	glycine receptor
GLYT	glcyine transporter
HEK	human embryonic kidney
I	current
ICP-MS	inductively-coupled plasma mass spectrometry

Iso	isoflurane
KCC2	potassium-chloride cotransporter
K_d	dissociation constant
LGIC	ligand-gated ion channel
MAC	minimum alveolar concentration
MIL	maximum interval likelihood
n	number
NAcc	nucleus accumbens
nAChR	nicotinic acetylcholine receptor
PMTS	propyl-methanethiosulfonate
P_o	open probability
REFER	rate-equilibrium free-energy relationship
SEM	standard error of the mean
SKM	segmental-k-means
SNK	Student-Newman-Keuls test
τ	time constant
Tau	taurine
TCE	1,1,1-trichloroethane
TCY	trichloroethylene
TM	transmembrane
TMA	tetramethylammonium
Tol	toluene
Tri	tricine
V	voltage

VGIC	voltage-gated ion channel
VIAAT	vesicular inhibitory amino acid transporter
VTA	ventral tegmental area
WT	wild type

AMINO ACID RESIDUE ABBREVIATIONS AND NAMING CONVENTIONS

Amino acid residues are often abbreviated using single letters (listed below). Point mutations to a protein structure are referred to using the following nomenclature: wild type amino acid abbreviation–residue number–mutation amino acid residue. Thus, a mutation from the arginine at position 131 of the glycine receptor to an aspartate would be referred to as R131D.

Single–letter amino acid abbreviations

A	Alanine	M	Methionine
C	Cysteine	N	Asparagine
D	Aspartate	P	Proline
E	Glutamate	Q	Asparagine
F	Pheynlalanine	R	Arginine
G	Glycine	S	Serine
H	Histidine	T	Threonine
I	Isoflurane	V	Valine
K	Lysine	W	Tryptophan
L	Leucine	Y	Tyrosine

1.0 | INTRODUCTION

1.1 – Cys-Loop Ligand Gated Ion Channels: Basic Structure and Function

The nervous system contains billions of neurons that form interconnected networks necessary for functioning of all other systems. Information conveyance is achieved through both electrical and chemical means. Neurons use a multitude of ion channels in their membranes to propagate electrical signals towards synapses with other neurons, where the electrical signal is converted into a chemical signal, with the presynaptic neuron releasing neurotransmitters that activate receptors on the postsynaptic cell, thus achieving information transfer. These neurotransmitter receptors are generally one of two types, either termed metabotropic and activating signaling cascades utilizing guanosine nucleotide-binding proteins, or termed ionotropic and being directly coupled to an ion channel in the neuronal membrane. These ionotropic receptors are also termed ligand-gated ion channels (LGICs) as they are directly activated by a chemical signal and to distinguish them from the many families of voltage-gated ion channels (VGICs). LGICs generally contain an extracellular domain, multiple transmembrane domains, and intracellular domains important for functioning of the channel.

One family of LGICs is the cys-loop receptor superfamily of ion channels. This family contains the nicotinic acetylcholine receptor (nAChR) as its prototypical member, being the ion channel first and most studied among this family. Other family members include the γ-aminobutyric acid type A receptor ($GABA_AR$), glycine receptor (GlyR), and the serotonin type 3 receptor ($5\text{-}HT_3R$). These receptors are composed of a pentameric

arrangement of protein subunits around a central ion conducting pore, and varyingly can be composed of all five subunits being identical (homomeric) or differing in protein sequence (heteromeric). Individual subunits in this family generally have similar structural components, with a large extracellular domain at the N-terminus, four transmembrane domains (TM), an intracellular domain of varying size between TM3 and TM4, and an extracellular C-terminus of variable length. The extracellular domain of each subunit in this family contains the characteristic cys-loop, a highly conserved sequence of 13 amino acids held into a loop by a cysteine-cysteine disulfide bond. In the pentameric arrangement, TM2 of each subunit lines the ion-conducting pore, with the nAChR and 5-HT_3R allowing cationic flow and the $GABA_A$R and GlyR allowing anionic flow.

Structural information regarding this family of ion channels has been achieved by studying related ion channels and proteins then using homology modeling to investigate the channels that have not been crystallized as of this date. Initial studies used the crystal structure of the acetylcholine binding protein (AChBP) from the great pond snail *Lymnaea stagnalis* (Brejc et al., 2001). The AChBP is a protein released from glia into the synaptic cleft to bind acetylcholine and modulate neuronal transmission. This snail protein is very similar in structure to the extracellular domain of the nAChR, which allowed for comparison with other cys-loop family members in terms of ligand binding. Subsequent to this characterization, the nAChR found in the electric organ of the marbled electric ray *Torpedo marmorata* was analyzed using electron microscopy to reveal the structure of the nAChR pore region (Miyazawa et al., 2003). Whole prokaryotic ligand gated ion channels homologous to human cys-loop receptors were subsequently crystallized and used for homology modeling comparison to mammalian channels. These

include channels from the bacterium *Gloeobacter violaceus* (GLIC) and the cyanobacterium *Erwinia chrysanthemi* (ELIC) (Hilf and Dutzler, 2008; Bocquet et al., 2009). More recently, a glutamate activated cys-loop receptor (GluCl) from the nematode *Caenorhabditis elegans* was crystallized, and marked the first crystallized receptor known to contain an anion-selective pore responsible for inhibitory neurotransmission (Hibbs and Gouaux, 2011). All structural determinations regarding cys-loop receptors that have not been crystallized utilize homology modeling with one or more of the previously mentioned structures, and will be assumed in this and following chapters. An example structure of the *Torpedo* nAChR showing the basic structural features of a cys-loop receptor can be seen in **Fig. 1.1** below.

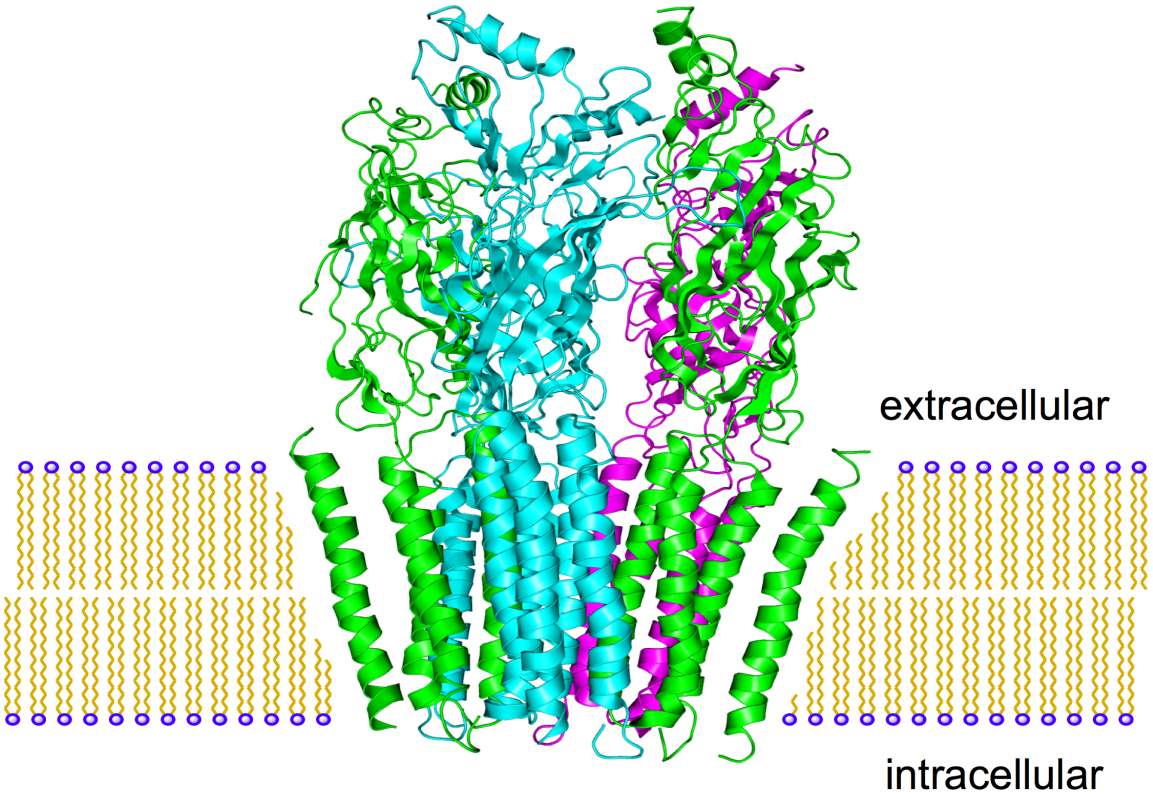

Figure 1.1 – Structure of a nicotinic acetylcholine receptor

Structure of the Torpedo nicotinic acetylcholine receptor. Viewed from inside the membrane at the side of the channel. Different colors denote different subunits. Adapted from derivation of the structure (PDB ID: 2BG9) from *Unwin N. (2005). Refined structure of the nicotinic acetylcholine receptor at 4 Å resolution. J Mol Biol 346: 967.*

Cys-loop receptor pentameric stoichiometry varies among the different receptor types. Receptors may be comprised of five identical subunits (termed homomeric) or a combination of different subunits (termed heteromeric). The number of subunits that can form functional channels can vary greatly between the different cys-loop receptors, and are usually classified by homology with other receptor subunits. For example, the nAChR has seventeen subunits in five classes, though not all subunits are found in all species. These include 10 α subunits, 4 β subunits, and one each of a δ, ε, and γ subunits. This results in a multitude of subunit combinations possible to create the pentameric channel. However, not all combinations have been found *in vivo* nor can all possible combinations even assemble into functional channels. For example, to date in the case of the nAChR, only the α_7 and α_8 subunits has been found to form functional homomeric channels in humans. Heteromeric channels are usually comprised of multiple α and β subunits that may contain one or more of the other subunit classes. This structural variability also contributes to functional variability both in terms of biophysical characteristics of the channels themselves as well as modulation by allosteric compounds. In this way, different regions of the nervous system may express specific subtypes of these receptors as needed for specialized functioning in that region, though there is often overlap.

The first functional characteristic to examine in cys-loop receptors is ligand binding. A hallmark of the ligand gated ion channels is that they are stably in a closed pore confirmation when no ligand is around. Upon ligand binding, the channel will change conformation allowing ionic conductance through the pore. The channel then closes in one of two ways, with ligand unbinding or by entering a desensitized state where ligand may be bound but the pore does not conduct ions. Although some

mechanisms for desensitization have been proposed, it is still a poorly understood process and may vary between cys-loop receptors. The ligand-binding domain for cys-loop receptors occurs in the large extracellular domain found near the N-terminus of the protein. Generally, ligands bind in the interface between adjacent subunits, with one subunit side (the "principal" or + side) comprised of a series of loops and the adjacent subunit side (the "complementary" or – side) composed of strands of β-sheets (Brejc et al., 2001). Thus, up to five ligands may bind a single receptor and the subunit stoichiometry determines if specific interfaces comprise a ligand binding site. The extracellular domain must convey ligand binding to the pore region in order for the channel to open. This occurs through a conformational wave of residue motion that allows loops from the extracellular domain to interact with the transmembrane regions considered next (Purohit et al., 2007).

The transmembrane domain is comprised of four α-helices with hydrophobic residue side chains anchoring the protein in the membrane. These helices are numbered according to the order they occur in the protein's amino acid sequence. Although the extracellular domain is directly connected to TM1, the extracellular linking region between TM2—TM3 has been shown to be important for transmission of the binding signal to gating of the pore (Kash et al., 2003). This may occur due to TM2 lining the pore for each subunit. Unlike other transmembrane helices, TM2 contains hydrophilic residues pointing into the pore, creating a strip of hydrophilicity along the hydrophobic TM2 helix of each subunit. In some positions of the pore lining residues there are charged amino acids that are of opposite charge to the ions the receptor conducts. This creates rings of charges from the five subunits, that are believed to help attract and propagate ions through the pore (Corringer et al., 1999; Gunthorpe and Lummis, 2001).

Thus cationic channels like the nAChR have negatively charged amino acid rings in the pore, while anionic channels like the $GABA_AR$ and GlyR have positively charged amino acid rings along the channel pore.

The large intracellular loop of cys-loop receptors occurs as the linking sequence between TM3-TM4 and varies considerably among family members in amino acid sequence and length. Although this region may contain necessary sites for signaling cascades and modulation of functioning of these channels, such as phosphorylation sites, or motifs necessary for cytoskeleton anchoring, the variability among family members leads to differences in functioning among them. For example, in the nAChR and the 5-$HT_{3A}R$ these domains seem to form hanging structures around the intracellular pore opening with holes connecting through to the cytoplasm that are similar in size to the hydrated ions conducted through the channel, thus influencing ion permeation through the channel (Miyazawa et al., 1999; Kelley et al., 2003). As a counter example, while the GlyR contains sites for phosphorylation and other signaling similar to other cys-loop receptors, the large intracellular loop, specifically in the β subunit, of this channel seems to play more of a role in anchoring the protein to certain membrane locations, such as at synapses.

Finally, cys-loop receptors contain a short extracellular C-terminus proceeding from TM4. This C-terminal peptide is quite variable in length among family members and generally has not been studied in great detail. A study of the structure of ELIC suggests that while TM1 and TM3 may help to shield and stabilize the pore formed by the TM2 domains, TM4 seems to only moderately interact with TM1 and TM3 and does not participate in subunit-subunit interactions. As the generally short C-terminus protrudes from TM4, it may have been thought to be unlikely to participate in

interactions with other parts of the receptor. Interestingly, recent research has shed light on some possible roles of the C-terminus. Deletion of the three amino acid C-terminus of the 5-HT_{3A}R significantly decreased membrane expression of the receptor, indicating a role in formation and stabilization of the mature protein or a binding/recognition site for trafficking proteins (Butler et al., 2009). Additionally, towards the goal of obtaining a better understanding of the structure function relationship of cys-loop receptors, Corringer's group created a chimeric channel with the extracellular domain of GLIC and the transmembrane domain of the α1 GlyR (Duret et al., 2011). In order to facilitate native interactions between the domains they mutated other sites, including changing the C-terminus from the GlyR sequence to that of the GLIC channel. When mutated back to the GlyR terminus in the chimera, the channel had faster desensitization, with a left shift in the concentration response curve, indicating a role of the C-terminus in modulating channel kinetics. Further explanation of the GlyR in detail follows in the next section.

1.2 – The Glycine Receptor

As previously mentioned, the GlyR is a member of the cys-loop ligand gated ion channel family. The namesake neurotransmitter that activates it, glycine, has the simplest structure of the biological amino acids. Inhibitory neurotransmission through ligand gated ion channels was first proposed by Coombs et al. (1955) who examined IPSP inhibition of motor neurons and the anions involved. Building upon this work, a pair of papers from Davidoff, Werman, and colleagues (Davidoff et al. 1967; Werman et al. 1967) proposed and confirmed glycine's role as an inhibitory neurotransmitter on postsynaptic spinal cord motor neurons of the cat. Glycine is not an essential dietary

component as it can be readily synthesized in the body via two enzymatic pathways. The first pathway utilizes the enzyme serine hydroxymethyltransferase to convert serine and tetrahydrofolate to glycine and N^5,N^{10}-Methylene tetrahydrofolate and H_2O, and is the main pathway used in the central nervous system (CNS). The second reaction occurs in the liver by the enzyme glycine synthase (glycine cleavage enzyme) which converts N^5,N^{10}-Methylene tetrahydrofolate with the cofactors CO_2, NH_4^+, NADH, and H^+ to glycine, tetrahydrofolate, and NAD^+. The reverse of this second reaction is the major catabolic pathway for glycine. Glycine packed into synaptic vesicles for neurotransmitter release comes from both the synthetic pathway mentioned earlier and reuptake of released glycine via glycine transporters GLYT1 and GLYT2 (Legendre, 2001). Although there is some disagreement as to which transporter is generally expressed more on glia vs. neurons, the GLYT2 is the major contributor of extracellular glycine uptake into presynaptic boutons despite a lack of expression seen in synapses (Jursky et al., 1994; Zafra et al., 1995a, 1995b; Poyatos et al., 1997; Spike et al., 1997; Belachew et al., 2000). Packaging of glycine into synaptic vesicles is accomplished by the vesicular inhibitory amino acid transporter (VIAAT) which also transports GABA (Dumoulin et al., 1999).

Like other cys-loop family members, the GlyR is comprised of a pentameric arrangement of subunits around a central ion conducting pore. The GlyR contains a strong anion conducting pore, and due to the overwhelming prevalence of the chloride anion *in vivo*, it mainly conducts chloride. However, the GlyR has been tested for anion permeability *in vitro*, and contains an anion permeability preference of $SCN^- > NO_3^- > I^- > Br^- > Cl^- > F^-$, which corresponds to the hydration energies of these anions indicating that removal of waters of hydration is the major hurdle to ion permeability

through the pore (Bormann et al., 1987; Fatima-Shad and Barry, 1993; Lynch, 2004). The chloride reversal potential *in vivo* varies but is usually close to the resting membrane potential of neurons. Thus activation of GlyR at rest don't drastically change membrane voltage but prevent further depolarization away from the chloride resting potential, an effect known as shunting inhibition (Lynch, 2004). During embryonic development, GlyR currents can be depolarizing and excitatory before expression of a potassium-chloride cotransporter (KCC2) that lowers internal concentrations of chloride in mature neurons (Stein and Nicoll, 2003).

The GlyR contains somewhat less subunit variability compared to other cys-loop receptor family members, with only five total identified subunits, four α subunits, and one β subunit. The α subunits have high homology of their sequences on the order of 80-90% while the β subunit has approximately 47% homology with the α1 subunit, though only the first three α subunits and the β are found in humans (Lynch, 2004). Thus, the GlyR exists as homomeric α receptors, or heteromeric receptors comprised of one member of the α subunit class in conjunction with the β subunit. Although the β subunit is expressed throughout the nervous system, it cannot form a functional channel on its own (Malosio et al., 1991). During development, GlyR exist predominantly as α2 homomers (Becker et al., 1988), with a switch to α1β heteromers being the predominant form in adult neurons (Lynch, 2004). Although various localization studies have found evidence of all mammalian α subunits expressed in the adult in various regions. For instance, the α3 subunit has been implicated in nociceptive signaling in the spinal cord (Zeilhofer, 2005). As mentioned previously, the β subunit seems to anchor the GlyR to synaptic locations through its interaction with the scaffolding protein known as gephyrin. Clustering of GlyR at synapses through gephyrin binding would indicate that synaptic

GlyR are heteromeric receptors containing the β subunit (Kirsch and Betz, 1995). However, there is growing evidence for functional homomeric α receptors in perisynaptic regions, perhaps acting as autoreceptors or in a neuromodulatory role distinct from synaptic transmission. For example, α2 receptors are preferentially expressed in the nucleus accumbens (NAcc) and may play a role in the rewarding effects of alcohol consumption which will be discussed later in more detail (Molander et al., 2005; Jonsson et al., 2014).

Although previously believed to be responsible for inhibitory neurotransmission in the spinal cord and brainstem, GlyR have more recently been found in many higher brain regions as well. The β subunit is expressed throughout the brain, but that is not a direct indicator of expression of functional channels. However, studies using antibodies against GlyR, *in situ* hybridization against GlyR transcripts, or electrophysiological characterization have found GlyR in regions such as the cerebellum, olfactory bulb, hippocampus, basal ganglia, and prefrontal cortex (Araki et al., 1988; van den Pol and Gorcs, 1988; Malosio et al., 1991; Waldvogel et al., 2007; Baer et al., 2009; Jonsson et al., 2009, 2012; Lu and Ye, 2011). GlyRs have also been found to function in the off-channel of the rod pathway in the retina, the initiation of the acrosome reaction in the plasma membrane of the acrosome region of spermatozoa, and may play a role in the functioning of pancreatic islet cells, adrenomedullary cells, and the specialized macrophage Kupffer cells of the liver (Lynch, 2004).

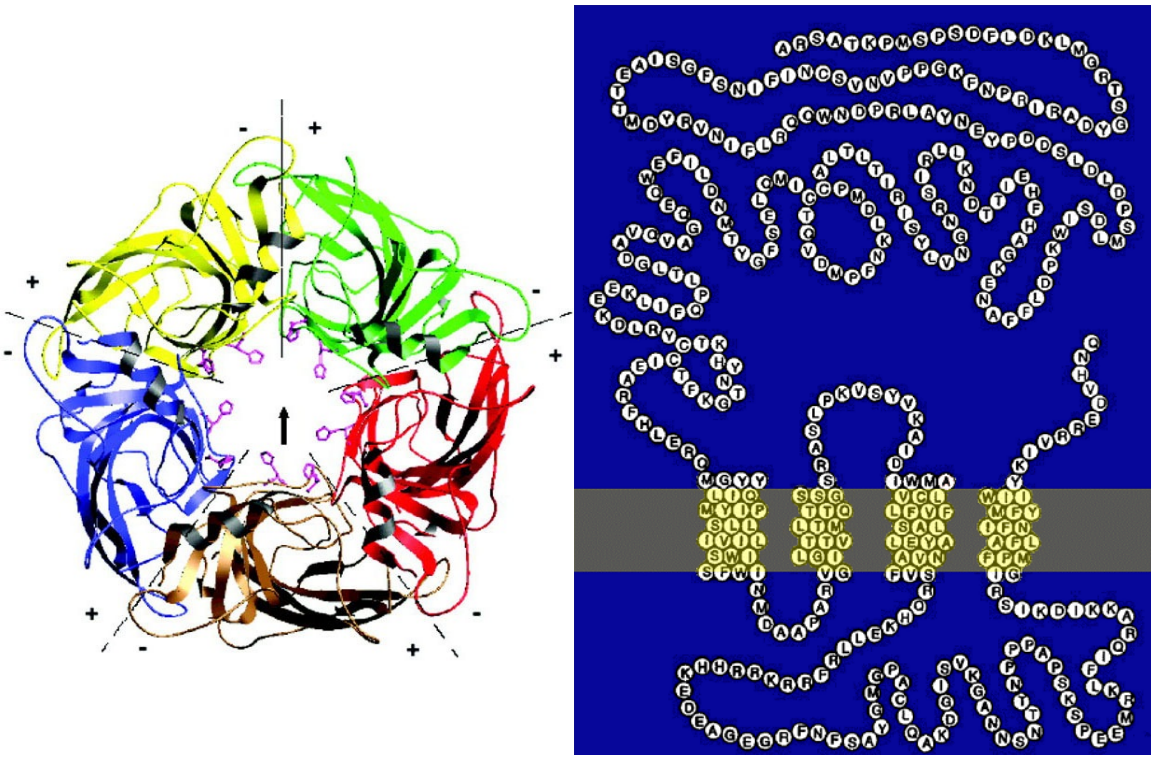

Figure 1.2 – Structure of the glycine receptor

Left: Homology model of the ligand-binding domain of the α1 GlyR viewed top down from the extracellular side of the membrane. Each color denotes a separate subunit. The principal (+) and complementary (-) sides of the intersubunit interface are shown. Adapted from *Lynch JW. (2004). Molecular structure and function of the glycine receptor chloride channel. Physiol Rev 84: 1051.*
Right: Cartoon representation of a single subunit of the α1 GlyR. Each circle represents a single amino acid residue with the single letter code denoting the amino acid inside the circle. The yellow band denotes the plasma membrane, with the residues of the transmembrane domains shown clustered in the membrane. The two cys-loops can be seen in the extracellular domain. Adapted from *Rajendra et al. (1997). The glycine receptor. Pharmacol Ther 73: 121.*

As mentioned in Section 1.1, the GlyR structure has not been specifically resolved, and thus is always compared to an existing structure like the nAChR or one of the non-mammalian channels. A homology model of the GlyR extracellular domain can be seen in **Fig 1.2**, along with a cartoon representation of a single subunit. Mutational analyses have allowed elaboration on the assumed structural similarities with other cys-loop receptors. The ligand-binding domain between adjacent subunits is composed of loops A, B, and C on the principal side and β domains D, E, and F on the complementary side. It is believed that the glycine molecule binds in an orientation with its amino group towards the principal side, and its carboxylic acid group towards the complementary side. The α1 subunit has been the most extensively studied subunit of the GlyR, and references to GlyR residues will use the residue number associated with the α1 subunit unless stated otherwise.

Charged residues from these loops and domains that point into the intersubunit interface interact with the end groups of glycine to stabilize the molecule in the binding area. However, a recent study found two residues to be the primary binding partners. On the principal side, E157 provides negative charge to interact with the amino group of glycine, and on the complementary side, R65 provides positive charge to interact with the carboxylic acid group of glycine (Grudzinska et al., 2005). Thus, in α homomeric receptors, up to five glycine molecules can bind, though only three bound glycine molecules are necessary for full activation of the channel (Beato et al., 2004). For αβ heteromers then, the stoichiometry of the subunits would become important if glycine could only bind between α subunits. Evidence has been found for both 3α:2β or 2α:3β configurations, with the latter being the currently accepted theory (Langosch et al., 1988; Burzomato et al., 2003; Grudzinska et al., 2005). Interestingly, in the same study

suggesting the 2α:3β configuration, the authors also found the corresponding glycine binding residues on the β subunit can also participate in stabilizing glycine, suggesting up to four possible glycine binding sites. Recent functional studies utilizing the newer cys-loop crystal structures have found that even the ββ interface can bind glycine and may be important for functional modification of heteromeric GlyR (Dutertre et al., 2012).

Mutations of additional residues in these binding regions can directly affect agonist affinity for the receptor. When residues F159 and Y161, on the same loop as the proposed binding partner E157, are mutated, the resultant receptors have drastic changes to agonist affinity for a variety of agonists (Schmieden et al., 1993). The same is true for residues on the complementary subunit, with mutations to the R119 residue causing great changes to multiple agonist and antagonist binding (Grudzinska et al., 2005). The Y202 residue on loop C has also been implicated in possible ligand binding, as mutations to this residue and nearby ones affect receptor sensitivity to glycine, though mutations in this region may also affect gating as efficacy of some agonists is increased (Vandenberg et al., 1992a, 1992b; Rajendra et al., 1995). Interestingly, loop C is contained within the second cys-loop unique to GlyR that may be involved in communicating binding to the pore in a similar way as the conserved cys-loop (Lynch, 2004). Whole cell electrophysiological characterization of these mutants does not allow for distinguishing between pure changes to affinity or gating of the receptor, though many studies view mutations of residues near the binding pocket to be more involved in affinity. This problem will be discussed in detail later.

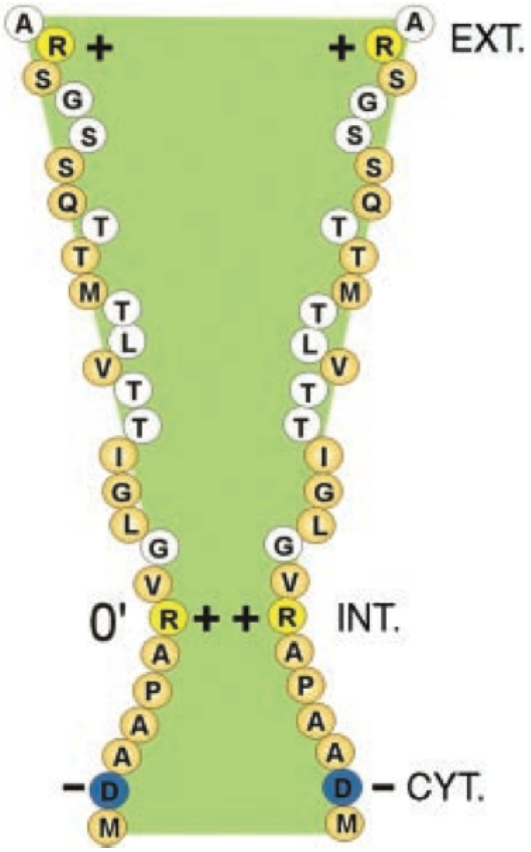

Figure 1.3 – Hypothetical cross-section of the glycine receptor pore

Cartoon model of the GlyR pore, showing the TM2 residues of two subunits. Pore-lining residues have white backgrounds. Positively charged residues are shaded yellow and negatively charged residues are shaded blue. Rings of positive charge are denoted by the "+" sign. Adapted from *Lynch JW. (2004). Molecular structure and function of the glycine receptor chloride channel. Physiol Rev 84: 1051. 967.*

The pore of the GlyR, like other cys-loop receptors, is made up of the TM2 domain of each subunit. As mentioned previously, ion selectivity is achieved through rings of charged amino acid side chains of the opposite polarity of the ions being conducted. Unlike the cationic channels, the GlyR only has two rings of positively charged amino acids formed by arginines. The first is located at position 252 near the intracellular side of the pore, and the second is located at position 271 near the extracellular side of the pore. Additionally the GlyR contains a proline at position 250 that likely changes the pore geometry compared with the cationic cys-loop receptors that do not have this proline. The pore lining residues between these charged residues are generally hydrophilic. The ring of R252 residues is believed to be in the narrowest part of the channel, and thus essential for determining ion selectivity. Mutations to both the nAChR and the 5-HT_3R at positions equivalent to the GlyR A251 and T265, along with insertion of a proline in the narrow part of the channel, to make the pore more closely resemble the GlyR were enough to convert these channels into anion conducting pores (Galzi et al., 1992; Gunthorpe and Lummis, 2001). By probing the pore with various anions and examining their size, the pore diameter was determined to be at least 5.2 Å (Bormann et al., 1987; Fatima-Shad and Barry, 1993; Rundstrom et al., 1994). Thus, anions are attracted to the extracellular side of the pore, shed their waters of hydration along the hydrophilic strip of residues, and pass through the narrowest part of the channel according to the exclusion preference listed previously.

The GlyR exhibits almost no spontaneous activity in the absence of ligand, unlike the nAChR (Twyman and MacDonald, 1991). Thus, ligand binding in the large extracellular domain must in some way transmit the occurrence of this binding to TM2 domains lining the pore to induce gating. Investigation into a GlyR associated disease

helped to elucidate this mechanism. Hyperekplexia or "startle disease" is a human hereditary disorder characterized by exaggerated startle responses to tactile or acoustic stimuli, resulting in generalized stiffness. Hyperekplexia results from mutations that reduce GlyR functioning, disrupting inhibitory tone resulting in increased excitability of motor neurons. The most common form of hyperekplexia is due to an autosomal dominant mutation in the gene for the GlyR α1 subunit that changes the residue R271 into either R271L or R271Q (Ryan et al., 1992). These mutations were shown to decrease both agonist sensitivity and single channel conductance (Langosch et al., 1994, Rajendra et al., 1994). Many other hyperekplexia related GlyR mutations have been identified, a fair number of which occur at residues in the extracellular loop between TM2 and TM3 (termed the TM2—TM3 linker), including Y279C, K276E, Q266H, and S267N among others (Lynch et al., 1997, Becker et al., 2008). Interestingly, each of these mutations have similar effects on GlyR functioning, causing a decrease in agonist sensitivity and changes to generated currents. The S267N mutation is particularly interesting as the residue has been proposed as a site of action for modulation by alcohols and volatile anesthetics (Mihic et al., 1997). In particular, these mutations converted two GlyR agonists into competitive antagonists without affecting binding of these compounds (Lynch et al., 1997). This interpretation was supported by kinetic fits of K276E single channel currents (Lewis et al., 1998). As these mutations seemed to affect efficacy without affecting ligand binding, this TM2—TM3 linker was proposed to be an important domain in channel gate activation (Lynch et al., 1997).

Additional evidence suggests how the binding signal is communicated from the ligand-binding domain to this crucial TM2—TM3 linker in order to activate the channel. Structural analysis of the nAChR pore showed that the loop between β segments 1 and 2

(loop 2) interacts with the TM2—TM3 linker to open the pore (Miyazawa et al., 2003). Interestingly, a hyperekplexia related GlyR mutation to a residue in loop 2, A52S, results in decreased glycine sensitivity similar to TM2—TM3 linker hyperekplexia mutants (Saul et al., 1994, Plested et al., 2007). Functional characterization of $GABA_AR$ mutants identified an electrostatic interaction between residues D149 and K279 that was favored in the open state of the channel (Kash et al., 2003). The $GABA_AR$ D149 residue lies in the cys-loop conserved throughout the superfamily. The corresponding residues in the GlyR, D148 and K276, have also been shown to interact and alter receptor gating in similar fashion to the $GABA_AR$ experiments (Schofield et al., 2003). Additionally, the short peptide sequence connecting the extracellular domain to TM1 may be involved in this transduction process. The residue R209 in this region of the nAChR was shown to interact with E45 of loop 2 through single channel mutational analysis as well as structural modeling (Lee and Sine, 2005). Lee and Sine (2005) also found that residue P272 in the extracellular portion of TM2 was able to interact with E45, showing the proximity of these three regions and ability for interaction, with each of these residues conserved in the GlyR. Thus, loop 2 and both cys-loops may contact and interact with the extracellular loops of the TM domains to transmit the binding signal to the pore.

Additional evidence of this transition comes from the Auerbach group's work on the nAChR. They utilize rate-equilibrium free-energy relationships (REFERs) on sequential nAChR point mutations to identify a ratio describing that residue's effects on the opening and closing rate constants. This ratio, termed Φ-value, varies from 0 to 1 and can be used to group residues in terms of the timing of their movements in the gating transition. A Φ-value of 0 is a late movement and a value of 1 is an early movement. Thus residues with similar Φ-values are likely to transition together in the conformation

wave of activity from binding to gating (Grosman et al., 2000; Purohit et al., 2007). A mapping of these groupings can be seen in **Fig. 1.4** with the extracelluar domain loops in the orange region and the TM2—TM3 linker in the green region. Recent evidence from the prokaryotic channels supports this general model of receptor gating. A recent crystal structure of GLIC at neutral pH, believed to be in the resting-closed state, was compared to existing GLIC crystal structures, that are believed to be in the open state and a secondary closed state where some extracellular domain movement has occurred (termed locally closed), to determine a sequence of events from the closed to open states of the channel (Sauguet et al., 2014). In the model of Sauguet et al. (2014) three grouped movements make up the transition from the closed to open channel: First the majority of the extracellular domain and the linker to TM1; second the cys-loop, TM2—TM3 linker, and the extracellular portions of the TM domains; finally the rest of the TM domains. These motions result in an "unblooming" and rotation of the extracellular domain and a twisting of the TM domains resulting in channel opening, implicating many of the same loops and homologous residues described here suggesting a general mechanism for cys-loop receptors.

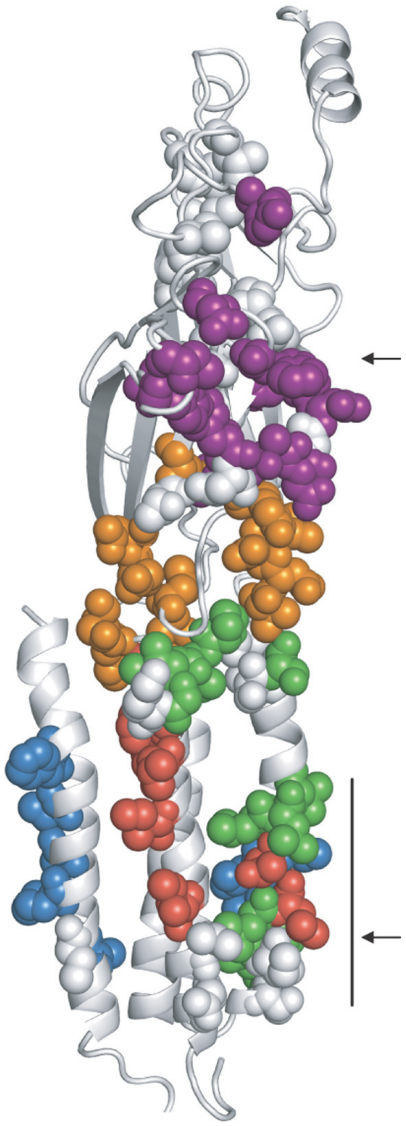

Figure 1.4 – Φ-values in the nAChR

An α subunit extracellular and TM domains from the nAChR with domains of synchronous Φ-values shown in color. The upper arrow denotes the ligand-binding domain with the lower arrow identifying the channel gate. The domains move from earliest to latest with Φ-values as follows: purple, > 0.90; orange, 0.75–0.85; green, 0.59–0.72; blue, 0.48–0.57; red, 0.26–0.35; white, no Φ-value. Adapted from *Purohit et al., 2007. A Stepwise mechanism for acetylcholine receptor channel gating. Nature 446:932.*

1.3 – Single Channel Kinetics of the Glycine Receptor

Single channel electrophysiological recording allows the study of the behavior of individual ion channels over time, and is still the standard for obtaining such rich information about these proteins' function. Neher and Sakmann (1976) developed this technique of using a glass pipette to isolate a single ion channel in a patch of the membrane (later termed patch-clamp), and were the first to observe currents through single nAChRs in frog muscle fibers. Development of this technique led to their award of the Nobel Prize in Physiology and Medicine in 1991. Key to the concept of single channel recordings was finding a way to reduce noise from the entirety of the membrane so that the very small currents through a single channel could be observed. Neher and Sakmann used a pipette with a very small open diameter, fire polished to have a smooth surface, to create a flush seal with the membrane around an ion channel. Applying a small amount of suction decreases any leakage between the glass and membrane interface resulting in a seal with gigaohm resistance (gigaseal). This allowed for recordings of single channels with very low background noise, as well as modified variants of the technique where a small piece of membrane is pulled from the cell (inside-out and outside-out patches) allowing fine control of the solutions on either side of this patch of membrane (Hamill et al., 1981).

Single channel openings occur in clusters of activity enclosed by periods of channel desensitization, where ligand may bind to the receptor but no current is generated. Within these clusters, receptors open in bursts of activity that begin when a ligand binds and opens the channel and end when the ligand unbinds and the channel is closed (Colquhoun and Hawkes, 1977; Pallotta, 1991). An example of these channel

behaviors can be seen in **Fig. 1.5**. The distinction between these two groupings is important, as closings within bursts are times when the channel is ligand-bound but the pore is closed or not conducting ions. Closings between bursts are indicative of ligand unbinding but are still within clusters. Therefore, two types of closings exist in clusters, which convey very different information. Thus, from recorded single channel currents, a lot of information about channel behavior can be obtained. Rates of ligand binding and unbinding can be determined from burst durations. Conductance of the ion channel can be obtained from the current amplitude measured using Ohm's Law:

$$g = I/V \qquad \textit{Equation 1.1}$$

Additionally, the length of time of openings and closings (lifetimes) can vary greatly over many orders of magnitude and can be used to gain kinetic information about channel states. Open and closed lifetime distribution histograms can be constructed with a logarithmic time scale to encompass the wide range of lifetimes seen, plotted against the square root of the number of events. From this distribution, exponential peaks can be identified and fit, the sum of which fit the entire distribution, which determine the time constants of the different states the channel occupies. The amplitude of these peaks determines the proportion of total open or closed time the receptor spent in each state (Pallotta, 1991). However, determination of these parameters is only useful if it describes channel functioning in a way that matches the observed behavior; especially in the case of separating the actions of binding and gating as population data from whole cell recordings can not distinguish between these phenomena (Colquhoun, 2006). Thus the entirety of the data is fit together and the subsequent states used to create a mechanism from which rate constants determining agonist binding and channel gating can be determined. An example of this type of mechanism can be seen in **Fig. 1.6**.

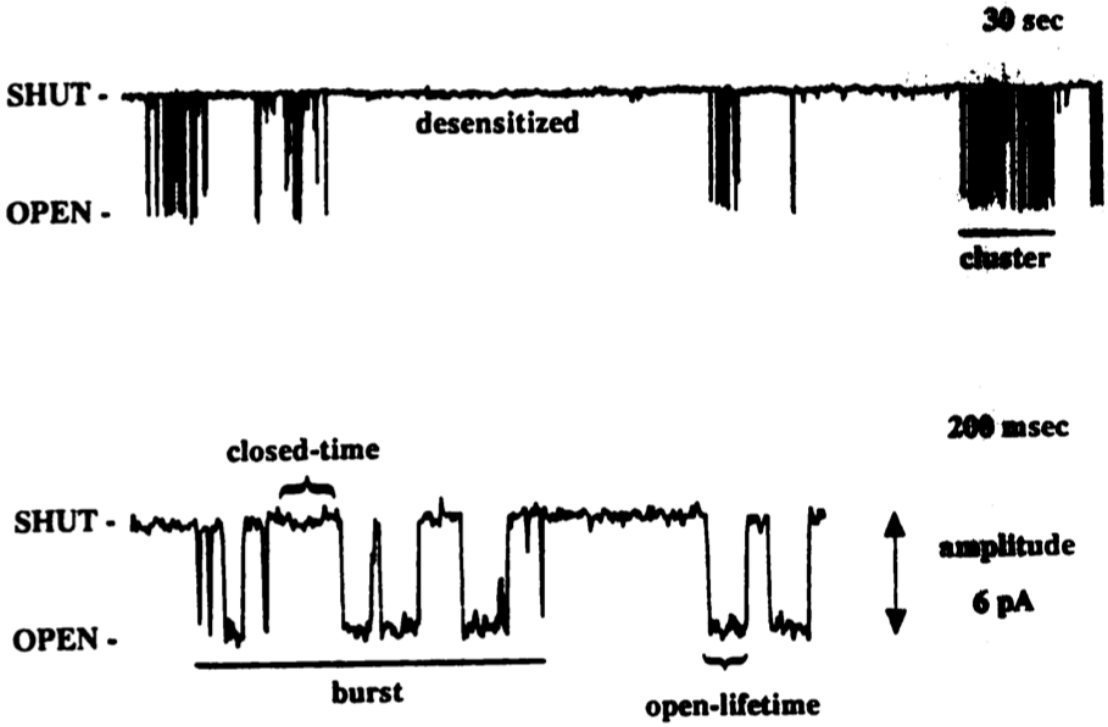

Figure 1.5 – Example single channel current tracing with labeled features

The top tracing shows single channel openings in clusters of activity separated by periods of desensitization. The bottom tracing shows an expanded view of activity showing open and closed times within bursts. Adapted from *Pallotta BS. 1991. Single ion channel's view of classical receptor theory. FASEB J 5:2035.*

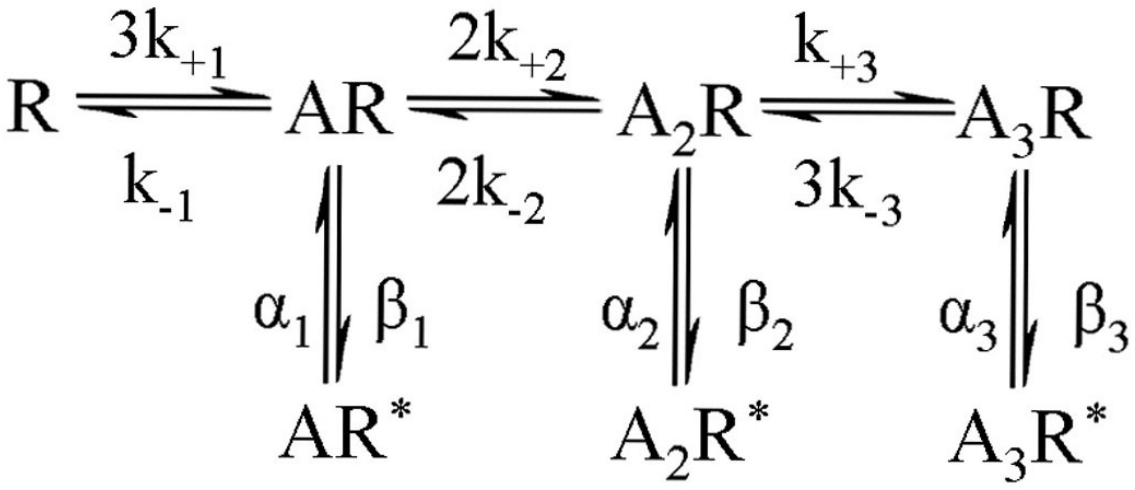

Figure 1.6 – Example kinetic mechanism of glycine receptor activation

Transitions from right to left signify ligand (A) binding, while transitions from top to bottom signify channel opening (*). In this mechanism three ligands can bind the receptor (R) and one is enough to open the channel. k_+ and k_- signify rates of ligand binding and unbinding respectively. β signifies rates of channel opening while α signifies channel closing rates. This mechanism has 12 free parameters describing 4 closed states and 3 open states. Adapted from *Beato et al., 2004. The activation mechanism of α1 homomeric glycine receptors. J Neurosci 24:895.*

The first single channel chloride currents recorded through GlyRs were obtained from patches pulled from cultured mouse spinal neurons (Hamill et al., 1983). This study examined conductance states of glycine- and GABA-activated channels, and found three different conductance states for the GlyR of 45, 31, and 21 pS, with openings displaying the highest conductance state occurring the most frequently. By measuring different conductance states elicited by glycine and GABA in these patches, that were unaffected by an antagonist of the other ligand, Hamill et al. (1983) provided evidence against a previous theory that glycine and GABA activate the same ion channel. Further characterization of conductance states was carried out in heterologously expressed GlyR in HEK-293 cells, examining both homomeric and heteromeric channels (Bormann et al., 1993). Three conductance states were measured for α1β GlyR in close agreement with the Hamill et al. (1983) study, indicating the cultured spinal neurons were indeed expressing these heteromeric channels. However, for the α1 GlyR, five conductance states were measured, 86, 64, 46, 30, and 18 pS, with the last three states corresponding to those seen in α1β GlyR. Six conductance states were observed with α2 and α3 homomeric GlyR with the five seen in α1 GlyR plus a higher conductance state around 111 pS. α3β GlyR had the same conductance states as α1β GlyR, while α2β no longer have the lowest conductance state in favor of the two highest conductance states seen in α2 GlyR. Interestingly, in all GlyR except the α2B, the highest conductance state observed was also the most frequently observed conductance state.

In an effort to better understand how GlyR conductance states relate to channel gating, Twyman and MacDonald (1991) investigated GlyR of cultured spinal neurons with varying concentrations of glycine. They found two conductance states occurred most often, a 42 pS main conductance state with a subconductance state of 27 pS, with

both single openings and bursts of each conductance state. By fitting each conductance state separately, they found that three open state exponential components were necessary to fit the open dwell time histograms in each conductance state (Twyman and MacDonald, 1991). They also noted that increasing glycine concentration resulted in an increase of mean open time for both conductance states, with a shift to spending more time in the longer lived open states. The closed dwell times were also fit by multiple components, with the shorter closed times occurring independent of concentration of agonist. Thus they proposed a kinetic model of binding and gating, similar to **Fig. 1.6**, with four closed states and three open states, with each subsequent open state corresponding to another agonist molecule up to three glycines bound (Twyman and MacDonald, 1991).

Following this study, research into the kinetics of GlyR shifted to heterologous expression systems. Beato et al. (2002) investigated the single channel characteristics of the α1 GlyR expressed in HEK-293 cells, reasoning that the five-fold symmetry of the homomeric channel could lead to a better understanding of the relationship between structure and function. This study also used a range of concentrations, but to a higher top concentration of 10 μM. The resulting open dwell time histograms were fit with four exponential components, with the longest three states having the same time constants as those found in the Twyman and MacDonald study. The fourth state had a much faster time constant, and tended to only be prevalent at lower concentrations of glycine. As the recording sensitivity had increased to this point, it was reasoned that the fastest time constant state was likely missed in previous studies. Like the previous study, Beato and colleagues found the time constants describing the four open states did not vary greatly with increasing concentration of glycine, and that an increase in the mean open time with

increasing glycine was due to spending more time in the longer lived open states. However, at the highest concentration tested, they found that burst length distributions contained a very long lifetime component, where bursts tended to exhibit less single burst behavior (Beato et al., 2002). They fit the data to a kinetic mechanism designed to make sense structurally. As the α1 GlyR has five binding sites, their model contained six closed states and five open states to account for each possible glycine binding. This model then predicted that a single glycine molecule bound was sufficient to open the channel, though with a greatly reduced efficacy compared to when more glycine molecules were bound (Beato et al., 2002).

Beato and colleagues (2004) followed up on their original study with an expansion to include even higher concentrations of glycine, up to 1 mM. They noted that at these higher concentrations, only one conductance level was seen, in contrast to the multiple conductance levels seen in other studies. This may have been due to different test systems, receptor types, concentration of agonist, or other possible reasons, though this issue has not been resolved as of yet. Additionally, at high concentrations, burst behavior tended to give way to clusters of activity, where long lived open states are broken by very short lived closed states, that ended with long lived receptor desensitization periods. The intracluster open probability (P_o), defined as the ratio between total open time per cluster and cluster length, increased with higher glycine concentrations, to a level of 0.96 with 1 mM glycine (Beato et al., 2004). In agreement with this data, only recordings at 10 μM had all three of the previously identified open states. Higher glycine concentrations resulted in increased mean open time with receptors spending more time in longer lived open states, up to 1 mM glycine responses only being fit by the single longest lived open time component. Similarly, increasing

glycine concentration caused receptors to increase the frequency of the shortest lived closed states at the expense of the longer lived closed states. The data was fit to multiple kinetic mechanisms, including three and five open state models, as well as multiple variations that looked at cooperativity of subsequent binding events. Both the three open state and five open state models fit the data, though the three open state model gave a better prediction of the Hill slope of the P_o curve. When the five open state model was fit with the constraint that all gating rate constants for four or five glycine bound was equal to those when three glycine were bound, the extra parameters allowed for a slight but insignificant improvement to the fit of the data. Therefore, three bound glycine molecules are sufficient to fully gate the channel though four or five glycine can bind (Beato et al., 2004).

Following characterization of α1 GlyR single channel behavior, the α1β GlyR was examined in HEK-293 cells (Burzomato et al., 2004). This study used similar concentrations of glycine from 10 μM — 1 mM, to investigate fully bound GlyR activity. As in the Beato et al. (2004) study, higher glycine concentrations resulted in clusters with more time occupying longer lived open states and shorter lived closed states, with the highest concentration showing only a single open time component and 94% of intracluster closings described by the fastest time constant exponential (Burzomato et al., 2004). Multiple kinetic schemes were fit to the data, but despite all open times being fit with at most two exponentials, kinetic schemes with only two open states were poor fits of the data. A kinetic mechanism similar to **Fig. 1.6** with three open states was then found to give a good initial fit of the data. However, it was reasoned that if extra open states were necessary for a better fit of the data, extra closed states may also result in a better fit. Thus many additional kinetic mechanisms were fit with extra closed states

modeled as either desensitized states or additional pre-open closed states. As previous kinetic mechanisms had all shown non-independence of subsequent agonist bindings, it was reasoned that if these additional closed states were modeled between agonist binding and channel opening, then differences in affinity could be modeled between the two different closed conformations. Thus, a change in agonist affinity after glycine binding is modeled as a separate closed state from which additional glycine binding occurs independently as long as in that same conformation. This intermediate closed state was termed "flipped" and the entire mechanism can be seen in **Fig. 1.7** (Burzomato et al., 2004). This mechanism contains three open states and seven closed states, but only 16 free parameters with fewer affinity rates than other models. This flipped mechanism fit the data the best out of the mechanisms tested and was also used to refit the α1 GlyR data from the Beato et al. (2004) study. The flipped mechanism fit was indistinguishable from the mechanism used in that study, despite the differences in affinity parameter constraints (Burzomato et al., 2004). The flipped model has also been used to model glycinergic IPSCs from spinal cord motorneurons and single channel behavior of the nAChR (Burzomato et al., 2004, Lape et al., 2008), thus increasing the complexity of and need for better understanding of the differences between binding and gating of GlyR.

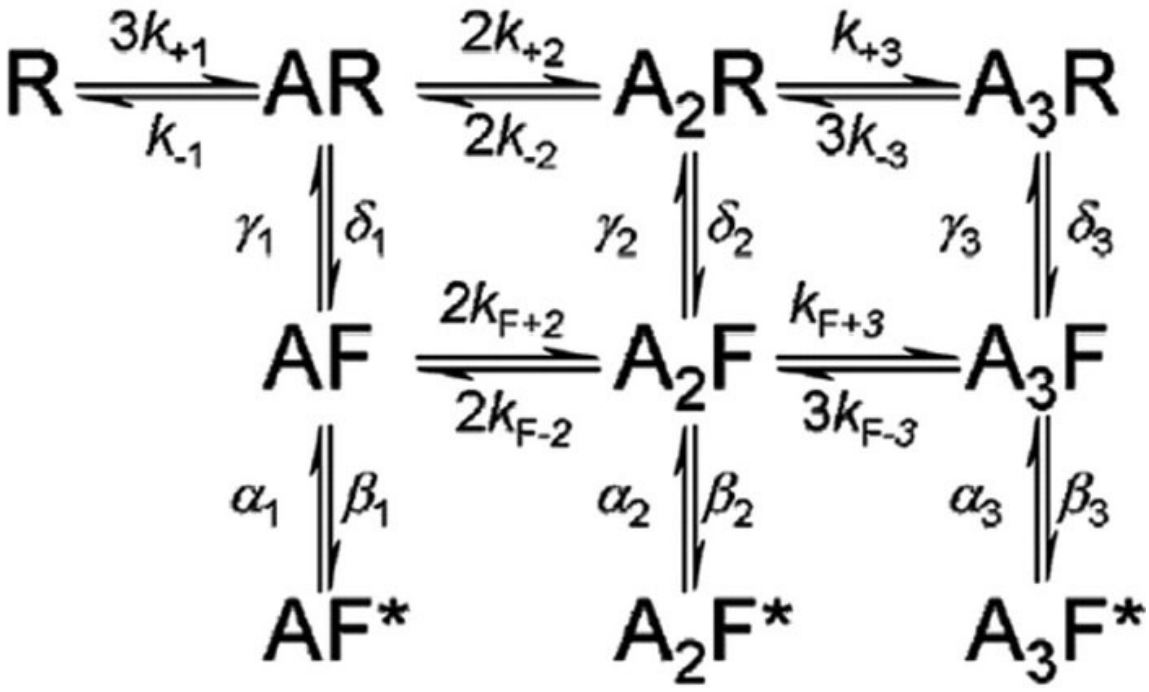

Figure 1.7 – Flipped kinetic mechanism of glycine receptor activation

Transitions from right to left signify ligand (A) binding. Transitions from receptor in the closed (R) to open (F*) states must first transition to a "flipped" (F) conformation. k_+ and k_- signify rates of ligand binding and unbinding respectively. β and α signify rates moving towards and away from channel opening respectively, while δ and γ signify rates moving towards and away from the flipped state. This mechanism has 16 free parameters describing 7 closed states and 3 open states. Adapted from *Burzomato et al., 2004. Single-channel behavior of heteromeric α1β glycine receptors: An attempt to detect a conformational change before the channel opens. J Neurosci 24:10924.*

1.4 – Partial Agonism of the Glycine Receptor

GlyR can be activated by many agonists other than glycine. These include ions such as cesium, macrocyclic lactones such as ivermectin, and amino acids and their derivatives such as alanine, β-alanine, taurine, serine, sarcosine, and GABA (Smith and McBurney, 1989; Rajendra et al., 1997; Shan et al., 2001; Lynch, 2004; Zhang et al., 2009; Dutertre et al., 2012). However, these compounds vary in the magnitude of response generated upon channel activation, with some differing in the method of activation. Agonists that have reduced maximum responses compared to that of glycine are generally known as partial agonists. Of these partial agonists, β-alanine and taurine may be of particular importance due to their abundance in the brain (Shibanoki et al., 1993, Albrecht and Schousboe, 2005). The mechanisms underlying partial agonism have not been fully characterized, as the degree of partial agonism is dependent on subunit composition, expression system, and possibly even membrane composition, resulting in great variability amongst even similar preparations (Lynch, 2004). For example, both β-alanine and taurine can sometimes elicit the same maximum whole cell currents as glycine on α1 GlyRs expressed in HEK-293 cells, though the concentration of agonist required to achieve the same response is increased (Lynch et al., 1997). However, β-alanine and taurine maximum whole cell currents are reduced in comparison to glycine when α1 GlyRs are expressed in *Xenopus* oocytes, with taurine having a larger reduction (Schmieden et al., 1992). In individual experiments, maximum elicited taurine responses as a percentage of glycine responses on α1 GlyR in *Xenopus* oocytes can range from approximately 20% to around 75%. Additionally, on α2 homomeric receptors expressed in oocytes, both β-alanine and taurine become much weaker agonists in comparison to

glycine responses (Schmieden et al., 1992). This reduction in partial agonism was seen for these compounds in α3 GlyR expressed in HEK-293 cells as well, though both partial agonists are weaker on α2 GlyR (Chen et al., 2009). Despite shifts in the degree of partial agonism with subunit or expression system changes, the rank order of agonist efficiency seems to be held constant, e.g. glycine > β-alanine > taurine (Lynch, 2004).

The effects of taurine on GlyR functioning may be of more importance than β-alanine as taurine may have a role as an endogenous GlyR ligand in the brain (Shibanoki et al., 1993; Mori et al., 2002; Albrecht and Schousboe, 2005; Choe et al., 2012). Taurine is the second most abundant amino acid in the brain, found in varying concentrations by brain region into the low mM range, with cerebral cortex, basal ganglia, and hypothalamus among the regions containing high concentrations of taurine (Palkovits et al., 1986; Banay-Schwartz et al., 1993; Albrecht and Schousboe, 2005). However, taurine has also been shown to be released from glia, where internal concentrations may reach up to ~20 mM (Shibanoki et al., 1993; Mori et al., 2002; Albrecht and Schousboe, 2005; Choe et al., 2012). Taurine is known to be released due to osmotic pressure (Albrecht and Schousboe, 2005; Choe et al., 2012), but release can also be induced in hippocampus through activation of NMDA receptors (Shibanoki et al., 1993; Mori et al., 2002) and this release can occur through non-osmotic mechanisms (Rodriguez-Navarro et al., 2009).

Although release of taurine does not guarantee action on GlyR *in vivo*, some studies have found evidence for taurine-activated currents on GlyR in hippocampus, hypothalamus, and nucleus accumbens. Strychnine-sensitive currents in hippocampal CA3 pyramidal neurons were increased by guanidinoethanesulfonic acid (GES), a taurine reuptake inhibitor, but not by sarcosine, a glycine reuptake inhibitor (Mori et al., 2002).

This study also found that GlyR were not involved in evoked synaptic currents, thus taurine may act on hippocampal GlyRs to regulate inhibitory tone (Mori et al., 2002). Blockade of osmotic release mechanisms or cellular depletion of taurine was found to excite neurons in the supraoptic nucleus of the hypothalamus, indicating glial release of taurine regulates inhibitory tone in this area as well (Choe et al., 2012). In the nucleus accumbens , a brain region believed to be important in reward and addiction, taurine may act in modulating the rewarding effects of drugs of abuse. Acute administration of alcohol increases taurine concentration in the NAcc by well over 100% (Dahchour et al., 1996), and taurine perfused into the NAcc causes a release of dopamine that can be blocked by strychnine (Ericson et al., 2006). Recently, Ericson et al. (2011) found that the dopamine release into NAcc associated with the rewarding effects of ethanol required an increase in taurine in this area, as inhibiting taurine release blocked the subsequent release of dopamine.

Partial agonists have been studied in kinetic models to better differentiate their differences in affinity for the channel or efficacy at opening it. Efficacy can be defined as:

$$E = \beta/\alpha \qquad \textit{Equation 1.2}$$

Where β is the rate constant of channel opening and α is the rate constant of channel closing. Determining efficacy for partial agonists using single channel studies is of great importance as whole cell concentration response curves can not distinguish between effects of binding and gating (Colquhoun, 1998); as seen in the equation for the effective concentration giving 50% of the maximum response (EC_{50}), a common parameter used to compare concentration response curves:

$$EC_{50} = K_d/(1 + E) \qquad \textit{Equation 1.3}$$

Partial agonism would then be described by a decrease in efficacy caused by either a decrease in β, an increase in α, or both. Subsequently, the efficacy at high concentrations of agonist can then be used to calculate the P_o using the equation:

$$P_o = E/(1+E) \qquad \textit{Equation 1.4}$$

The P_o then can be used to differentiate the max response seen between agonists. A study by Lewis et al. (2003) looked at kinetic parameters for glycine, β-alanine, and taurine activation of α1 homomeric GlyR expressed in HEK-293 cells, and found that the partial agonists had reduced β compared to glycine with no change in α. Thus glycine had a high efficacy of 16 and a P_o of 0.94, while β-alanine and taurine had efficacies of 8.4 and 3.4 with P_o of 0.89 and 0.77 respectively, in agreement with the high maximum effect of these partial agonists on HEK-293 whole cell GlyR currents (Lewis et al., 2003).

However, a study investigating taurine activated α1β GlyR at the single channel level found that partial agonism is determined earlier than the final opening transition. Unlike the Lewis study, Lape et al. (2008) fit single channel openings over a range of concentrations of both glycine and taurine with the flip kinetic mechanism (**Fig. 1.7**) used previously in the Burzomato et al. (2004) study. They determined the efficacy (Equation 1.2) of both the transition from the flipped state to the open state, and the closed state to the flipped state which they termed F. Comparing these model fits between glycine and taurine activated GlyR revealed that when fully bound (high concentration of agonist), E for both glycine and taurine was high (20 and 9.2 respectively). These efficacies would result in P_o values of 0.95 for glycine and 0.90 for taurine, which is incongruent with taurine acting as a partial agonist. However, the F values were very different between glycine and taurine (27 and 0.15 respectively). This placed the determination of partial

agonism earlier than the final opening transition, with taurine favoring the closed state over the flipped state; however when the flipped state was obtained for either agonist, transitions to the open state were heavily favored. Including both transitions from closed to open leads to a P_o calculation of:

$$P_o = EF/(1+F+EF) \qquad \textit{Equation 1.5}$$

Using Equation 1.5 gives a Po of 0.95 for glycine and 0.53 for taurine, which matches with previous data on taurine partial agonism (Lape et al., 2008). This study also found similar results for the partial agonist tetramethylammonium (TMA) on the nAChR, providing evidence that this early determinant of partial agonism may be generalizable to the cys-loop receptor family (Lape et al., 2008).

The Lape study also revealed another interesting feature of taurine activation of GlyR. In their kinetic mechanism, Lape et al. (2008) ignored flip and open transitions for the singly liganded GlyR. They were able to fit these transitions with rate constants for glycine, but taurine concentrations less than 1 mM did not produce reliable openings. Thus, they fit only the doubly and triply liganded rate constants, as they believed at these high concentrations only these two bound states were likely to occur. Although the doubly liganded state may not have been very prevalent, it was clear that the γ_2 rate constant was extremely high for taurine. This results in the GlyR doubly liganded by taurine almost never being able to attain the flipped state (Lape et al., 2008). The implication being that the taurine-bound GlyR needs to be fully liganded to open. If this is indeed the case, comparisons of taurine and glycine at low concentrations are comparing different phenomena.

In light of this evidence placing the root of partial agonism early in the transitions from closed to open, it is of interest to determine where in the GlyR structure these

differences are determined. The extracellular domain is a good candidate as binding causes a conformational wave of activity that allows extracellular loops to interact with the TM domains to open the pore (Lynch, 2004; Purohit et al. 2007). Taurine binding may induce less of a conformational change or align the extracellular domain in such a way that interaction with the TM2-TM3 linker is possible but difficult. Interestingly, charge reversal mutations to residues E53 and D57 in loop 2 have been shown to change taurine from a partial agonist into an antagonist (Absalom et al., 2003). Additionally, a charge reversal mutation in the intersubunit interface of residue D97 that renders the receptor spontaneously active turns taurine into an equally efficacious agonist as glycine, while a mutation in the TM domains at residue K281 that also results in a spontaneously active GlyR does not change taurine efficacy (Welsh et al., *In Prep*.).

1.5 – Allosteric Modulation of the Glycine Receptor

An allosteric modulator is generally thought of as a compound that binds somewhere other than the active site that changes function of the protein in a positive or negative way, i.e. favoring one conformation over another. This definition was useful when describing enzymes where the catalytic site is the active site and any compound that binds elsewhere and favors the active or inactive forms of the enzyme could be considered an allosteric modulator; however, defining allosterism for ion channels becomes a more complex problem (Colquhoun, 1998). For example, is the pore region where ions flow through the channel the active site, or is the active site the ligand binding site which begins the process of channel activation? Additionally, if the Φ-analysis of Purohit et al. (2007) and the flip mechanism of Burzomato et al. (2004) and Lape et al.

(2008) are taken into consideration, an ion channel can exist in multiple discreet states; thus, is it necessary examine the effects of a compound on each state? Some receptors have co-agonist sites that are required to activate the channel but bind somewhere other than the ligand, so are these compounds allosteric modulators? Many of these concerns have not been addressed in the literature, as allosteric modulation has been used to mean a great many things (Colquhoun, 1998). Thus here we will define an allosteric modulator as anything that binds the GlyR at a site other than the agonist binding site and modulates the activity of the channel.

The GlyR has many compounds that fit this definition of allosteric modulators, including divalent cations, alcohols, halogenated compounds, cannabinoids, neurosteroids, tropeines, plant derived poisons, and even other proteins (Lynch, 2004; Yevenes and Zeilhofer, 2011). A large amount of research has been done into the binding locations and functional effects of almost all of these compounds, though complete understanding of the actions of these compounds has not yet been achieved. Some of these GlyR modulators that are relevant to this work will be considered individually below.

1.5.1 – ALCOHOL

Ethanol (ethyl alcohol), commonly known as alcohol, is a drug consumed in beverages throughout the world and has been for most of human history (McGovern et al., 2004). Alcohol is commonly used, with over half of Americans identifying as current drinkers (Johnston et al., 2013b). The highest levels of binge drinking were found among young adults, with more minors using alcohol than tobacco or illicit drugs (Johnston et

al., 2013a, 2013b). However, the potential for abuse of alcohol is high, with abuse leading to large impacts at the individual and societal levels. The United States Centers for Disease Control and Prevention (CDC) estimate alcohol-attributable deaths due to excessive use to average ~88,000 per year. This makes excessive alcohol use the third leading cause of lifestyle choice related deaths in the United States (Mokdad et al., 2004). Therefore, an understanding of the mechanisms behind alcohol actions are necessary to effectively develop treatment for and aid in prevention of alcohol abuse.

Alcohol is known to be a CNS depressant which results in behavioral disinhibition, but at the molecular level it has a wide variety of targets throughout the brain that include ion channels of the cys-loop family, including the GlyR. However, the diversity of targets has complicated the interpretation of which molecular effects are relevant to the behavioral phenotypes. Recent evidence has indicated alcohol effects on GlyR *in vivo* may mediate some of the rewarding effects of ethanol. GlyR are found in the NAcc, where drug induced dopamine release is believed to modulate the rewarding properties of these drugs (Waldvogel et al., 2007; Soderpalm and Ericson, 2013; Jonsson et al., 2014). Infusion of glycine into the NAcc increased the concentration of dopamine there and decreased alcohol consumption in alcohol-preferring rats, while infusion of the GlyR antagonist strychnine decreased dopamine release in NAcc (Molander et al., 2005). Additionally, a glycine reuptake inhibitor Org 25935, which would increase the amount of glycine present extracellularly, decreased ethanol intake in rats in agreement with the previous study (Molander et al., 2007).

Ethanol effects on GlyR have been well characterized at the whole cell level. Ethanol potentiates GlyR responses generated by low concentrations of glycine in a concentration dependent manner, ranging from biologically relevant recreational

concentrations to anesthetic doses (Mascia et al., 1996a). However, ethanol potentiation of glycine currents decreases with increasing glycine concentration to the point of having no effect on saturating concentrations of glycine (Mascia et al., 1996a). Ethanol action was greater on α1 GlyR than α2 GlyR, and the α1 mutant GlyR A52S had responses similar to α2 GlyR, indicating a possible role of this residue in ethanol action (Mascia et al, 1996a). Further investigation of ethanol binding to GlyR was carried out by Mihic et al. (1997), who created various chimeric channels comprised of pieces of α1 GlyR and $GABA_A$-ϱ1 subunits, which are less sensitive to the effects of ethanol. Investigation of these chimera led to the identification of two residues important in the actions of ethanol, S267 and A288 in the TM2-TM3 region (Mihic et al., 1997), which were believed to line a water filled pocket separate from the pore where ethanol could bind. S267 mutations could affect the potentiation by ethanol as a function of side chain residue size, yielding information about the size of this binding pocket as large residue side chains converted ethanol from potentiating to inhibiting GlyR responses (Ye et al., 1998). Similar characterization of the A288 residue revealed this residue was a crucial determinant of volatile anesthetic sensitivity, indicating a common binding pocket for alcohols and volatile anesthetics (Mihic et al., 1997; Yamakura et al., 1999).

At the single channel level, few studies have investigated the effects of ethanol on GlyR. Eggers and Berger (2004) examined GlyR in outside-out patches pulled from rat hypoglossal motor neurons. Ethanol was found to enhance GlyR currents by increasing binding rates and decreasing unbinding rates when fit with a simple kinetic model (Eggers and Berger, 2004). A more recent study examining the effects of ethanol on single channel GlyR currents was carried out with low concentrations of glycine and two concentrations of ethanol. Ethanol increased duration of burst activity without affecting

open or closed dwell times by decreasing unbinding of glycine (Welsh et al., 2009). These two studies are in agreement then that ethanol appears to act by increasing affinity for glycine.

1.5.2 – ANESTHETICS

Anesthetics are a broad group of compounds that produce a similar group of physiological effects including analgesia, amnesia, immobility, hypnosis, and sedation. They are widely used in clinical settings to induce these effects for surgery and other medical procedures, and can be administered as an injection or via inhalation, where inhalational anesthetics are usually volatile halogenated compounds. Although most anesthetics are not available to the general public, they do have the potential for abuse mainly with anesthesiologists who have access to the them. A study by Wilson et al. (2008) found that 22% of anesthesiologist training programs had at least one case of inhalational anesthetic abuse, with only 22% of abusers able to return to practice. Like alcohol, anesthetics cause a depression of nervous system functioning, though they are much more potent in their effects, with high concentrations leading to a risk of death. In order to equate effective concentrations of various anesthetics, a measure of potency was developed known as the minimum alveolar concentration (MAC), defined as the concentration at which 50% of patients are unable to respond to a painful stimulus (Eger et al., 1965).

Like ethanol, anesthetics can affect a large number of targets, though direct binding of anesthetics to proteins was only shown in the last 30 years. Originally anesthetics were thought to work by disruption of the lipid bilayer comprising the cell

membrane, where compounds with higher lipid solubility would exhibit higher potency as an anesthetic (Franks and Lieb, 1997). This idea, known as the Meyer-Overton hypothesis was called into question when compounds were found that had increased lipid solubility without an increase in anesthetic potency (Pringle et al., 1981; Mihic et al., 1994), as well as the finding that clinically relevant concentrations of anesthetics had almost undetectable effects on membrane fluidity (Franks and Lieb, 1982). This led Franks and Lieb to search for anesthetics acting by binding directly to proteins to elicit their effects (Franks and Lieb, 1982). They subsequently showed that a variety of anesthetics, alcohols, and other compounds could directly bind to and inhibit a completely soluble protein, firefly luciferase, devoid of any lipid (Franks and Lieb, 1984).

As mentioned previously, Mihic et al. (1997) found residues S267 and A288 in the TM2-TM3 region of the α1 GlyR that are important for ethanol and anesthetic binding. Subsequent research into these residues confirmed their importance for anesthetic action. S267C mutant GlyR responses were potentiated by anesthetics, but when covalently bound and potentiated by propyl-methanethiosulfonate (PMTS), a thiol reagent that forms a disulfide bond with a cysteine to mimic binding of an alcohol to this residue, anesthetics no longer potentiated GlyR responses (Mascia et al., 2000). Additionally, the S267I mutant GlyR, which negates ethanol potentiation was shown to retain anesthetic potentiation of responses; however, ethanol was found to competitively inhibit anesthetic potentiation of the mutant receptor responses (Beckstead et al., 2001). These studies showed that binding to discrete residues in this pocket for alcohols and anesthetics can indeed potentiate GlyR responses and that this pocket is of a limited size.

1.5.3 – INHALANTS

Inhalants are a broad group of volatile chemical compounds which can be inhaled to produce a rapid but quickly reversible high (Evans and Balster, 1991). Inhalants have no common defining structural characteristics, as a loose definition of inhalants can also include alcohols and anesthetics. The recent distinction between inhalants and these other drugs comes from differences among use patterns and ease of obtaining the drugs. The inhalants then are usually solvents which are legally obtained in many household items. The ease with which they are obtained combined with the rapid high have led to the highest prevalence of abuse of these drugs being amongst young teens and adolescents. Inhalants have the second highest prevalence of use among this age group, and are often the first drug tried for adolescents (Johnston et al., 2013a).

The inhalant toluene, like other drugs of abuse, causes a release of dopamine into the NAcc (Riegel et al., 2007), and has modulatory effects on other receptors also affected by ethanol (Bale et al., 2002; Del Re et al., 2006). Thus it was likely that inhalants exhibiting similar effects to GlyR modulators would themselves modulate GlyRs. Inhalant modulation of GlyR functioning was shown for both halogenated solvents like 1,1,1-trichloroethane (TCE) and trichloroethylene (TCY) and aromatic compounds like toluene (Beckstead et al., 2000). Testing of these compounds on mutant GlyRs previously identified to alter ethanol and anesthetic potentiation altered inhalant modulation as well, and ethanol antagonism of an inhalant on one such mutant was similar to antagonism seen for anesthetics, indicating inhalants bind in the same pocket as alcohols and anesthetics (Beckstead et al., 2000; Beckstead et al., 2001).

1.5.4 – ZINC

The divalent cation zinc may be unique as a GlyR modulator in that it is biphasic in its modulation of GlyR currents. At low concentrations up to ~10 μM, zinc potentiates GlyR responses, while at concentrations above this range, zinc inhibits GlyR responses (Laube et al., 1995, 2000; Harvey et al., 1999). Zinc has been studied extensively for its effects on GlyR functioning because it may have physiological relevance. Zinc is present throughout the brain at nM concentrations in the range of potentiation for GlyR (Frederickson et al., 2006b). Zinc has been found to be released by some synaptic terminals, the most well studied being the glutamatergic mossy fiber synapse in the hippocampus (Frederickson, 1989). However, there is evidence of zinc co-localization with glycine in presynaptic terminals of lamprey spinal cord (Birinyi et al., 2001). While it was originally thought that zinc concentration could reach into the high μM range with release (Lynch, 2004), recent calculations of zinc concentration following synaptic release determined that concentrations never exceed 10 μM, at the end of the potentiating range for GlyR (Frederickson et al., 2006a).

The biphasic nature of zinc modulation for the GlyR arises from two separate binding sites, a high affinity potentiating site and a low affinity inhibitory site (Laube et al., 1995). The inhibitory site was identified in the intersubunit interface, where H109 from the principal subunit and H107 from the complementary subunit both act to stabilize zinc. Mutation of these two residues to alanines were enough to abolish zinc inhibition of GlyR functioning. Conformation that the zinc ions are stabilized between subunits rather than within each subunit was achieved by expressing single mutation H107A and H109A subunits with each other to abolish intrasubunit but retain intersubunit zinc coordination. These heteromeric mutant GlyR retained zinc inhibition similar to that seen in wild type

(WT) GlyR (Nevin et al., 2003). These histidine residue can be seen in **Fig. 1.2** as the pink colored histidine side chains in the lumen of the ligand-binding domain pentamer.

The potentiation binding site for zinc has been more elusive to discover. Functional characterization of GlyR potentiation by zinc revealed that zinc increases mean open time and burst durations, by increasing the occurrence of longer lived open states and decreasing glycine unbinding (Laube et al., 2000). This suggested the zinc potentiating site might be in the extracellular domain near the ligand-binding domain. In agreement with this hypothesis, Laube et al. (2000) found that the residue D80 was important for zinc potentiation of GlyR responses. However, while the mutant GlyR D80A was able to abolish zinc potentiation of glycine-activated GlyR, it had no effect on zinc potentiation of taurine-activated GlyR (Lynch et al., 1998). This study also investigated various residues throughout the TM2-TM3 region, but no mutation was able to abolish zinc potentiation of both glycine and taurine activated GlyR currents (Lynch et al., 1998). Kinetic analysis of zinc potentiation of taurine activated GlyR revealed that zinc was able to increase taurine efficacy, an effect not seen for glycine (Laube et al., 2000). This led to speculation that the activation mechanism for the two agonists were separate, and thus zinc would modulate the two pathways separately.

However, two subsequent studies give evidence of an alternative zinc potentiating site. The first found mutations in the β sheets of the extracellular domain near the external perimeter of the domain. Three residues, E192, D194, and H215 were found to abolish zinc potentiation of glycine and taurine activated GlyR currents (Miller et al., 2005). These mutations were all made on a H107N background to eliminate the possibility of zinc inhibition, though high concentrations of zinc still caused inhibition of glycine and taurine activated GlyR currents (Miller et al., 2005). Thus the interpretation

of zinc effects on these mutants is somewhat muddled. However, a recent study looking at a hyperekplexia mutation of W170S GlyR found that while these receptors behaved relatively similar to wild type GlyR, zinc potentiation of glycine, β-alanine, and taurine activated GlyR currents was greatly reduced or abolished all together (Zhou et al., 2013). This W170 residue resides near those found in the Miller study, thus this external region may incorporate the zinc potentiating site.

1.6 – Dissertation Aims

The objective of the research presented in this dissertation was to investigate allosteric modulation of the taurine activated GlyR to elucidate differences in glycine vs. taurine activation and the nature of partial agonism. This objective was divided into the following three specific aims.

Aim 1. To examine differential modulation of the GlyR when activated by taurine vs. glycine. The hypothesis to be tested was that ethanol, anesthetics, inhalants, and zinc would enhance GlyR currents activated by maximally effective concentrations of taurine but not glycine.

Aim 2. To investigate the kinetic mechanisms underlying allosteric modulation of the taurine activated GlyR. The hypothesis to be tested was that ethanol and the anesthetic isoflurane would enhance the taurine activated GlyR by stabilizing the open state.

Aim 3. To investigate the effects of an intersubunit electrostatic bond and its implications for partial agonist activation of the GlyR. The hypothesis to be tested was that a mutation at residue R131 would destabilize the closed state and thus increase the efficacy of the partial agonist taurine.

2.0 | MATERIALS AND METHODS

2.1 – Molecular Biology

Human wild type GlyR subunit cDNA was previously subcloned into a modified pBK-CMV vector modified to delete the region coding for the *lac* promoter and the *lacZ* start codon (Mihic et al., 1997). The GlyR cDNA is under the control of a Cytomegalovirus (CMV) promoter that allows the α1 subunit to be expressed in heterologous expression systems, and the vector contains a gene conferring resistance to the antibiotic kanamycin. GlyR cDNAs were produced using supercompetent XL1-Blue *E. Coli* (Stratagene) that were transformed with the plasmid and grown on LB agar plates containing 50 μg/ml kanamycin to select for transformed cells. From these plates, individual colonies were selected and used to inoculate LB broth which was subsequently allowed to grow overnight in a shaker incubator. Plasmid cDNA was isolated using either Mini or Maxi prep kit protocols (Qiagen). Isolated plasmid was tested for concentration and quality using a NanoDrop spectrophotometer (Thermo Scientific). Plasmid samples with an A_{260}/A_{280} ratio determined to be near 1.8 were considered acceptable for use in heterologous expression systems.

Point mutations to the α1 GlyR subunit cDNA sequence were made using a QuickChange Mutagensis kit (Stratagene). Custom oligonucleotide primers (Integrated DNA Technologies) were designed to contain the point mutation(s) in the middle of the primer sequence. Primers were combined with template α1 GlyR cDNA and a high fidelity DNA polymerase, and run through a thermocycling protocol that led to

production of new plasmids that incorporated the primers coding for the point mutation(s). The original template cDNA was digested using the *DpnI* restriction enzyme. Resulting primers were grown in supercompetent XL1-Blue *E. Coli* and isolated as described above. Samples were sent for sequencing using a dideoxy fluorophore method to verify incorporation of the mutation.

2.2 – *Xenopus* Oocyte Harvesting, Isolation, and cDNA Injection

Xenopus laevis frogs were purchased from Xenopus Express (Homosassa, FL) or Nasco (Fort Atkinson, WI) and housed at 19°C on a 12 h light/dark cycle. Surgeries were performed in accordance with the Association for Assessment and Accreditation of Laboratory Animal Care regulations. Briefly, frogs were anesthetized, a small incision was made through the lower abdomen and a portion of ovary was removed and placed in a modified Barth's saline (MBS) solution. Incision was closed with sutures and frogs were allowed to recover for future oocyte harvesting, up to two more times.

Harvested oocytes were placed in a hypertonic isolation media to slightly shrink the oocytes and loosen the thick protective membrane. Forceps were used to manually remove the thecal and epithelial layers from stage V and VI oocytes. Isolated oocytes were than placed in a collagenase solution for 10 min to remove the follicular layer. Fully isolated oocytes were then washed with and placed in an isotonic MBS solution.

cDNA constructs used for oocyte injection were diluted to 50 ng/μl using sterile deionized water (diH_2O). An injector tip (10-15 μm) was created by pulling a piece of capillary glass using a Sutter Intruments P-30 Flaming/Brown Puller. The injector was backfilled with mineral oil and attached to a Drummond Nanoject II injector. cDNA to be

injected was front loaded into the injector tip. The animal poles of oocytes were impaled with the injector tip and 30 nl of cDNA (1.5 ng) was injected near the nucleus of each oocyte. Injected oocytes were then placed into 96-well plates containing incubation media that had been sterilized by passage through a 0.22 μm filter. The plates were stored in the dark. Oocytes expressed GlyR within ~24 h, and all electrophysiological measurements were made within 1-7 days of cDNA injection.

2.3 – Two-Electrode Voltage-Clamp of *Xenopus* Oocytes

Before electrophysiological recording, oocytes were placed in a 100 ml bath with the animal poles facing upwards. Electrodes were pulled from capillary glass using a Sutter Instrument P-97 Flaming/Brown Micropipette Puller to tip resistances of 0.5-10 MΩ. Glass electrodes were filled with 3 M KCl and used to impale the animal pole of oocytes. Cells were voltage-clamped at –70 mV using an OC-725C oocyte clamp (Warner Instruments, Hamden, CT) and perfused with MBS or MBS + drug solutions at a rate of 2 ml/min using a Masterflex USA peristaltic pump (Cole Parmer Instrument Co., Vernon Hills, IL) through 18-gauge polyethylene tubing. A waste line removed build up of the excess fluids from the chamber. One of the electrodes measures the voltage of the cell while the other injects current in order to maintain a set potential. Activation of the GlyRs opens the channels and allows chloride ions to flow outward. The voltage electrode detects this flux as a depolarizing force, causing the current electrode to inject negative current in order to keep the cell clamped at the desired voltage. This feedback loop occurs continuously while the output from the amplifier is acquired at a rate of 1 kHz using a Powerlab 4/30 digitizer with LabChart version 7 software (ADInstruments,

Bella Vista, NSW, Australia). All drug applications were followed by 6-15 min washout periods to allow for complete receptor resensitization. All concentrations reported are the bath concentrations to which the oocytes were exposed.

2.4 – Patch Clamp Electrophysiology

Patch clamp electrophysiology was used to record currents from outside-out patches pulled from *Xenopus* oocytes expressing either mutant or WT GlyRs. Before outside-out patches can be pulled, the vitelline membrane must be removed to obtain a proper seal. Thus, prior to recording, the oocyte was placed in a high-osmolarity stripping solution to aid in manual removal of the vitelline membrane using forceps. Once removed, the oocyte was transferred to the recording chamber filled with external solution, using a Pasteur pipette being careful to ensure that the oocyte is not exposed to the air. The oocyte was turned in the bath, so that the animal pole faced upwards towards the recording electrode, and allowed to adjust to the external solution for at least 5 min. Thick-walled borosilicate glass (WPI, Sarasota, FL) was pulled using a P-97 Flaming/ Brown Micropipette Puller (Sutter Instruments) to form patch pipettes. These pipettes were coated with wax or with Sylgard 184 (Dow Corning, Midland, MI) just above the tips and fire-polished with an MF-830 Microforge (Narishige, Japan) to obtain a smooth tip with resistances of 5 to 15 MΩ. Pipettes were then tip-filled with internal solution by applying suction to the back of the electrode while the tip was held in a bead of internal solution resting on a piece of Parafilm (Pechiney Plastic Packaging Company, Chicago, IL). Pipettes were then backfilled with inline-filtered internal solution using quartz flexible tubing (WPI).

Outside-out patches were held at –80 mV, and recordings were made according to standard methods (Hamill et al., 1981) using an Axopatch 200B amplifier (Molecular Devices, Sunnyvale, CA). First, a slight positive pressure was applied to the electrode before it was lowered into the bath to prevent clogging of the tip. The electrode tip was moved into close proximity with the edge of the oocyte such that the positive pressure began to dimple the membrane. The tip was then slowly pressed against the oocyte until a small increase (0.5-1 MΩ) in tip resistance was observed. Positive pressure was released and the membrane was allowed to seal around the electrode tip until a resistance of at least 1 GΩ was measured. In order to obtain a gigaseal, it was often necessary to apply a small amount of negative pressure to the electrode. Once a gigaseal was achieved, the "Zap" button was pressed to break into the cell. This was visible by a drop in the measured resistance, and the electrode was then slowly pulled away from the oocyte until a patch was pulled from the membrane and re-sealed resulting in a resistance again exceeding 1 GΩ. The outside out patch configuration results in the extracellular patch membrane facing into the bath while the intracellular side of the patch membrane faces the interior of the patch pipette. The amplifier gain was then increased to 50x and the holding current was set to –80 mV.

Agonist and drug solution were prepared in external solution before being perfused over outside-out patches using an SF-77B Perfusion Fast Step apparatus (Warner Instruments, Hamden, CT). The bath chamber was continuously filled using a 50 ml syringe containing external solution, via gravity flow. A vacuum line attached to an L-shaped metal piece of tubing in a separate portion of the recording chamber provided an outlet and maintained a steady bath level. Solutions were loaded in 20 ml glass syringes that were held above the recording chamber and connected to one of three

manifolds with polyethylene tubing. The output of the manifold was connected to a piece of three-barrel square glass and its tip was submerged in the bath. Bubbles were expelled from each line that was in use to ensure that the gravity flow delivery worked properly and that bubbles would not break patch seals. The three-barrel glass was moved and placed where the patch was directly under the middle chamber perfusing external solution. Rapid re-positioning of the perfusion barrel could be achieved to switch the patch from external solution perfusion to solution + drug perfusion when necessary. Steady state patches remained in the solution for the duration of the recording.

The analog output of the Axopatch 200B was filtered at 10 kHz though the internal 4-pole lowpass Bessel filter and then again at 10 kHz through an external 8-pole lowpass Bessel filter. This signal was then digitized at 50 kHz with a Digidata 1322A (Molecular Devices) and recorded on a PC hard drive using the Clampex program from the pClamp 9 software suite (Molecular Devices). Membrane voltage, sampling rate, and the perfusion motor were all controlled via computer using the Clampex software interface.

2.5 – Analysis of Macroscopic Currents

Macroscopic currents of the peak amplitude resulting from GlyR activity in *Xenopus* oocytes were measured in the LabChart software program and recorded in an Excel spreadsheet (Microsoft, Redmond, WA). These values were grouped according to condition and the mean and standard error of the mean (SEM) were determined. Statistical analyses were performed using SigmaPlot 11.0 software (Systat Software, San Jose, CA). Differences between treatment groups were considered significant when $p <$

0.05 following appropriate statistical tests as indicated. Concentration-response data were fit using the following four-parameter Hill equation in SigmaPlot 11.0.

$$y = \min + (\max - \min)/(1+(x/EC_{50})^{-Hillslope}) \qquad \textit{Equation 2.1}$$

2.6 – Analysis of Single Channel Data

Single-channel data were analyzed using the single-channel analysis programs in QuB (Qin et al., 2000a, 2000b). The data were converted in the Clampfit program (Molecular Devices) to a QuB-compatible format for clean up and analysis. Preprocessing of the data involved removal of noise spikes and other errant signals, baseline correction, and the deletion of multiple openings (when present). The current amplitude and standard deviation used to represent the open and closed states was determined by selecting only clusters of activity by eye and removing any channel desensitization periods, plotting the amplitudes, and fitting two Gaussian functions. The mean amplitude corresponding to the open state was used to determine the conductance using Ohm's Law (Equation 1.1). The tracings were then idealized using the segmental-k-means algorithm (Qin et al., 2000a, 2000b). Data were initially idealized with a simple two-state C↔O model.

This initial idealization was then fit with multiple exponentials added sequentially to a star model (closed state as the center) using the maximum interval likelihood (MIL) method after imposing a dead time resolution of 60 μS. MIL fits the open and closed dwell time histograms with the following probability density function:

$$f(t) = \Sigma\, a_i \tau_i^{-1} e^{-t/\tau i} \qquad \textit{Equation 2.2}$$

The appropriate numbers of open and closed components in this star model were determined by increased log likelihood, a measure of the quality of fit. The data were then re-idealized using this model and used for dwell-time analyses. Dwell-time distributions were constructed and fit with a mixture of exponential components again using the MIL function, after the data had been binned using a log-time abscissa axis and a square-root count/total ordinate axis. The mean open and closed times were calculated as the weighted mean of the time constants according to the following function:

$$\text{Mean} = \Sigma\, a_i\tau \qquad \textit{Equation 2.3}$$

The probability of the channel being in the open state (P_o) during a cluster was determined as a ratio of the total open time and the total cluster duration for each patch.

$$P_o = \text{Mean}_{open}(n_{events}/2)/(\text{Mean}_{open}(n_{events}/2) + \text{Mean}_{closed}(n_{events}/2)) \qquad \textit{Equation 2.4}$$

This method of determining P_o was used by Burzomato et al. (2004) and provides an accurate estimate of P_o without assumption of any particular kinetic model. Mean values for all parameters were calculated individually per patch and then averaged for each condition. Statistical analyses were performed using SigmaPlot 11.0 software (Systat Software, San Jose, CA), using appropriate statistical tests as indicated.

2.7 – Chemicals and Preparation of Drug Solutions

All reagents used were purchased from Sigma-Aldrich (St. Louis, MO) with the exception of isoflurane which was obtained from Anaquest (New Providence, NJ). All solutions were made up in filtered diH_2O. All drug solutions were made up in MBS or external solution as appropriate. Loss of volatile compounds through tubing and evaporation from the bath was previously measured (Mihic et al., 1994; Yamakura et al.,

1999; Beckstead et al., 2000, 2002), and accounted for when making up these solutions. Thus all concentrations reported are the bath concentrations to which the GlyR were exposed. Volatile solutions were made by pipetting the appropriate volume of drug into MBS or external solution, covering with Parafilm and aluminum foil, and then mixing well.

All buffers were pH adjusted with HCl, NaOH, or CsCl as appropriate. The recipes for all buffers are as follows:

MBS — 88 mM NaCl, 1 mM KCl, 2.4 mM $NaHCO_3$, 10 mM HEPES, 0.82 mM $MgSO_4 \cdot 7H_2O$, 0.33 mM $Ca(NO_3)_2$, and 0.91 mM $CaCl_2$, pH 7.5

Isolation Media — 108 mM NaCl, 1 mM EDTA, 2 mM KCl, and 10 mM HEPES

Collagenase Solution — 83 mM NaCl, 2 mM $MgCl_2$, and 5 mM HEPES, 0.5 mg/ml Sigma Type 1A collagenase

Incubation Media — MBS + 2 mM sodium pyruvate, 0.5 mM theophylline, 10 U/ml penicillin, 10 mg/l streptomycin, and 50 mg/l gentamicin

Stripping Solution — 200 mM sodium methyl sulfate, 20 mM KCl, 10 mM HEPES, and 1 mM $MgCl_2 \cdot 6H_2O$, pH 7.4

External Solution — 100 mM NaCl, 2 mM KCl, 1 mM $MgCl_2 \cdot 6H_2O$, 10 mM HEPES, 2 mM $CaCl_2$, pH 7.4

Internal Solution — 102 mM CsCl, 10 mM HEPES, 10 mM EGTA, 1 mM $CaCl_2$, 2 mM $MgCl_2 \cdot 6H_2O$, pH 7.2

3.0 | POSITIVE ALLOSTERIC MODULATORS DIFFERENTIALLY AFFECT FULL VERSUS PARTIAL AGONIST ACTIVATION OF THE GLYCINE RECEPTOR[1]

3.1 – Introduction

The glycine receptor (GlyR) is responsible for the majority of neuronal inhibition in the brainstem and spinal cord but is also found in a variety of higher brain regions, such as the basal ganglia, cerebellum, hippocampus, and the prefrontal cortex (Lynch, 2004; Baer et al., 2009; Lu and Ye, 2011). It is a member of the Cys-loop family of ligand gated ion channels composed of five subunits that co-assemble around a central ion-conducting pore. Many compounds are known modulators of the GlyR, including alcohols, volatile anesthetics, zinc, and inhaled drugs of abuse (Lynch, 2004), and the GlyR has been implicated in their effects in vivo (Downie et al., 1996; Beckstead et al., 2000; Yamashita et al., 2001; Cheng and Kendig, 2002; Molander et al., 2005, 2007). Ethanol (EtOH) is the second most widely abused drug behind tobacco, and its use leads to depression of nervous system functioning. Volatile anesthetics are characterized by their propensities to readily vaporize at room temperature and, like ethanol, to cause central nervous system depression. In the clinical setting, they produce a myriad of

---

[1]Portions of this chapter have previously been published in *The Journal of Pharmacology and Experimental Therapeutics.* Kirson D, Todorovic J, Mihic SJ (2012) Positive allosteric modulators differentially affect full versus partial agonist activation of the glycine receptor. J Pharmacol Exp Ther 342:61–70. Reprinted with permission of the American Society for Pharmacology and Experimental Therapeutics.

effects, including analgesia, amnesia, immobility, hypnosis, and sedation. Inhalants are a heterogeneous class of industrial solvents that are often abused by adolescents because they quickly produce a rapidly reversible high (Evans and Balster, 1991).

Ethanol, anesthetics, and inhalants enhance GlyR function in a concentration-dependent manner. They act by left-shifting the glycine concentration-response curve, thus decreasing the EC_{50} of glycine (Mascia et al., 1996a; Mihic, 1999; Beckstead et al., 2000; Welsh et al., 2010). Thus, these compounds enhance currents elicited by low concentrations of glycine but have minimal effects at saturating concentrations of glycine (Mascia et al., 1996a; Beckstead et al., 2000; Welsh et al., 2010). These modulators are thought to bind in a water-filled pocket near the second transmembrane domain of each subunit of the GlyR (Mihic et al., 1997; Yamakura et al., 1999; Beckstead et al., 2001; Roberts et al., 2006).

At a saturating concentration, taurine acts as a partial agonist with ~50% efficacy in activating the GlyR compared with glycine. This refers to the proportion of time the receptor spends in the open state (P_o) while agonist is bound. At saturating concentrations, glycine and taurine produce P_o values of 0.96 and 0.54, respectively (Lape et al., 2008). Ethanol, anesthetics, and inhalants have no effects at saturating concentrations of glycine, and one reason for this may be attributed to the GlyR already spending ~95% of its time in the open state. Such a ceiling effect would not be expected to occur with saturating concentrations of taurine. Another possibility is that these allosteric modulators do not affect P_o, as suggested by a recent single channel study conducted by Welsh et al. (2009) and, in which case, no enhancement of GlyR function should be observed in the presence of a maximally effective concentration of taurine. In light of recently obtained evidence of a role for taurine as a GlyR activator in vivo

(Dahchour et al., 1996; Mori et al., 2002; Ericson et al., 2006, 2011; Rodríguez-Navarro et al., 2009), we tested ethanol, anesthetics, and inhalants for their enhancing effects on taurine-activated GlyR. In addition, if enhancement were to be seen at saturating taurine concentrations, it would suggest differences in the mechanisms of allosteric modulation of receptors activated by full versus partial agonists.

3.2 – Materials and Methods

Isolation, injection, and two-electrode voltage-clamp of *Xenopus* oocytes were described in Chapter 2. Specific methods pertaining to the experiments in this chapter are outlined below.

All chemicals were purchased from Sigma-Aldrich (St. Louis, MO). *Xenopus laevis* were obtained from Nasco (Fort Atkinson, WI) and housed at 19°C on a 12-h light/dark cycle. During surgery performed in accordance with the Association for Assessment and Accreditation of Laboratory Animal Care regulations, portions of ovaries were removed and placed in isolation media containing 108 mM NaCl, 1 mM EDTA, 2 mM KCl, and 10 mM HEPES. Forceps were used to manually remove the thecal and epithelial layers from stage V and VI oocytes. The oocyte follicular layer was removed using a 10 min incubation in 0.5 mg/ml type 1A collagenase (Sigma-Aldrich) in buffer containing 83 mM NaCl, 2 mM $MgCl_2$, and 5 mM HEPES. Animal poles of oocytes were injected with 30 nl of the glycine α1-receptor subunit cDNA (1.5 ng/30 nl) in a modified pBK-cytomegalovirus vector (Mihic et al., 1997) by the "blind" method of Colman (1984), using a micropipette (10–15 μm tip size) attached to an electronically activated microdispenser. For α1β experiments, a 1:30 ratio of α to β cDNAs was

injected to ensure incorporation of the β subunit. Oocytes were stored in the dark at 19°C in 96-well plates containing modified Barth's saline (MBS) [88 mM NaCl, 1 mM KCl, 2.4 mM $NaHCO_3$, 10 mM HEPES, 0.82 mM $MgSO_4 \cdot 7H_2O$, 0.33 mM $Ca(NO_3)_2$, 0.91 mM $CaCl_2$ at pH 7.5] supplemented with 2 mM sodium pyruvate, 0.5 mM theophylline, 10 U/ml penicillin, 10 mg/l streptomycin, and 50 mg/l gentamicin and sterilized by passage through a 0.22 μm filter. Oocytes expressed the wild-type and S267F (Ye et al., 1998) GlyR within 24 h, and all electrophysiological measurements were made within 5 days of cDNA injection. Replacement of a serine residue with phenylalanine at residue 267 within the second transmembrane segment of the α1 subunit yields the S267F mutant.

Before electrophysiological recording oocytes were placed in a 100-μl bath with the animal poles facing upwards and impaled with two high-resistance (0.5–10 MΩ) glass electrodes filled with 3 M KCl. Cells were voltage clamped at –70 mV using an OC-725C oocyte clamp (Warner Instruments, Hamden, CT) and perfused with MBS at a rate of 2 ml/min using a Masterflex USA peristaltic pump (Cole Parmer Instrument Co., Vernon Hills, IL) through 18-gauge polyethylene tubing. All drug solutions were prepared in MBS. When saturating concentrations of agonists were applied, applications lasted for 15 s for the short-application experiments and for 13 min for the long-application experiments. Sub-maximally effective concentrations of agonist (glycine or taurine) were applied for 60 s. Modulators were either pre-applied to oocytes for 30 s before being co-applied with agonist for an additional 15 s for short-application experiments or co-applied with agonist for 60 s for long-application experiments. All drug applications were followed by 6 to 10 min washout periods to allow for complete receptor resensitization. Loss of volatile compounds through tubing and evaporation

from bath was previously measured (Mihic et al., 1994; Yamakura et al., 1999; Beckstead et al., 2000, 2002). All concentrations reported are the bath concentrations to which the oocyte was exposed. Currents were acquired using either a Powerlab 4/30 digitizer with LabChart version 7 software (ADInstruments, Bella Vista, NSW, Australia) or a strip-chart recorder (Cole Parmer Instrument Co.) with a < 0.5-s full-scale pen movement response time. Peak currents were measured and used in data analysis. Currents observed in the presence of agonist plus modulators were compared with currents generated by agonist alone.

Experimental values are listed as the mean ± SEM. Significant differences between experimental conditions were determined using paired or unpaired t-tests, the Wilcoxon signed rank test or the Mann-Whitney rank sum test as indicated. Equation 2.1 was used to fit agonist and agonist + isoflurane concentration-response curves to determine the half-maximally effective concentrations (EC_{50}). SigmaPlot version 11.0 (Systat Software, San Jose, CA) was used for statistical testing.

3.3 – Results

3.3.1 – Preincubation of allosteric modulators is necessary to unmask true effects of these compounds on GlyR functioning

The enhancing actions of ethanol, volatile anesthetics, and inhaled drugs of abuse were compared for their effects on currents generated by glycine versus taurine on wild-type α1-homomeric GlyRs. We first tested 1.1 mM isoflurane for its abilities to enhance GlyR function in receptors activated by glycine or taurine (**Fig. 3.1**). As expected,

isoflurane left-shifted the glycine concentration-response curve without having any effect at maximally effective glycine concentrations. Isoflurane also left-shifted the taurine concentration-response curve but also markedly increased the effects of maximally effective taurine concentrations.

We previously examined the effects of ethanol on GlyR using short and long applications of saturating concentrations of glycine or taurine (Welsh et al., 2010) and found minor enhancing effects during long applications of the latter. In these long-application experiments, ethanol was applied for 60 s and thus had sufficient time to equilibrate within its binding pocket. In experiments involving brief applications of saturating concentrations of agonists, the peak current is reached in less than 100 ms in our hands, concurrent with rapid desensitization of the GlyR. If ethanol is co-applied with agonist, the ethanol may not have sufficient time to reach equilibrium within the binding pocket. Therefore, we first tested whether preincubation of modulator was necessary for this equilibrium to occur before desensitization predominated, allowing us to see the full effects of the modulator on the activated GlyR. Because isoflurane was previously shown to have enhancing effects on saturating concentrations of taurine (Downie et al., 1996), we chose to use the structurally similar anesthetic enflurane for these experiments. **Fig 3.2A**, left panel, shows sample tracings of the effects of 100 mM taurine co-applied with 1.2 mM enflurane for 15 s, with 15 s applications of 100 mM taurine alone (before and after application). The tracing in the right panel shows the effects of a 30-s preincubation of 1.2 mM enflurane immediately before co-application with taurine. Co-application of 100 mM taurine plus 1.2 mM enflurane resulted in a 99.4 ± 14% increase in current above that produced by 100 mM taurine alone (**Fig. 3.2B**). However, preincubation of 1.2 mM enflurane before co-application with 100 mM taurine

resulted in a current 209 ± 24.4% above that produced by taurine alone, suggesting that preincubation with anesthetics is required for enflurane to come to equilibrium with receptors before agonist is co-applied. There was a statistically significant effect of preincubation [$t(4) = 9.3, p < 0.001$].

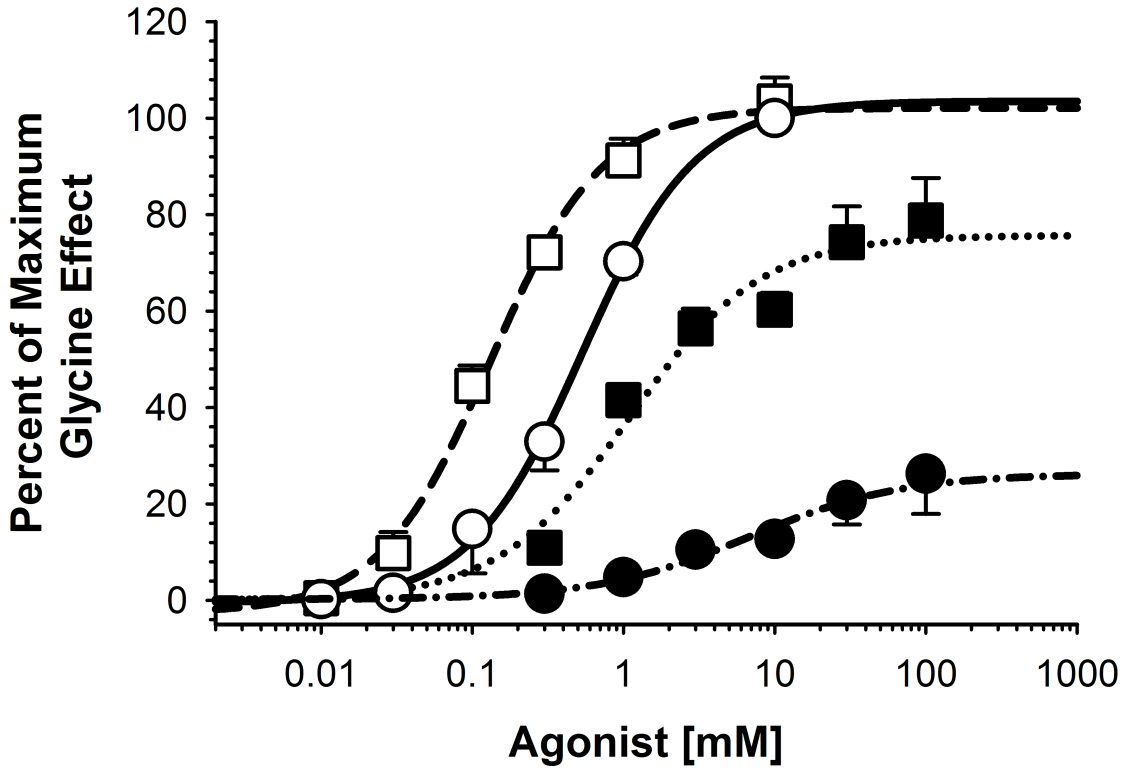

Figure 3.1 – Isoflurane decreases agonist EC_{50} and increases taurine mediated peak currents

Isoflurane shifts α1-homomeric GlyR glycine and taurine concentration-response curves to the left and increases the maximal response to the partial agonist. Open symbols represent glycine-mediated responses, and filled symbols show taurine-mediated responses. Circles represent agonist applied alone, with squares showing agonist + 1.1 mM isoflurane. Each line is a logistic fit to the respective set of data. Glycine activation of the GlyR produced an EC_{50} of 0.54 mM with a Hill coefficient (n_H) of 1.2. The addition of 1.1 mM isoflurane decreased the EC_{50} to 0.13 mM and an n_H of 1.2. Taurine alone had an EC_{50} of 6.9 mM, with an n_H of 0.9, decreasing to an EC_{50} of 1.1 mM and an n_H of 1.0 in the presence of isoflurane. Data are shown as mean ± SEM of 4 oocytes.

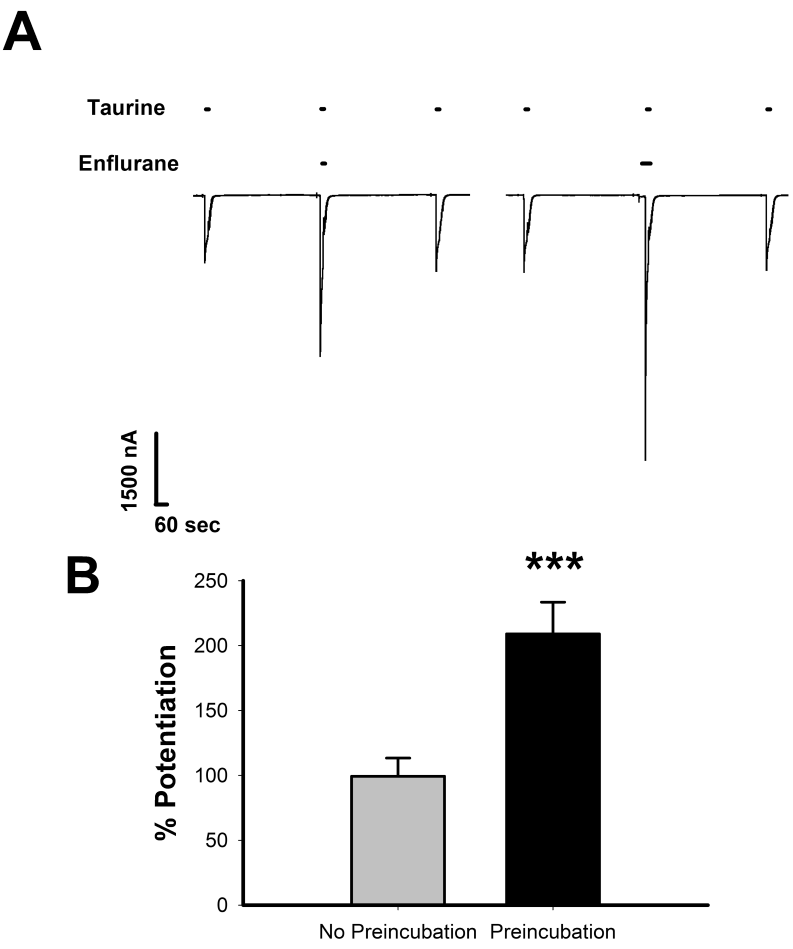

Figure 3.2 – Preincubation enhances the potentiating effects of enflurane on taurine-activated GlyRs

A) sample tracings showing enflurane potentiation of taurine responses with and without preincubation. The left tracing shows co-application of 100 mM taurine and 1.2 mM enflurane, with applications of taurine alone (before and after). The right tracing shows the effect of preincubation with 1.2 mM enflurane, immediately followed by co-application of 100 mM taurine and 1.2 mM enflurane. Again bracketed by taurine alone. Horizontal bars over tracings indicate the time of exposure to taurine or enflurane. B) summary of the effects of 100 mM taurine and 1.2 mM enflurane with and without preincubation. The y-axis represents the percentage increase in current observed in the presence of enflurane compared with that produced by taurine alone. Data are shown as mean ± SEM of 5 oocytes. ***, $p < 0.001$.

3.3.2 – Ethanol potentiates GlyR currents activated by maximally effective concentrations of taurine but not glycine

We have previously demonstrated that ethanol acts as an allosteric modulator by left-shifting glycine and taurine concentration-response curves without an effect when maximally effective concentrations of either glycine or taurine were tested (Welsh et al., 2010). Here, we further investigated the effects of ethanol on maximally effective concentrations of glycine and taurine using two different experimental designs. Since we showed that preincubation was necessary to reveal the full enhancing effect of enflurane (**Fig. 3.2**), we also tested ethanol using the same preincubation experimental design (**Fig. 3.3A**). Preincubation of 200 mM ethanol for 30 s was immediately followed by co-application with a maximally effective concentration of agonist (10 mM glycine or 100 mM taurine) for 15 s. Each co-application was preceded and followed by 15 s applications of glycine or taurine as appropriate (**Fig. 3.3A**). Ethanol (200 mM) slightly inhibited the glycine response, decreasing the peak current by 15.2 ± 5% (**Fig. 3.3B**). In contrast, ethanol moderately increased the peak taurine current by 42.2 ± 7.6%. The taurine + ethanol response was significantly different from the glycine + ethanol response [$t(5) = 8.81, p < 0.001$].

We next examined the effects of ethanol using a saturating concentration of agonist applied for 10 min to allow for a pseudo-equilibrium between the open and desensitized states of channels to become established before the co-application of ethanol (**Fig. 3.3C**). After a 10 min application of either 10 mM glycine (**Fig. 3.3C**, top) or 100 mM taurine (**Fig. 3.3C**, bottom), 200 mM ethanol was co-applied for 1 min followed by agonist alone for 2 min. The effects of ethanol were similar to those seen in the preincubation experiment but to a lesser degree. Ethanol had a negligible effect on the

saturating 10 mM glycine response (0.3 ± 12.3%) while potentiating the saturating 100 mM taurine response by 23.6 ± 7.6% (**Fig. 3.3D**), although these responses were not significantly different [Mann-Whitney U-Test $U = 4, n_1 = n_2 = 5, p > 0.05$].

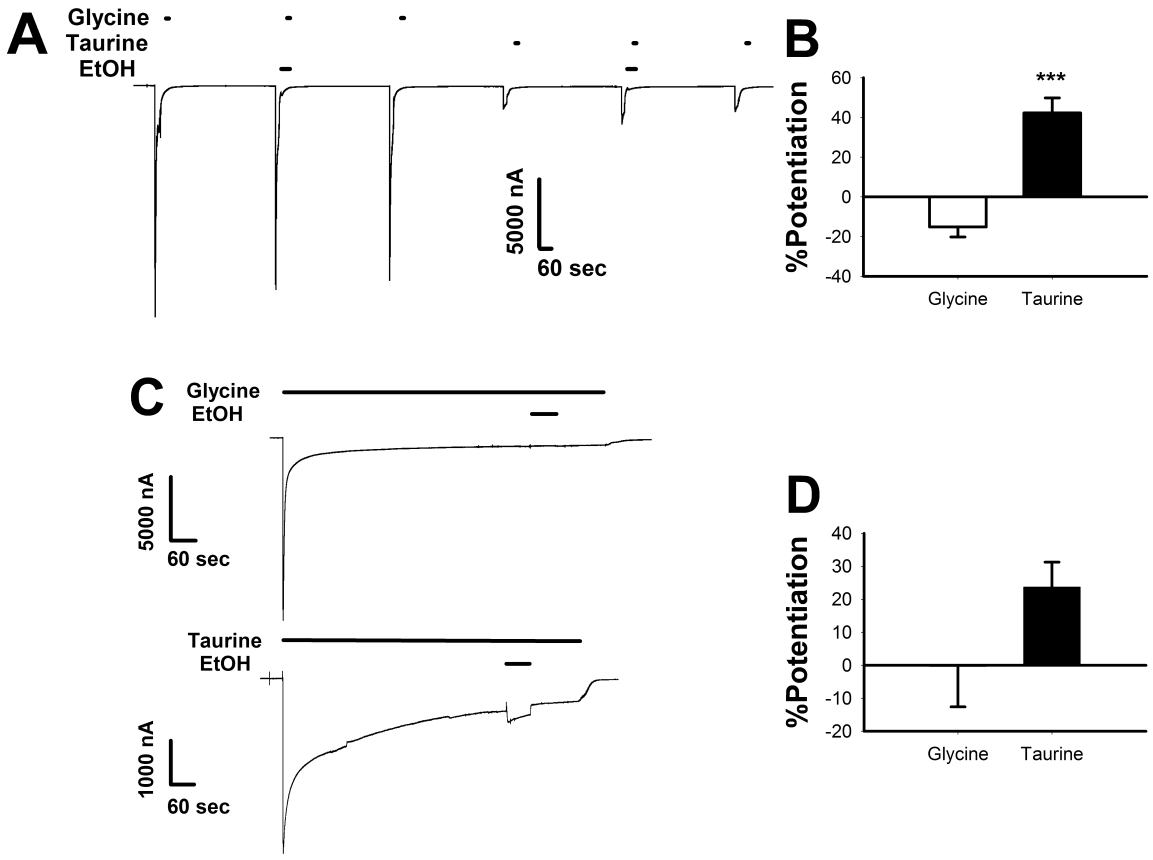

Figure 3.3 – Ethanol affects currents elicited by maximally effective concentrations of taurine but not glycine

A) tracing showing the effects of maximally effective concentrations of glycine and taurine applied with or without 200 mM EtOH. 30 s preincubations with 200 mM EtOH were followed immediately by 15 s applications of either 10 mM glycine or 100 mM taurine + EtOH. Each of these applications was preceded and followed by applications of agonist tested. Horizontal bars over tracings indicate time of exposure to glycine, taurine, or EtOH. B) summary of the effects of EtOH as seen in A. The *y*-axis is the percentage change in current with EtOH compared to that produced by agonist alone. Data are shown as mean ± SEM of 6 oocytes. ***, $p < 0.001$. C) sample tracings showing the effects of 200 mM EtOH co-applied with saturating concentrations of glycine or taurine, after the neurotransmitters had been applied for 10 min. Top: 10 mM glycine was applied for 10 min followed immediately by co-application of 10 mM glycine plus 200 mM EtOH for 1 min. Bottom: Same as top tracing but 100 mM taurine instead of glycine. D) summary of the effects of EtOH as seen in C. The *y*-axis is the percentage change in current observed with EtOH compared to the glycine or taurine current immediately preceding EtOH co-application. Data are shown as mean ± SEM of 4–5 oocytes.

3.3.3 – VOLATILE ANESTHETICS POTENTIATE GLYR CURRENTS ACTIVATED BY MAXIMALLY EFFECTIVE CONCENTRATIONS OF TAURINE BUT NOT GLYCINE

We next examined the effects of volatile anesthetics using the same experimental protocols used for ethanol. The concentrations of volatile anesthetics tested were 1.5 mM chloroform, 0.55 mM isoflurane, 0.5 mM halothane, 1.2 mM enflurane, and 1.76 mM desflurane. In **Fig. 3.4A**, desflurane was preapplied for 30 s before co-application with a saturating concentration of either glycine or taurine. None of the anesthetics tested in this manner showed any effect on 10 mM glycine responses, but all markedly enhanced currents elicited by 100 mM taurine (**Fig. 3.4B**). Each anesthetic showed significantly greater potentiation of maximal taurine responses compared with maximal glycine responses. Chloroform [Wilcoxon Signed-Rank Test W = 28, Z = 2.4, $p < 0.05$], isoflurane [$t(6) = 8.32$, $p < 0.001$], halothane [$t(6) = 3.11$, $p < 0.05$], enflurane [$t(6) = 6.31$, $p < 0.001$], and desflurane [$t(5) = 3.61$, $p < 0.05$] all produced significantly greater enhancement of maximal taurine responses.

The results for experiments involving long exposures to saturating concentrations of agonists were similar to the preincubation experiments, with marked potentiation of 100 mM taurine responses and minimal effects on 10 mM glycine responses (**Fig. 3.4C,D**). Again, for each anesthetic, potentiation of maximal taurine responses was significantly increased compared with their effects on maximal glycine responses. Chloroform [Mann-Whitney U-Test U = 0, n1 = n2 = 4, $p < 0.05$], isoflurane [$t(6) = 3.38$, $p < 0.05$], halothane [Mann-Whitney U-Test U = 6, n1 = 6, n2 = 8, $p < 0.05$], enflurane [$t(7) = 5.51$, $p < 0.001$], and desflurane [$t(8) = 3.7$, $p < 0.01$] displayed significantly greater enhancement of maximal taurine responses.

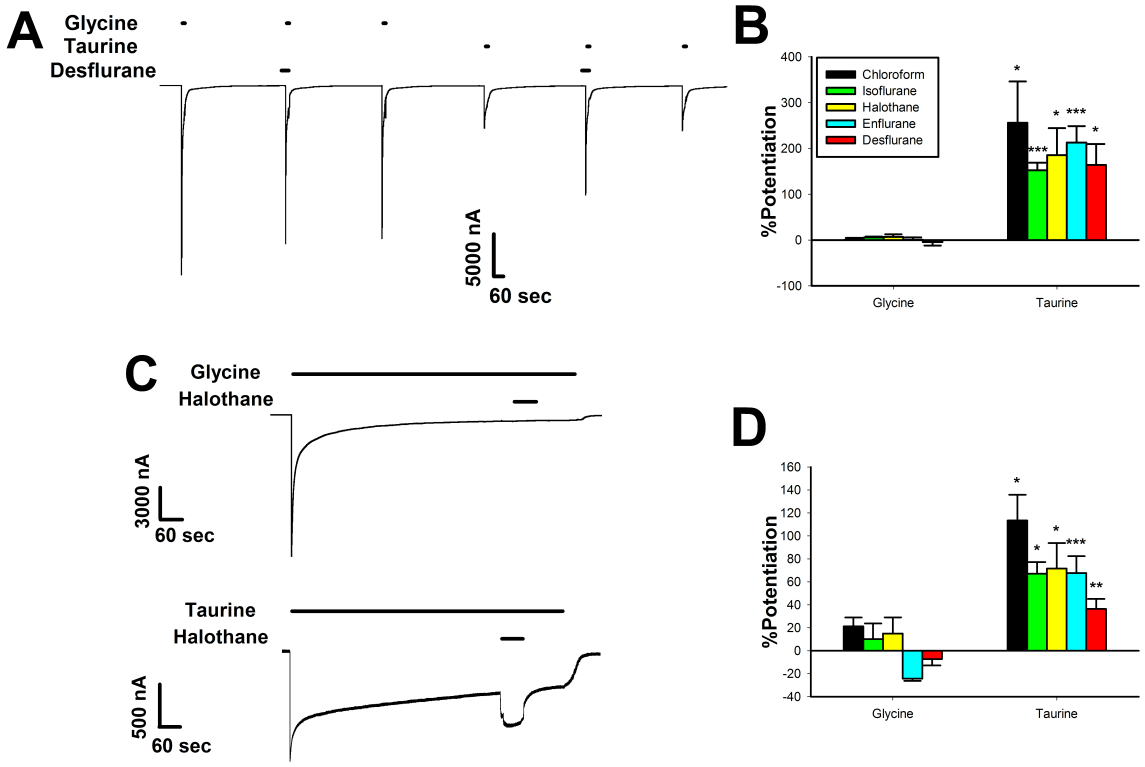

Figure 3.4 – Anesthetics affect currents elicited by maximally effective concentrations of taurine but not glycine

A) sample tracing of maximally-effective concentrations of glycine and taurine applied ± 1.76 mM desflurane. The tracing shows 30 s preincubations with desflurane followed immediately by 15 s applications of 10 mM glycine or 100 mM taurine + desflurane. Each application was preceded and followed by applications of agonist alone. Horizontal bars over tracings show time of exposure to glycine, taurine, or desflurane. B) summary of the effects of anesthetics on maximally effective concentrations of glycine or taurine as in A. The y-axis is the percentage change in current with anesthetic compared to agonist alone. Data are shown as mean ± SEM of 6–7 oocytes per anesthetic. C) sample tracings showing the effects of 0.5 mM halothane co-applied with saturating concentrations of glycine or taurine after the agonist had been applied for 10 min. Top: 0.5 mM halothane co-applied with 10 mM glycine after a 10 min exposure to glycine. Bottom: Same as top with 100 mM taurine instead of glycine. D) summary of the effects of anesthetics during long applications with saturating agonist. The y-axis is the percentage change in current with anesthetic compared to agonist current measured immediately before anesthetic co-application. Data are shown as mean ± SEM of 4–8 oocytes per anesthetic. *, $p < 0.05$, **, $p < 0.01$, ***, $p < 0.001$ for glycine vs. taurine.

3.3.4 – INHALANTS POTENTIATE GLYR CURRENTS ACTIVATED BY MAXIMALLY EFFECTIVE CONCENTRATIONS OF TAURINE BUT NOT GLYCINE

The inhaled drugs of abuse, toluene, 1,1,1-trichloroethane (TCE), and trichloroethylene (TCY) were also assayed using the same experimental protocols as before. The bath concentrations of these inhalants were 0.42 mM toluene, 0.56 mM TCE, and 0.39 mM TCY. **Fig. 3.5A,C**, shows tracings of these experiments by use of a sample inhalant in each case. Each of the inhalants slightly inhibited 10 mM glycine responses while potentiating 100 mM taurine responses in preincubation experiments (**Fig. 3.5B**). All three inhalants displayed significantly greater enhancement of maximal taurine responses: toluene [$t(4) = 4.31$, $p < 0.05$], TCE [$t(5) = 3.58$, $p < 0.05$], and TCY [$t(6) = 6.65$, $p < 0.001$].

The results for the long exposures to saturating concentrations of agonists were similar to the preincubation experiments, with marked potentiation of 100 mM taurine responses observed but small effects on 10 mM glycine responses, with the exception of TCY (**Fig. 3.5D**). TCY produced a potentiation of maximal glycine and maximal taurine responses that were not significantly different [$t(8) = 0.36$, $p > 0.7$], although the TCY + glycine responses were highly variable (**Fig. 3.5D**). For toluene [$t(10) = 3.59$, $p < 0.01$] and TCE [$t(9) = 3.38$, $p < 0.01$], potentiation of maximal taurine responses was significantly greater than inhalant effects on maximal glycine responses.

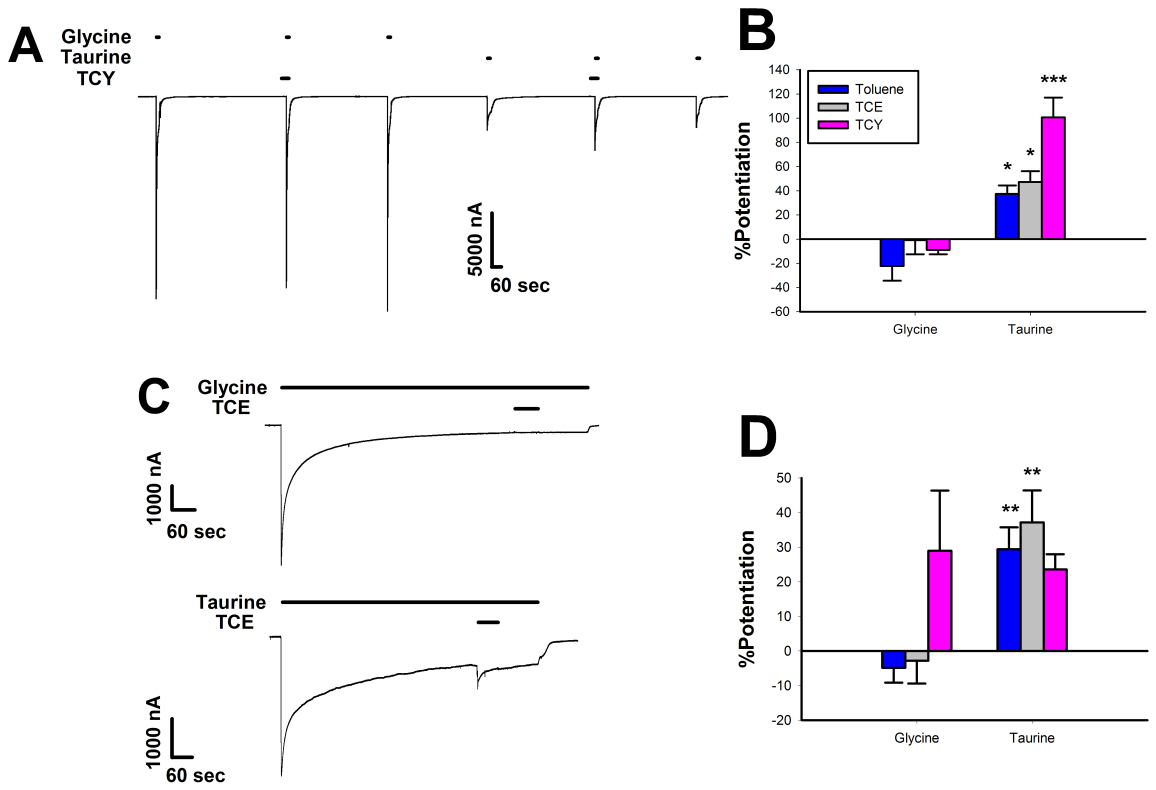

Figure 3.5 – Inhalants affect currents elicited by maximally effective concentrations of taurine but not glycine

A) tracing demonstrating the effects of maximally effective concentrations of glycine and taurine applied ± 0.39 mM TCY. The tracing shows 30 s preincubations with TCY followed immediately by 15 s applications of 10 mM glycine or 100 mM taurine + TCY. Each application was preceded and followed by applications of agonist alone. Horizontal bars over tracings indicate time of exposure to glycine, taurine, or TCY. B) summary of the effects of inhalants on maximally effective agonist as in A. The y-axis is the percentage change in current with inhalant compared to glycine or taurine applied alone. Data are shown as mean ± SEM of 5–7 oocytes for each inhalant. C) sample tracings showing the effects of 0.56 mM TCE co-applied with saturating concentrations of glycine or taurine, after the agonist had been applied for 10 min. Top: 0.56 mM TCE was co-applied with 10 mM glycine after 10 min exposure to saturating glycine. Bottom: the same for a sustained application of 100 mM taurine instead of glycine. D) summary graph of the effects of inhalants during long applications of saturating agonist. The y-axis is the percentage change in current with inhalant compared to the current seen immediately before inhalant co-application. Data are shown as mean ± SEM of 4–8 oocytes. *, $p < 0.05$, **, $p < 0.01$, ***, $p < 0.001$ for glycine vs. taurine.

3.3.5 – Allosteric modulators potentiate heteromeric GlyR currents activated by maximally effective concentrations of taurine but not glycine

We performed the same experimental protocol of modulator preincubation followed by short application of agonist on α1β heteromeric GlyR to confirm that the modulator effects seen on the homomeric α1 GlyR were also seen in the presence of the β subunit. For these experiments, we chose a representative compound from each of the categories of modulators tested previously. Ethanol, desflurane, and TCY were used at the same bath concentrations as in the previous experiments. **Fig. 3.6A** shows tracings of the effects of 1.76 mM desflurane on maximally effective concentrations of both glycine- and taurine-mediated currents. **Fig. 3.6B** shows a summary of the effects of each compound tested, with all three compounds showing negligible effects on maximal glycine responses and large potentiating effects on maximal taurine responses. Potentiation of maximal taurine responses was significantly greater than for glycine for all three modulators: ethanol [Wilcoxon Signed-Rank Test $W = 45$, $Z = 2.7$, $p < 0.01$]; desflurane [$t(8) = 17.15$, $p < 0.001$]; and TCY [$t(7) = 6.31$, $p < 0.001$)].

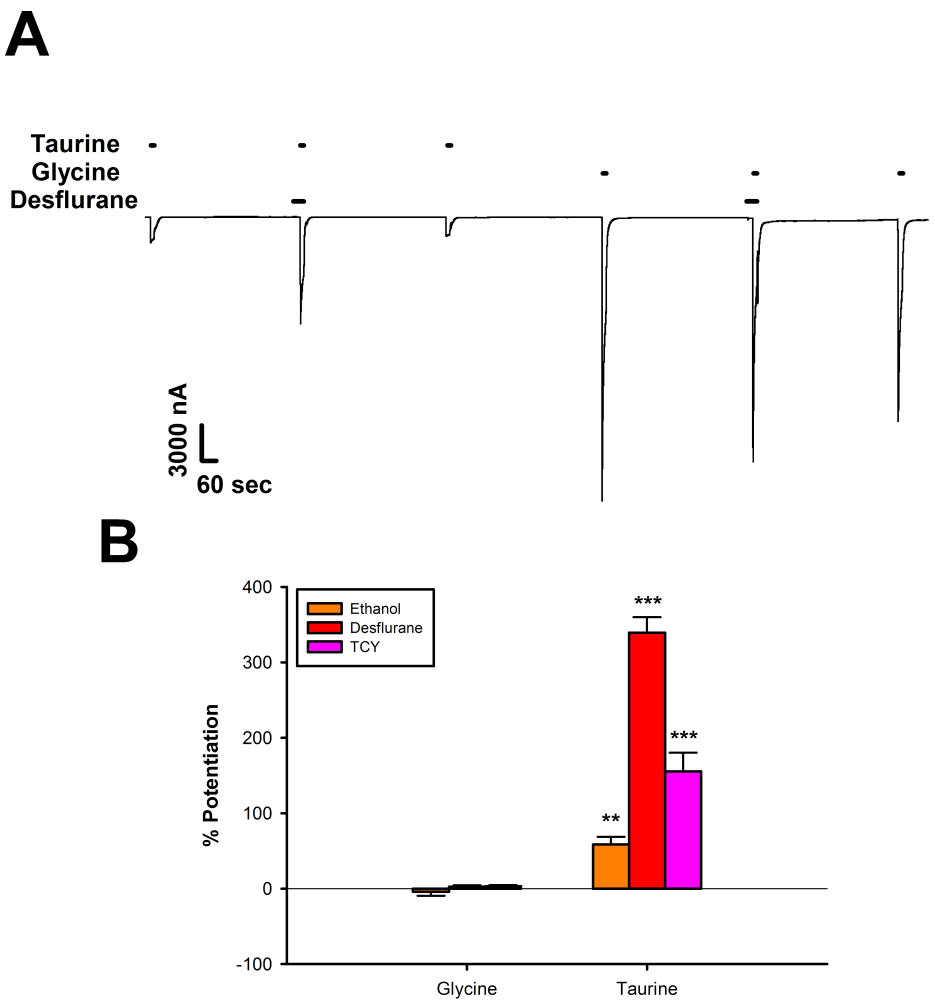

Figure 3.6 – Positive allosteric modulators affect α1β heteromeric GlyR in a similar manner to homomeric α1 GlyR

A) sample tracing demonstrating the effects of maximally effective concentrations of glycine and taurine applied ± 1.76 mM desflurane. The tracing shows 30 s preincubations with desflurane followed immediately by 15 s applications of either 10 mM glycine or 100 mM taurine + desflurane. Each of these applications was preceded and followed by applications agonist alone. Horizontal bars over tracings indicate time of exposure to glycine, taurine, or desflurane. B) summary of the effects of 200 mM ethanol, 1.76 mM desflurane, or 0.39 mM TCY on applications of maximally effective concentrations of agonist. The y-axis is the percentage change in current with modulator compared to agonist alone. Data are shown as mean ± SEM of 8–9 oocytes for each modulator tested. **, $p < 0.01$, ***, $p < 0.001$ for glycine vs. taurine.

3.3.6 – ANESTHETICS AFFECT DESENSITIZATION RATES OF TAURINE-ACTIVATED GLYR BUT NOT GLYCINE-ACTIVATED GLYR

We compared tracings from the brief application experiments to contrast the effects of modulators on desensitization rates after activation by glycine or taurine. **Fig. 3.7** shows sample tracings for four of the modulators tested: ethanol, isoflurane, desflurane, and TCY. None of the modulators affected desensitization rates after receptor activation by glycine, which was expected because none of the modulators had large effects on glycine peak currents in these brief application experiments. However, both isoflurane and desflurane markedly increased desensitization rates when GlyR was activated by taurine. A summary of the effects of modulators on glycine- and taurine-mediated desensitization is provided in **Table 3.1**. We hypothesized that there might be a direct correlation between the degree of potentiation of peak responses produced by allosteric modulators and their effects on desensitization. **Fig. 3.8** shows that, as the modulator-induced percentage enhancement of peak current responses increases, so does the rate of desensitization produced by the modulator.

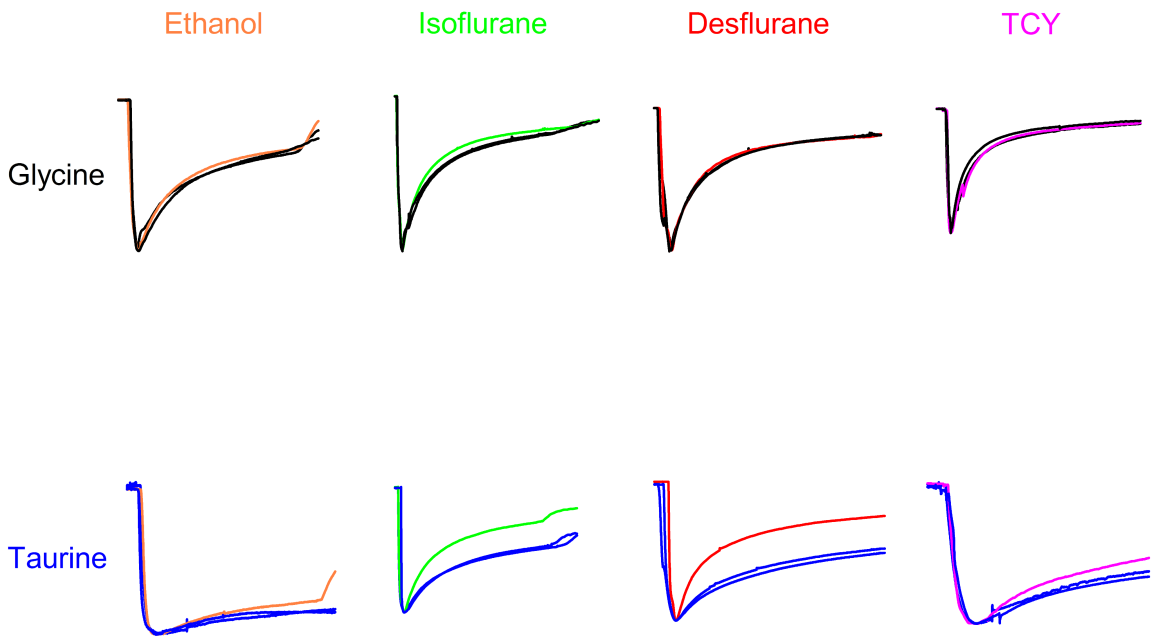

Figure 3.7 – Anesthetics increase desensitization rates of taurine- but not glycine-activated GlyR

Each set of the sample tracings shown depicts 15 s applications of agonist + modulator as well as the agonist-alone tracings that preceded and followed the agonist + modulator application. Oocytes were preincubated with modulators for 30 s before the incubations with agonists. For each set of tracings all responses were normalized to the peak response produced by the first application of glycine or taurine. Each column contains one of four different allosteric modulators: ethanol, isoflurane, desflurane, or TCY. Each row shows one of the agonists tested, glycine (black) or taurine (blue). Tracings are color coded by compound, and each column shows tracings from a single oocyte.

Modulator	Glycine	Taurine
Ethanol	2.3 ± 4.5%	16.3 ± 10.5%
Chloroform*	-4.5 ± 2.5%	120.0 ± 58.4%
Isoflurane*	3.6 ± 1.9%	68.6 ± 14.0%
Halothane	3.9 ± 6.2%	104.5 ± 52.5%
Enflurane*	20.5 ± 4.7%	128.3 ± 39.1%
Desflurane*	2.9 ± 5.8%	136.2 ± 83.2%
Toluene	2.3 ± 9.4%	-4.9 ± 10.1%
TCE	6.7 ± 11.4%	27.6 ± 19.4%
TCY*	-4.9 ± 6.4%	56.4 ± 23.1%

Table 3.1 – The effects of positive allosteric modulators on glycine- and taurine-activated GlyR desensitization rates

Currents were measured at the peak responses and 5 s later. The percentage drop in current observed within 5 s in the presence of the modulator was divided by the percentage drop seen in the absence of the modulator, multiplied by 100, and then had 100 subtracted to indicate the percentage change in desensitization produced by the modulator. Data are shown as the mean ± SEM of 5–7 oocytes per modulator per agonist. *, $p < 0.05$ for glycine vs. taurine.

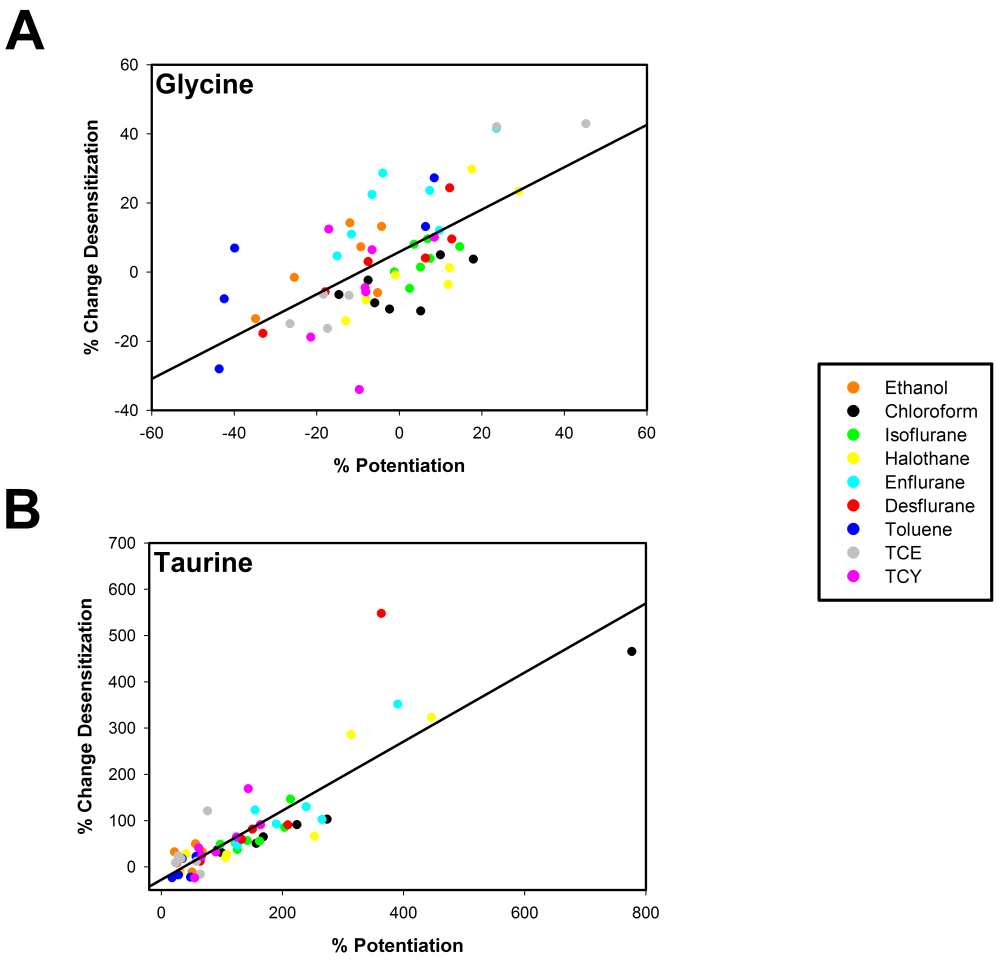

Figure 3.8 – Correlation between the degree of positive allosteric modulator enhancement of peak current levels and desensitization rates

A) correlation between positive allosteric modulator effects on peak current percentage potentiation and desensitization rate for glycine-activated GlyR. Each data point is from a single oocyte and a single modulator according to the color key shown. The x-axis is the percentage change in peak current produced by modulator, and the y-axis is the percentage change in desensitization rate seen with each modulator. The solid line is a linear regression through the data set with r = 0.67. Each modulator was tested on 5–7 oocytes. B) correlation between positive allosteric modulator effects on percentage potentiation and desensitization rate for taurine-activated GlyR. The axes and color coding are the same as in A. The solid line is a linear regression through the data set with r = 0.87. Each modulator was tested on 5–7 oocytes.

3.3.7 – ALLOSTERIC MODULATOR POTENTIATION OF TAURINE-ACTIVATED GLYR RESPONSES ARE EQUALLY CONCENTRATION DEPENDENT AT LOW AND HIGH TAURINE CONCENTRATIONS

We next investigated the differences in the magnitudes of effects of the volatile anesthetics and the inhaled drugs of abuse. Although all drugs in both categories showed enhancing effects when applied with maximal concentrations of taurine, the degree of potentiation was much larger for the volatile anesthetics than that for the inhaled drugs of abuse. We further examined this difference by testing whether the degree of efficacy inherent in each compound was simply concentration dependent by comparing sample modulators from each group. From the anesthetics, we chose isoflurane because of its high potentiation of maximal taurine responses coupled with a small error in the preincubation experiments, and from the inhalant class, we chose toluene because of its relatively low enhancement of maximal taurine effects in the preincubation experiments. For this experiment, the concentration of taurine producing a 5 to 10% effect ($EC_{5–10}$) of a maximally-effective taurine response was first determined in each oocyte. The concentrations of isoflurane and toluene producing ~200% potentiation of the $EC_{5–10}$ response were determined next (**Fig. 3.9A**). These concentrations of isoflurane and toluene were then tested using the maximally-effective concentration of taurine (EC_{100}), and the effects of isoflurane and toluene were compared (**Fig. 3.9B**). Concentrations of 0.42 mM toluene and 0.28 mM isoflurane produced ~200% potentiation of the $EC_{5–10}$ taurine response. When tested at EC100 taurine concentrations, isoflurane potentiated the taurine response by 107.7 ± 16.4%, and toluene potentiated the taurine response by 93.4 ± 11.5%; these responses were not significantly different from one another [$t(3) = 0.57$, $p > 0.6$].

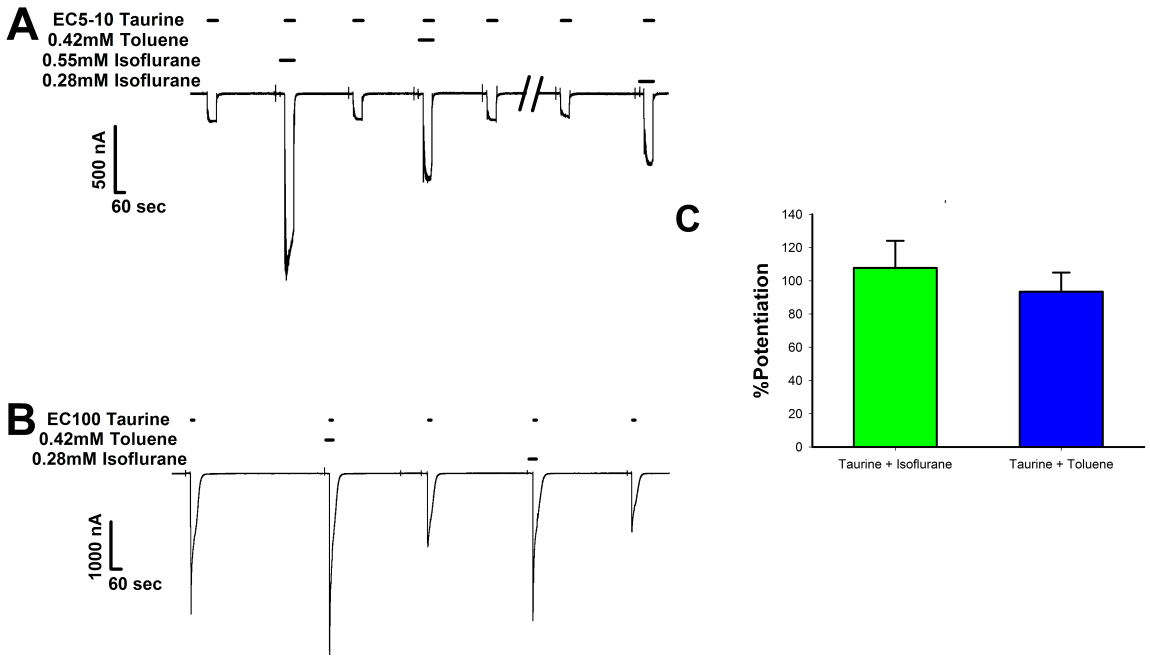

Figure 3.9 – Equi-effective concentrations of modulators at a low taurine concentration also have equal efficacy at a saturating taurine concentration

A) concentrations of toluene and isoflurane that yield an ~200% potentiation of $EC_{5–10}$ taurine were determined. Tracing shows the effect of $EC_{5–10}$ taurine ± several concentrations of isoflurane or toluene. Toluene (0.42 mM) potentiated $EC_{5–10}$ taurine ~200%, whereas 0.55 mM isoflurane potentiated to a higher degree, and 0.28 mM isoflurane produced ~200% potentiation of $EC_{5–10}$ taurine. Taurine applications preceded and followed each co-application with a modulator. Horizontal bars above tracings indicate the times of exposure to taurine, toluene, or isoflurane at the concentrations indicated. B) sample tracing demonstrating the enhancing effects of the toluene and isoflurane concentrations found in A, but co-applied with a saturating concentration (EC_{100}) of taurine. co-applications of taurine and modulator were preceded and followed by applications of taurine. C) summary of the effects seen in B. The y-axis is the percentage increase in current with modulator compared to taurine alone. Data are shown as mean ± SEM of 4 oocytes.

3.3.8 – MUTATIONS THAT AFFECT ALCOHOL BINDING HAVE SIMILAR EFFECTS ON THE GLYCINE- AND TAURINE-ACTIVATED GLYR

Lastly, we investigated whether mutation of a residue in the second transmembrane segment of the α1 subunit previously shown to alter alcohol modulation of glycine-activated GlyR would similarly affect receptors activated by taurine. **Fig. 3.10** shows that ethanol, isoflurane, and TCE had minimal effects on S267F homomeric α1 GlyR activated by sub-saturating concentrations ($EC_{5–10}$) of glycine or taurine.

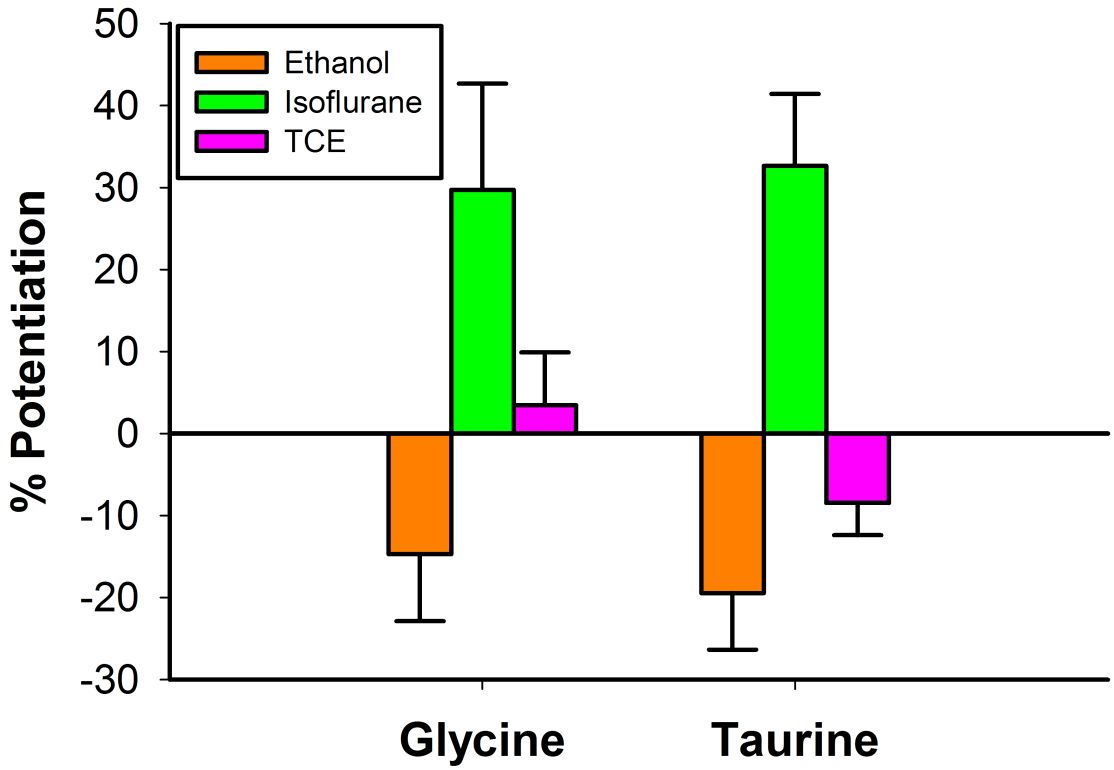

Figure 3.10 – The S267F mutation in the second transmembrane segment of the α1 subunit similarly affects modulator enhancement of glycine- and taurine-mediated GlyR function

The effects of 200 mM ethanol, 0.55 mM isoflurane, or 0.56 mM TCE were assayed with $EC_{5–10}$ concentrations of glycine or taurine. The y-axis represents the percentage change in current observed in the presence of modulator compared with that produced by glycine or taurine applied alone. Data are shown as mean ± SEM of 4–5 oocytes for each modulator.

3.4 – Discussion

Glycine receptors, traditionally thought to be responsible for inhibitory neurotransmission only in the brainstem and spinal cord, are also found in higher brain regions (Lynch, 2004). As a result, they have come to be considered possible sites of action for ethanol, volatile anesthetics, and inhaled drugs of abuse (Mihic, 1999; Bowen et al., 2006; Franks, 2008; Lubman et al., 2008; Chau, 2010; Yevenes and Zeilhofer, 2011). After release, the postsynaptic GlyR is initially exposed to millimolar concentrations of glycine, which then rapidly decrease. Enhancement of GlyR function by allosteric modulators is not seen at millimolar glycine concentrations because these compounds left-shift glycine concentration response curves and exert their greatest effects at low glycine concentrations (Downie et al., 1996; Mascia et al., 1996a; Beckstead et al., 2000). Thus, allosteric modulators function to extend the durations of synaptic effects at the GlyR. The partial agonist taurine may be an endogenous ligand at GlyR expressed in the hippocampus (Shibanoki et al., 1993; Mori et al., 2002), nucleus accumbens (Dahchour et al., 1996; Ericson et al., 2006, 2011), and the ventral tegmental area (Wang et al., 2005) where glycine has also been shown to work. This suggests the possibility that ethanol, volatile anesthetics, and inhaled drugs of abuse exert some of their effects through the taurine-activated GlyR and that these responses may differ from those of receptors activated by glycine.

On the basis of the importance of modulator preincubation as shown in **Fig. 3.2**, we replicated the saturating agonist and ethanol experiments that we had performed previously (Welsh et al., 2010) but with modifications to the experimental design. We previously tested whether ethanol had any effects on applications of saturating agonist

concentrations on the GlyR, and as expected, 200 mM ethanol had no effects on saturating glycine responses or on responses elicited by brief applications of a maximally effective concentration of taurine (Figs. 2 and 3A in Welsh et al., 2010). However, during a long application of a saturating concentration of taurine, 100 mM ethanol seemed to have a small enhancing effect (Fig. 3B in Welsh et al., 2010). Therefore, we tested the effect of preincubation of 200 mM ethanol in a short application protocol and compared its effects with those in the long application experiments. We used this concentration of ethanol to allow us to compare results with the approximately equivalent anesthetizing concentrations used for the anesthetics that we also tested. With preincubation of ethanol, followed by a brief co-application with agonist, we found no effects on saturating glycine responses and modest (~40%) potentiating effects in the presence of a saturating concentration of taurine. Ethanol had no effect when combined with glycine, consistent with previous findings that ethanol does not affect the P_o for individual glycine-activated GlyRs (Welsh et al., 2009). However, the modest potentiation of taurine-activated currents suggests that ethanol does increase P_o when receptors are activated by this partial agonist. An increase in single channel conductance could conceivably also explain the potentiation seen here, but it is unlikely given that partial and full agonists elicit the same conductance (Gardner et al., 1984; Lewis et al., 2003). In addition, ethanol does not affect unitary conductance of glycine-activated GlyRs (Welsh et al., 2009).

We sought to further examine the effects of ethanol by co-applying it with maximally effective concentrations of glycine or taurine for 10 min. During constant exposure to a saturating agonist concentration, essentially all receptors enter a fully liganded state, thus minimizing any possible modulator effects on agonist binding or

unbinding. When fully liganded, the GlyR exists in one of the three general states: closed, open, or desensitized. Channel activity is observed as a cluster of transitions between closed and open states terminated by receptor desensitization (Beato et al., 2004). Upon resensitization in the presence of a saturating concentration of agonist, the receptor will almost immediately initiate a new cluster of opening/closing events, meaning that for all practical purposes, all transitions leaving the desensitized state almost instantly lead to a fully liganded open state. Thus, long applications of saturating concentrations of agonist result in a pseudo-equilibrium of clusters of channel-opening events separated by sojourns into desensitized states, with no receptors found in the closed unliganded state. Any increases in current produced by allosteric modulators under these conditions could not be attributed to changes in agonist association or dissociation rates. Positive allosteric modulators must instead be acting by increasing the rates of entering (or decreasing the rates of leaving) open states within clusters to increase P_o or by increasing the rates of leaving (or decreasing the rates of entering) desensitized states. Ethanol did not affect currents elicited by long applications of glycine, consistent with our previous data showing that ethanol only affects glycine unbinding rates (Welsh et al., 2009). However, ethanol did seem to slightly potentiate taurine-mediated currents during long applications (**Fig. 3.3C,D**). This is not attributed to ethanol decreasing the rates of desensitization (**Fig. 3.7**; **Table 3.1**), so the most parsimonious explanation is that ethanol modestly affects taurine-activated intracluster P_o.

We next performed these same experiments using a series of inhaled anesthetics. For these experiments, we tested the alkyl halides chloroform and halothane and the halogenated ethers isoflurane, enflurane, and desflurane. None of the anesthetics tested had any effects on glycine-mediated currents in the brief application experiments, but all

produced striking (>150% potentiation) effects on taurine-mediated currents (**Fig. 3.4**). Similar to Downie et al. (1996), we found that isoflurane has no effects on maximally effective glycine concentrations but enhances maximal taurine currents. Because the anesthetics enhanced the rates of taurine- but not glycine-mediated desensitization (**Fig. 3.7**), this suggests that they increase P_o. If anything, one would expect a slowing of desensitization to increase peak heights. These structurally dissimilar anesthetics had very similar effects, suggesting a common mechanism of action. Lastly, we tested the effects of three inhaled drugs of abuse using the same experimental design, finding that the inhalants produced enhancement of taurine-mediated currents and desensitization rates similar to those seen with ethanol.

The different classes of modulators we tested produced variable enhancement of taurine-activated GlyR currents. We hypothesized that this may be simply attributed to differences in the concentrations used. To test this, we compared the weakly enhancing inhaled drug of abuse toluene with the strongly enhancing anesthetic isoflurane. We first identified the concentrations of each that produced ~200% potentiation of the effects of low (EC_{5-10}) concentrations of taurine. We next tested those modulator concentrations using a maximally effective taurine concentration, observing almost identical effects of the two. Thus, these classes of modulators may all act via a similar mechanism to enhance taurine currents. The greater percentage enhancement seen at low taurine concentrations probably reflects the dual effects of allosteric modulators on taurine unbinding as well as increasing P_o, whereas only the latter effect was observed at a maximally effective taurine concentration.

In summary, all modulators tested produced enhancement of peak current responses elicited by a saturating concentration of taurine but not glycine. In addition,

enhancement of desensitization rates was seen when modulators were applied with taurine but not glycine. Allosteric modulators potentiate both taurine- and glycine-elicited currents when either agonist is present at low concentrations. However, the concentration of either agonist found at the GlyR in vivo is probably high either through the synaptic release of glycine or the osmotic release of taurine. The effects of these modulators on saturating concentrations of taurine are especially interesting given that taurine is the second most abundant amino acid in the brain (Albrecht and Schousboe, 2005) and has also been shown to be released through an osmoresistant calcium-mediated mechanism in the hippocampus (Rodríguez-Navarro et al., 2009). Our findings suggest that allosteric modulators differentially affect the time courses of synaptic events at GlyR, depending on whether the receptor is activated by a full or partial agonist.

4.0 | PHYSIOLOGICAL CONCENTRATIONS OF ZINC REDUCE TAURINE-ACTIVATED GLYR RESPONSES TO DRUGS OF ABUSE[2]

4.1 – Introduction

The glycine receptor (GlyR) is a member of the cys-loop receptor superfamily of ligand-gated ion channels. It has a pentameric structure composed of either α (homomeric) or α & β (heteromeric) subunits arranged around a central anion-conducting pore. GlyR are responsible for the majority of fast inhibitory neurotransmission in the brainstem and spinal cord, with γ-aminobutyric acid type A ($GABA_A$) receptors primarily fulfilling this role in the brain. However, GlyR are also found in many brain regions including the hippocampus, NAcc and prefrontal cortex (Baer et al., 2009; Jonsson et al., 2012, 2009; Lu and Ye, 2011; Lynch, 2004; Malosio et al., 1991; van den Pol and Gorcs, 1988; Waldvogel et al., 2007). Because GlyR are found in brain regions associated with hypnosis, memory, and the rewarding properties of drugs of abuse, it is reasonable to hypothesize that these receptors may play a role in the effects of these agents in vivo.

A wide variety of compounds act as allosteric modulators of the GlyR, including alcohols, inhaled drugs of abuse and anesthetics, neurosteroids, tropeines, divalent cations, and many others (Beckstead et al., 2000; Cheng and Kendig, 2002; Downie et al., 1996; Harvey et al., 1999; Laube et al., 1995; Molander et al., 2007, 2005; Yamashita et

---

[2]Portions of this chapter have previously been published in *Neuropharmacology.* Kirson D, Cornelison GL, Philpo AE, Todorovic J, Mihic SJ (2013) Physiological concentrations of zinc reduce taurine-activated GlyR responses to drugs of abuse. Neuropharmacol 75:286–294.

al., 2001; Yevenes and Zeilhofer, 2011). Thus, the GlyR has emerged as a logical target for the possible development of pharmacological agents to treat substance abuse (Tipps et al., 2010). Allosteric modulators exert their greatest enhancing effects on low concentrations of glycine that are unlikely to be seen at GlyR *in vivo* except at the initiation or tail-end of synaptic events or perhaps at extrasynaptic receptors (Scimemi and Beato, 2009). Indeed these compounds have negligible effects when tested with saturating concentrations of glycine (Kirson et al., 2012; McCracken et al., 2010).

The sulfonic acid taurine acts as a partial agonist at the GlyR, possessing approximately 50% of the efficacy of glycine (Lape et al., 2008). Taurine is the second most abundant amino acid in the brain, and has been implicated as an endogenous ligand of the GlyR in multiple brain regions (Albrecht and Schousboe, 2005; Dahchour et al., 1996; Ericson et al., 2006; Mori et al., 2002; Rodríguez- Navarro et al., 2009). Although glycine receptors are found synaptically in a variety of brainstem nuclei (Ferragamo et al., 1998; Lim et al., 2000) and in cerebellum (Dieudonne, 1995) they are also found extrasynaptically, where taurine and β-alanine may be acting as the endogenous agonists (Mori et al., 2002). Taurine may reach concentrations as high as 20 mM in astrocytes, from which it is released by osmoregulatory mechanisms (Albrecht and Schousboe, 2005). Extracellular taurine concentrations measured by micro-dialysis range from 1 to 100 μM but, by their nature, likely underestimate concentrations found locally around astrocytes.

Taurine plays a role in the effects of ethanol in the NAcc (Ericson et al., 2011). Although allosteric modulators have no effects when tested using saturating concentrations of full agonists at the GlyR, this is not true when saturating concentrations of partial agonists are tested (Albrecht and Schousboe, 2005; Kirson et al., 2012;

Scimemi and Beato, 2009). In this paper we examined the possible interactions of these allosteric modulators with the ubiquitous GlyR modulator, zinc, on glycine- and taurine-activated GlyR.

Zinc modulation of the GlyR is biphasic in nature, with concentrations below 10 μM enhancing responses, while higher concentrations inhibit GlyR functioning (Harvey et al., 1999; Laube et al., 2000, 1995; McCracken et al., 2010). Zinc is present at low and variable levels in standard buffer solutions (Kay, 2004; McCracken et al., 2010), and is also present throughout the brain at low nM concentrations known to potentiate GlyR responses (Frederickson et al., 2006a, b; McCracken et al., 2010). Although zinc is packaged into some synaptic vesicles, even upon release concentrations remain below 10 μM (Frederickson et al., 2006a). Zinc modulation of the glycine-activated GlyR has been extensively studied but the interactions between zinc and the taurine-activated GlyR have not been characterized to the same extent, especially in conjunction with ethanol or other modulators. Previous studies of zinc modulation of taurine-activated GlyR responses focused on adding zinc at both enhancing and inhibiting concentrations, without controlling for the background zinc likely to be found at biologically-relevant concentrations (Laube et al., 2000). In this study we further characterize zinc modulation, as well as compare zinc's interactions with other allosteric modulators on the glycine- vs. taurine-activated GlyR.

4.2 – Materials and Methods

Isolation, injection, and two-electrode voltage-clamp of *Xenopus* oocytes were described in Chapter 2. Specific methods pertaining to the experiments in this chapter are outlined below.

All chemicals were purchased from Sigma–Aldrich (St. Louis, MO) except isoflurane which was obtained from Anaquest (New Providence, NJ).

Xenopus laevis were obtained from Nasco (Fort Atkinson, WI) and housed at 19°C on a 12-h light/dark cycle. During surgery, performed in accordance with the Association for Assessment and Accreditation of Laboratory Animal Care regulations, portions of ovaries were removed and placed in isolation media containing 108 mM NaCl, 1 mM EDTA, 2 mM KCl, and 10 mM HEPES. Forceps were used to manually remove the thecal and epithelial layers from stage V and VI oocytes. The oocyte follicular layer was removed using a 10 min incubation in 0.5 mg/ml type 1A collagenase in buffer containing 83 mM NaCl, 2 mM $MgCl_2$, and 5 mM HEPES. Animal poles of oocytes were injected with human glycine α1, α2, α1β or α2β receptor subunit cDNAs (1.5 ng/30 nl) in a modified pBK-cytomegalovirus vector (Mihic et al., 1997), using a micropipette (10–15 μm tip size) attached to an electronically-activated microdispenser. When heteromeric receptors were to be studied, α and β subunit cDNAs were injected in a 1:20 α:β concentration ratio to ensure incorporation of the β subunits into receptors. Oocytes were stored in the dark at 19°C in 96-well plates containing modified Barth's saline (MBS) [88 mM NaCl, 1 mM KCl, 2.4 mM $NaHCO_3$, 10 mM HEPES, 0.82 mM $MgSO_4 7{\cdot}H_2O$, 0.33 mM $Ca(NO_3)_2$, 0.91 mM $CaCl_2$ at pH 7.5] supplemented with 2 mM sodium pyruvate, 0.5 mM theophylline, 10 U/ml penicillin, 10 mg/l streptomycin and 50 mg/l gentamicin, and sterilized by passage through a 0.22 μm filter.

Oocytes expressed GlyR within 24 h, and all electrophysiological measurements were made within 5 days of cDNA injection. Before electrophysiological recording, oocytes were placed in a 100 µl bath with the animal poles facing upwards and impaled with two high-resistance (0.5–10 MΩ) glass electrodes filled with 3 M KCl. Cells were voltage-clamped at –70 mV using an OC-725C oocyte clamp (Warner Instruments, Hamden, CT) and perfused with MBS at a rate of 2 ml/min using a Masterflex USA peristaltic pump (Cole Parmer Instrument Co., Vernon Hills, IL) through 18-gauge polyethylene tubing. All drug solutions were prepared in MBS, MBS + 2.5 mM tricine, or MBS + 100 nM ZnCl. When saturating concentrations of agonists were applied, applications lasted for 15 s for the short application experiments and for up to 26 min for the continuous application experiments. For experiments using submaximal concentrations of taurine, concentrations that yielded 5 percent of the maximally-effective taurine response (EC_5) were applied for 30 s. For short application experiments, modulators were co-applied with agonists following a 30 s preincubation of modulator alone. For continuous application experiments, modulators were co-applied with agonist for 2 min following agonist application alone. All drug applications during short application experiments were followed by 6–10 min washout periods to allow for complete receptor resensitization. Loss of volatile compounds through tubing and evaporation from bath was previously measured (Beckstead et al., 2002, 2000; Mihic et al., 1994; Yamakura et al., 1999). All concentrations reported are the bath concentrations to which the oocytes were exposed. Data were acquired at a rate of 1 kHz using a Powerlab 4/30 digitizer with LabChart version 7 software (ADInstruments, Bella Vista, NSW, Australia).

Peak currents were measured and used in data analysis. Currents observed in the presence of agonist plus modulators were compared with currents generated by agonist without the modulator of interest present. Experimental values are listed as the mean ± SEM. Significant differences between experimental conditions were determined using ANOVA or repeated measures ANOVA and post-hoc tests, as indicated. SigmaPlot version 11.0 (Systat Software, San Jose, CA) was used for statistical testing.

4.3 – Results

4.3.1 – Chelation of endogenous zinc decreases responses to taurine

We previously showed that various allosteric modulators of GlyR, such as ethanol and some anesthetics, have different effects on currents generated by saturating concentrations of glycine versus taurine (Kirson et al., 2012). In order to compare zinc modulation of GlyR currents generated by maximally-effective concentrations of glycine and taurine, we compared currents generated by co-applications of agonist and either 100 nM zinc or 2.5 mM of the zinc chelator tricine with currents generated by agonist alone. **Fig. 4.1A** shows a sample tracing of successive 15 s applications of 10 mM glycine in the presence of a background concentration of zinc, 2.5 mM tricine, or 100 nM zinc. **Fig. 4.1B** shows the same experimental protocol as in A but with 100 mM taurine instead employed as the agonist. Addition of 100 nM zinc enhanced saturating taurine currents almost 60% (**Fig. 4.1C**) while leaving saturating glycine-mediated currents unchanged. Elimination of background levels of zinc in the perfusion buffer by co-application of

tricine decreased saturating taurine currents while having no effects on saturating glycine currents. A two-way ANOVA showed a significant interaction effect between the concentration of zinc in the buffer and the agonist tested [$F(1,37) = 34.4$, $p < 0.001$]. A Student-Newman-Keuls (SNK) multiple comparison post-hoc test showed significant differences between glycine and taurine both in the presence of 2.5 mM tricine [$q = 4.6$, $p < 0.01$] and 100 nM zinc [$q = 7.1$, $p < 0.001$], as well as a significant effect of zinc concentration when taurine was the agonist [$q = 12.3$, $p < 0.001$].

We next looked at the effects of zinc modulation using saturating agonist concentrations that were applied continuously for 10 min, followed by 2 min co-applications of agonist and either 2.5 mM tricine or 100 nM zinc. This continuous agonist application approach allows for channels to equilibrate between the open and desensitized states (**Fig. 4.2A,B**). Under these conditions all receptors have bound agonist and are either activated (opening) or desensitized. In this experimental paradigm the effects of modulators can thus only be due to their effects on channel opening/closing kinetics (P_o) or desensitization/resensitization rates and not on possible effects on agonist affinity. As seen in **Fig. 4.2C**, the effects exhibited by zinc trended in the same directions as those seen in **Fig. 4.1C**, but to a smaller degree. Co-application of 100 nM zinc produced greater potentiation of saturating taurine currents compared to saturating glycine currents. Co-application of tricine showed a decrease in saturating taurine responses compared to a negligible increase in saturating glycine. Similar to the short application experiments, a two-way ANOVA showed a significant interaction effect between the concentration of zinc in the buffer and the agonist tested [$F(1,16) = 34.3$, $p < 0.001$]. A SNK multiple comparison post-hoc test revealed significant differences between glycine and taurine both in the presence of 2.5 mM tricine [$q = 7.1$, $p < 0.001$]

and 100 nM zinc [$q = 4.6$, $p < 0.01$], as well as a significant effect of zinc concentration when taurine was the agonist [$q = 11.6$, $p < 0.001$].

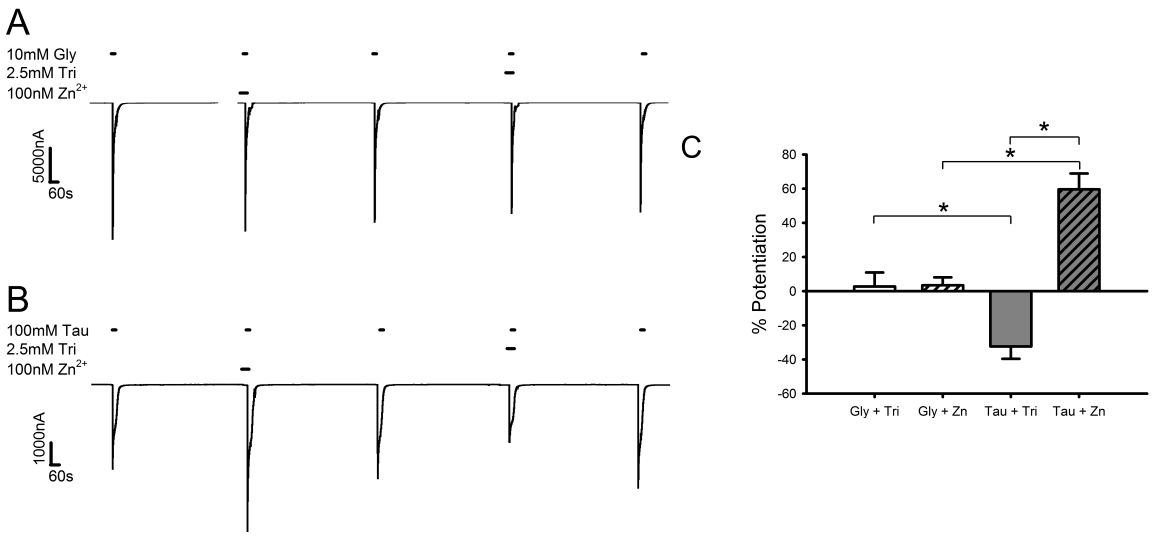

Figure 4.1 – Zn^{2+} affects currents elicited by maximally-effective concentrations of taurine but not glycine

A) tracings showing the effect of a maximally-effective concentration of glycine applied in the presence or absence of Zn^{2+}. The tracing shows 15 s co-applications of 10 mM glycine with either 2.5 mM tricine or 100 nM Zn^{2+} following a 30 s preincubation with tricine or Zn^{2+}. Each application was preceded and followed by applications of 10 mM glycine alone in buffer containing background levels of Zn^{2+}. Horizontal bars over tracings indicate time of exposure to glycine, tricine, or Zn^{2+}. 10 min washouts separated agonist applications. B) tracing showing the effect of a maximally-effective concentration of taurine applied in the presence or absence of Zn^{2+}. The tracing follows the same protocol as in panel A. Horizontal bars over tracing indicate time of exposure to taurine, tricine, or Zn^{2+}. C) Summary of the effects of Zn^{2+} on maximally-effective concentrations of glycine or taurine. The y-axis represents the percent current potentiation observed in the presence or absence of Zn^{2+} compared with that produced by glycine or taurine in background levels of Zn^{2+}. Data are shown as mean ± SEM of 9–11 oocytes. *, $p < 0.05$.

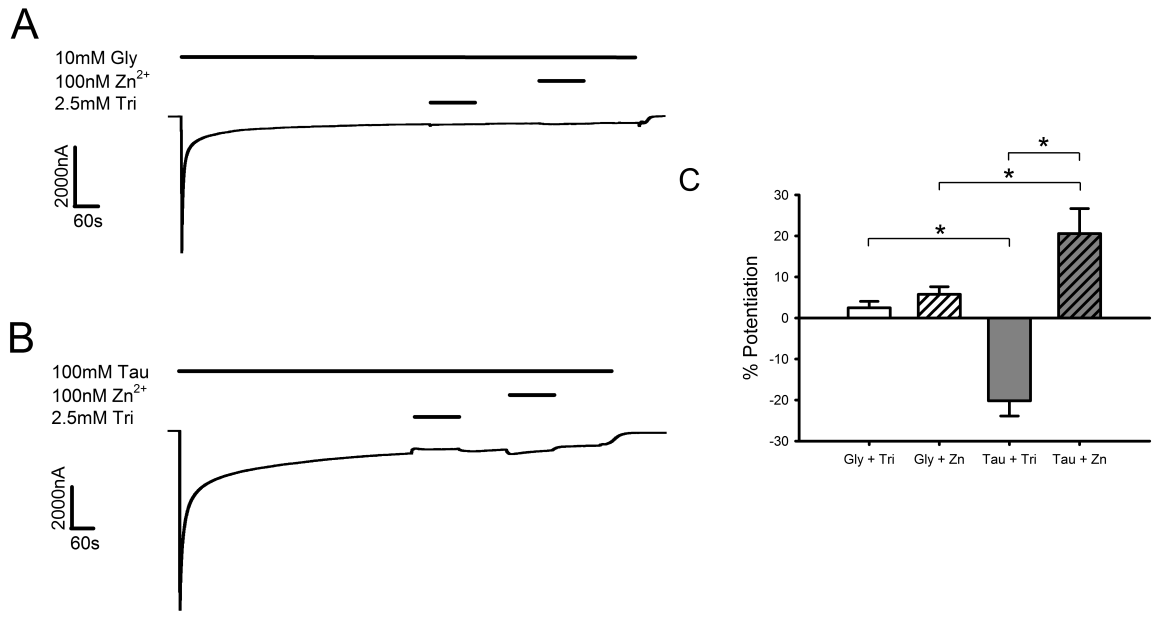

Figure 4.2 – Zn^{2+} affects currents elicited by long exposures to maximally-effective concentrations of taurine but not glycine

A) Sample tracing showing the effects of 2.5 mM tricine or 100 nM Zn^{2+} co-applied with saturating concentrations of glycine after 10 min of continuous glycine application. Two minute applications of 10 mM glycine in either 2.5 mM tricine or 100 nM Zn^{2+} were preceded and followed by 10 mM glycine in buffer containing background levels of Zn^{2+}. Horizontal bars over the tracing indicate time of exposure to glycine, tricine, or Zn^{2+}. B) Sample tracing showing the effects of 2.5 mM tricine or 100 nm Zn^{2+} co-applied with saturating concentrations of taurine, after 10 min of continuous taurine application. The tracing follows the same protocol as in panel A. Horizontal bars over the tracing indicate time of exposure to taurine, tricine, or Zn^{2+}. C) Summary of the effects of maximally-effective concentrations of glycine or taurine in the presence or absence of Zn^{2+} during continuous agonist exposures. The y-axis is the percent current enhancement observed in the presence or absence of Zn^{2+} compared with the glycine or taurine current level immediately preceding tricine or zinc co-application. Data are shown as mean ± SEM of 4–6 oocytes. *, $p < 0.05$.

4.3.2 – ZINC AND ETHANOL INTERACTIONS

Physiologically-relevant low nM concentrations of zinc enhance ethanol modulation of GlyR currents generated by submaximal but not maximally-effective concentrations of glycine (McCracken et al., 2010). As these two modulators are likely to be present concurrently at GlyR in vivo, we compared the effects of enhancing concentrations of zinc on ethanol modulation of GlyR activated by maximally-effective glycine or taurine concentrations. We first looked at the effects of 15 s co-applications of maximally-effective concentrations of agonist and 200 mM ethanol in the presence of background levels of zinc and also in the presence of 2.5 mM tricine or 100 nM zinc. **Fig. 4.3A** shows that ethanol modulation of the maximally-effective taurine response is present in all three different zinc concentrations. However, 100 nM zinc significantly decreased [Two-way Repeated Measures (RM) ANOVA with SNK multiple comparison procedure; $q = 5.0, p < 0.01$; $q = 4.6, p < 0.01$, respectively] the degree of ethanol percent potentiation of a saturating taurine concentration compared to the potentiation seen in either the background zinc level or after zinc chelation. In background levels of zinc, or in the presence of 2.5 mM tricine, or 100 nM zinc, 200 mM ethanol produced significantly greater enhancement of responses in saturating taurine than glycine [$q = 12.9$, $p < 0.001$; $q = 11.6$, $p < 0.001$; $q = 8.3$, $p < 0.001$, respectively], as there was negligible inhibition of glycine currents observed instead (**Fig. 4.3B**). The same trends were observed using 50 mM ethanol, just with a lower degree of ethanol potentiation (**Fig. 4.3C**) [$q = 3.85, p < 0.05$, comparing taurine alone with taurine plus zinc].

We next looked at the combined effects of zinc and ethanol on receptors comprised of different subunits. The heteromeric $\alpha1\beta$ GlyR is the predominant adult form found in brainstem and spinal cord of mammals and is likely to be found

synaptically, as the β subunit is involved in anchoring the GlyR via its interactions with gephyrin (Kirsch and Betz, 1995). As shown in **Fig. 4.4A**, the effects of combined ethanol and zinc on the heteromeric channel exhibit the same trends as those seen on the homomeric channel but with slightly increased enhancement of taurine currents for the heteromeric channel. A two-way RM ANOVA with SNK multiple comparison procedure showed ethanol potentiation of currents in 100 nM zinc significantly decreased from both background zinc [$q = 3.8$, $p < 0.05$] and 2.5 mM tricine [$q = 3.1$, $p < 0.05$], as well as significantly greater ethanol percent potentiation of taurine vs.glycine currents [$q = 7.5$, $p = 0.001$]. We also performed equivalent experiments on α2 homomeric (**Fig. 4.4B**) and α2β (**Fig. 4.4C**) heteromeric receptors. Two-way RM ANOVAs with SNK multiple comparison procedures showed significantly greater ethanol percent potentiation of taurine vs.glycine currents [α2, $q = 7.14$, $p < 0.01$; α2β, $q = 4.6$, $p < 0.05$]. We found that taurine had very low efficacy on GlyR containing α2 subunits: 13.2 ± 5.4% in α2 homomers and 6.1 ± 1.4% in α2β heteromeric GlyR, compared to the effects produced by a saturating concentration of glycine.

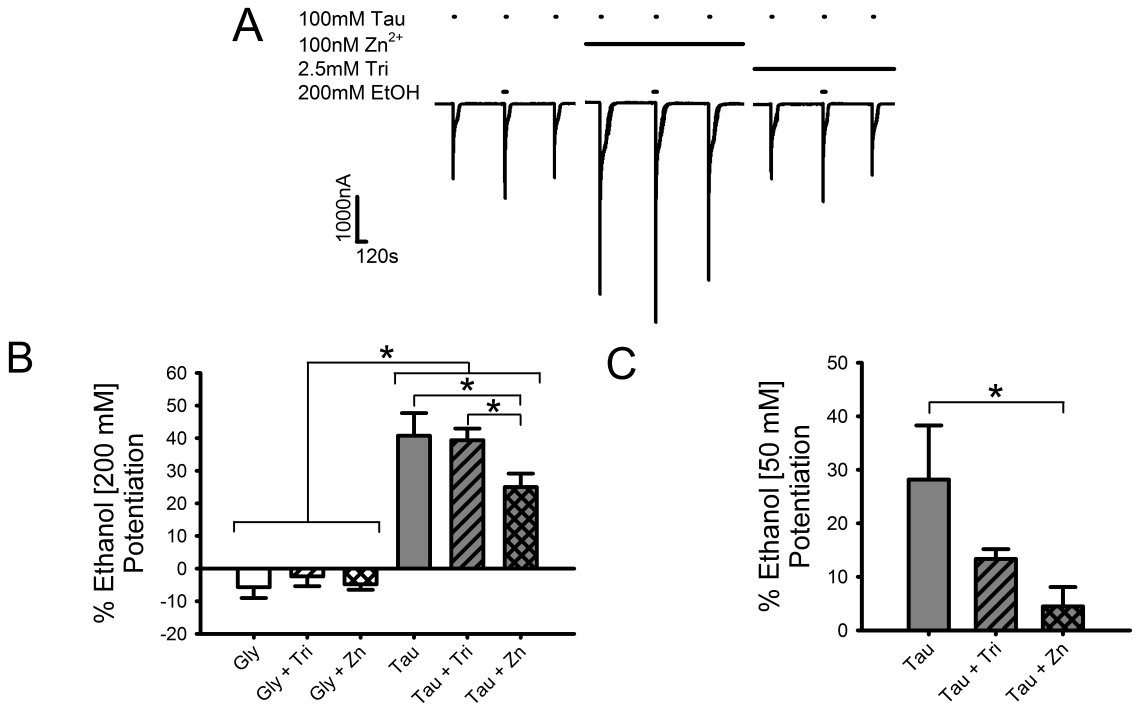

Figure 4.3 – Zn^{2+} affects ethanol potentiation of currents elicited by maximally-effective concentrations of taurine but not glycine

A) tracings showing the effect of Zn^{2+} on brief applications of maximally-effective concentrations of taurine. Taurine (100 mM) was co-applied with 200 mM ethanol for 15 s following a 30 s preincubation with 200 mM ethanol. Ethanol applications were flanked by 15 s applications of taurine applied alone. Series of applications were carried out in buffer containing background levels of Zn^{2+}, 2.5 mM tricine or 100 nM Zn^{2+}. Horizontal bars over tracings indicate time of exposure to taurine, tricine, Zn^{2+} or ethanol. B) Summary of the effects of 200 mM ethanol on maximally-effective concentrations of glycine or taurine in the presence of a background level of Zn^{2+}, the absence of Zn^{2+} produced by tricine, or the addition of 100 nM Zn^{2+}. The y-axis is the percent current potentiation with ethanol co-application, in background Zn^{2+}, 2.5 mM tricine or 100 nM Zn^{2+}. Data are shown as mean ± SEM of 6 oocytes. C) Summary of the effects of 50 mM ethanol on maximally-effective concentrations of taurine in the presence of a background level of Zn^{2+}, the absence of Zn^{2+} produced by tricine, or the addition of 100 nM Zn^{2+}. The y-axis is the percent current potentiation with ethanol co-application, in background Zn^{2+}, 2.5 mM tricine or 100 nM Zn^{2+}. Data are shown as mean + SEM of 8 oocytes. *, $p < 0.05$.

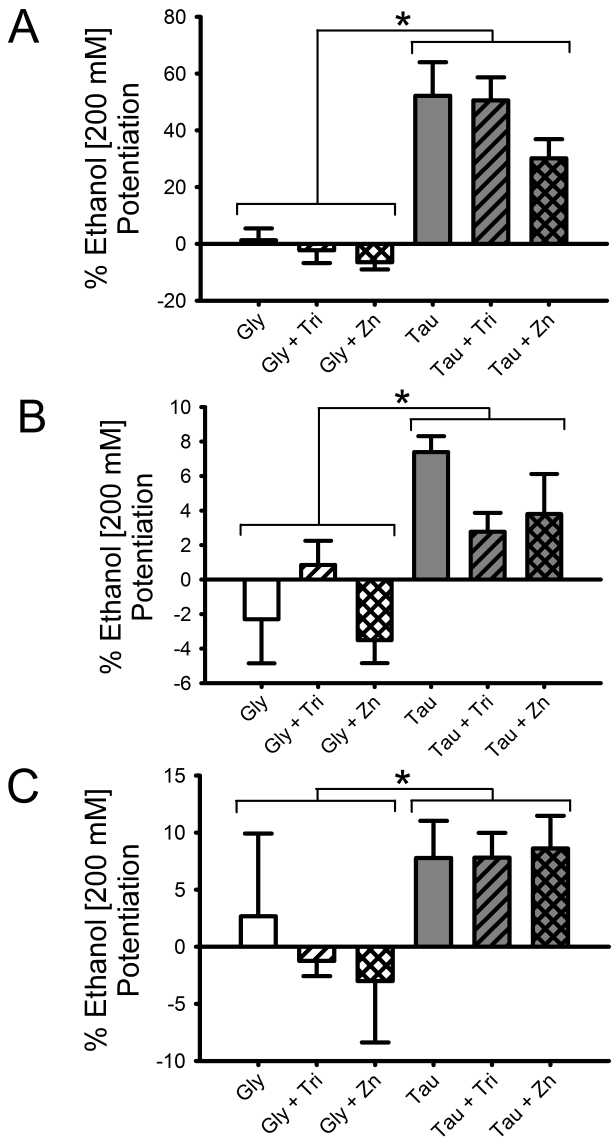

Figure 4.4 – Zinc/ethanol interactions on GlyR composed of a variety of different subunits

Summaries of the effects of ethanol on brief applications of maximally-effective concentrations of glycine or taurine in the presence of a background level of Zn^{2+}, the absence of Zn^{2+} produced by tricine, or the addition of 100 nM Zn^{2+} on the α1β GlyR (A) α2 GlyR (B) or α2β GlyR (C). The y-axes represent the percent current potentiation observed with ethanol co-application, in background Zn^{2+}, 2.5 mM tricine or 100 nM Zn^{2+}. Data are shown as mean ± SEM of 5–8 oocytes. *, $p < 0.05$.

4.3.3 – ZINC AND ISOFLURANE INTERACTIONS

Because biologically-relevant concentrations of zinc affect ethanol potentiation of saturating taurine currents, we investigated other allosteric modulators of the GlyR for zinc-modulator interactions. The inhaled volatile anesthetic isoflurane was tested using the same experimental protocols as those used for ethanol. **Fig. 4.5A** shows the results of 15 s co-applications of 0.55 mM isoflurane with either 10 mM glycine or 100 mM taurine in the presence of background levels of zinc, 2.5 mM tricine or 100 nM zinc. As for ethanol, isoflurane potentiation of saturating taurine currents in either background zinc or 2.5 mM tricine were very similar, while the addition of 100 nM zinc significantly decreased the isoflurane percent potentiation from those levels [Two-way RM ANOVA with SNK multiple comparison procedure; q = 4.1, $p < 0.02$; q = 4.4, $p < 0.05$, respectively]. Saturating glycine-mediated currents were minimally affected by isoflurane whether in background levels of zinc, 2.5 mM tricine, or 100 nM zinc. Isoflurane enhancement was significantly different between glycine and taurine in the presence of a background level of zinc [q = 7.4, $p < 0.001$] and in 2.5 mM tricine [q = 7.8, $p < 0.001$].

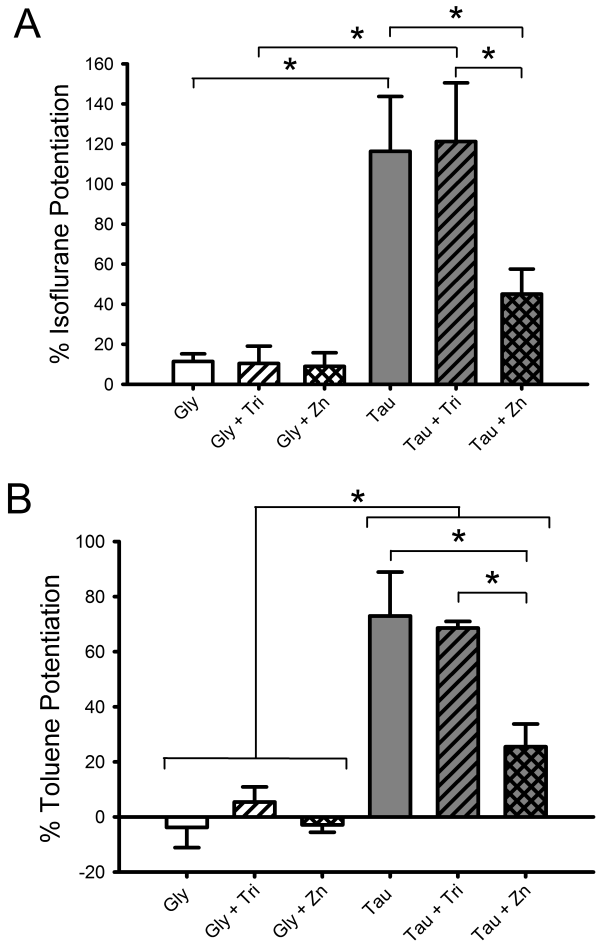

Figure 4.5 – Zn^{2+} decreases isoflurane and toluene potentiation of currents elicited by maximally-effective concentrations of taurine but not glycine

These experiments were carried out in the same manner as the ethanol experiments described in **Fig. 4.3**. A) Effect of isoflurane on currents elicited by brief applications of maximally-effective glycine (10 mM) or taurine (100 mM) in the presence or absence of Zn^{2+}. Agonist was co-applied with 0.55 mM isoflurane for 15 s following a 30 s preincubation with 0.55 mM isoflurane. Data are shown as mean + SEM of 6 oocytes. B) Effect of toluene on currents elicited by brief applications of maximally-effective glycine (10 mM) or taurine (100 mM) in the presence or absence of Zn^{2+}. Agonist was co-applied with 0.42 mM toluene for 15 s following a 30 s preincubation with 0.42 mM toluene. Data are shown as mean ± SEM of 4 oocytes. *, $p < 0.05$.

4.3.4 – Zinc and toluene interactions

The next allosteric modulator tested was the inhaled drug of abuse toluene. **Fig. 4.5B** shows the results of the brief co-applications of 0.42 mM toluene with either 10 mM glycine or 100 mM taurine in the presence of background levels of zinc, 2.5 mM tricine, or 100 nM zinc. Toluene had negligible effects on 10 mM glycine currents and its effects on 100 mM taurine currents were similar to effects seen with ethanol and isoflurane. Again, similar to ethanol and isoflurane, toluene percent potentiation of saturating taurine-mediated currents was significantly reduced in the presence of 100 nM zinc, compared to the other two zinc conditions [Two-way RM ANOVA with SNK multiple comparison procedure; q = 6.3, $p < 0.002$; q = 5.7, $p < 0.002$, respectively]. Toluene enhancement of saturating taurine was significantly greater than effects on saturating glycine in background levels of zinc [q = 8.8, $p < 0.001$], 2.5 mM tricine [q = 7.2, $p < 0.001$], and 100 nM zinc [q = 3.3, $p < 0.05$].

4.3.5 – Zinc & ethanol interactions at a low taurine concentration

We previously found that zinc enhances ethanol potentiation of low concentrations of glycine, and that the degree of ethanol enhancement is reduced when zinc is chelated by tricine (McCracken et al., 2010). Although we saw minor ethanol effects with changing zinc levels at saturating concentrations of glycine, we did see changes in ethanol potentiation of saturating concentrations of taurine based on the level of zinc present (**Fig. 4.2B**). Thus we extended the observations made in the McCracken et al. (2010) paper, this time using EC_5 concentrations of taurine. We first tested whether

ethanol potentiation of EC_5 taurine currents in α1 GlyR depends on the concentration of zinc. **Fig. 4.6A** shows that when zinc is chelated with tricine, the degree of ethanol potentiation of EC_5 taurine-mediated currents is the same as EC_5 glycine-mediated currents for both 50 mM and 200 mM ethanol. We next tested if chelation of zinc significantly reduces ethanol potentiation of EC_5 taurine-mediated currents as it does for glycine-mediated currents. **Fig. 4.6B** shows the results of 200 mM ethanol effects on EC_5 glycine and taurine currents, with and without the addition of 2.5 mM tricine. With no differences between agonists, ethanol potentiation was significantly lower in 2.5 mM tricine compared to background levels of zinc [Two-way ANOVA with SNK multiple comparison procedure; $q = 3.7, p < 0.05$].

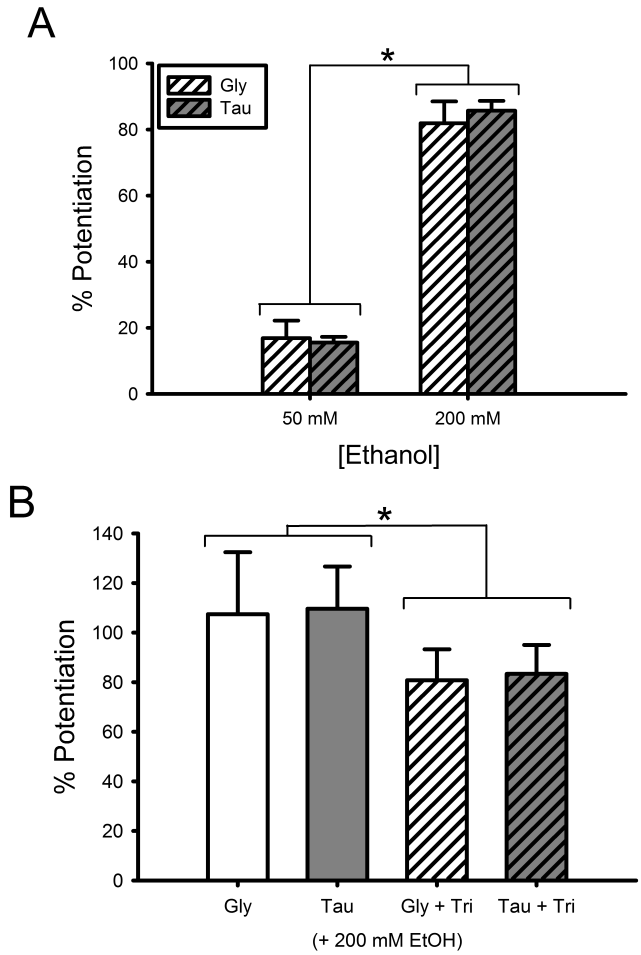

Figure 4.6 – Zn^{2+} affects ethanol potentiation of low concentrations of full and partial agonists

A) Ethanol potentiation of the effects of 5% maximal (EC_5) glycine- or taurine-mediated currents in the presence of 2.5 mM tricine (i.e., in the absence of Zn^{2+}). EC_5 glycine and taurine were co-applied with either 50 mM or 200 mM ethanol following a 30 s preincubation with ethanol. Data are shown as mean + SEM of 5 oocytes. B) Ethanol potentiation of EC_5 glycine and taurine is enhanced by Zn^{2+}. EC_5 glycine or taurine were co-applied with 200 mM ethanol following preincubation with ethanol, in the presence of either background Zn^{2+} (left two bars) or 2.5 mM tricine (right two bars). Data are shown as mean + SEM of 9 oocytes. *, $p < 0.05$.

4.3.6 – ZINC/MODULATOR INTERACTION EFFECTS ON DESENSITIZATION RATES

We next looked at the effects of changing zinc concentration on desensitization rates. Desensitization rates were determined by comparing the peak current to that measured five seconds post-peak for saturating glycine and taurine currents, in the presence of background levels of zinc or in the presence of 2.5 mM tricine or 100 nM zinc. Changing the zinc concentration did not affect the desensitization rates of glycine-activated currents in α1 GlyR (**Fig. 4.7A**). Taurine-mediated desensitization was significantly slower than for glycine-mediated currents in background zinc [Two-way ANOVA with SNK multiple comparison procedure; $q = 8.5$, $p < 0.001$], as well as in 2.5 mM tricine [$q = 10.4$, $p < 0.001$], and in 100 nM zinc [$q = 4.2$, $p < 0.01$]. Additionally, desensitization of taurine-mediated currents in 2.5 mM tricine and 100 nM zinc were significantly different [$q = 3.7$, $p < 0.05$].

Because drugs of abuse and zinc are likely to be found concomitantly at receptors *in vivo*, we examined the effects of different allosteric modulators on desensitization rates in the presence of background zinc, 2.5 mM tricine, or 100 nM zinc. **Fig. 4.7B** shows the desensitization rates produced by 10 mM glycine and 100 mM taurine applied with 200 mM ethanol in the three different zinc concentrations. Taurine + ethanol current desensitization was significantly slower than that seen in glycine + ethanol currents in background zinc [Two-way RM ANOVA with SNK multiple comparison procedure; $q = 7.7$, $p < 0.001$], 2.5 mM tricine [$q = 11.0$, $p < 0.001$], and 100 nM zinc [$q = 5.1$, $p < 0.01$]. Additionally, desensitization of glycine + ethanol currents in 2.5 mM tricine and 100 nM zinc were significantly different [$q = 4.3$, $p < 0.05$].

Fig. 4.7C shows the results for desensitization experiments involving isoflurane. Desensitization was similar for 10 mM glycine with 0.55 mM isoflurane currents and 100

mM taurine with 0.55 mM isoflurane currents, with the only significant difference found between glycine + isoflurane and taurine + isoflurane in 100 nM zinc buffer [Two-way RM ANOVA with SNK multiple comparison procedure; $q = 3.5$, $p < 0.05$]. **Fig. 4.7D** shows the effects of toluene on desensitization mediated by either glycine or taurine. There was a significant effect of agonist [Two-way RM ANOVA with SNK multiple comparison procedure; $q = 4.2$, $p < 0.05$].

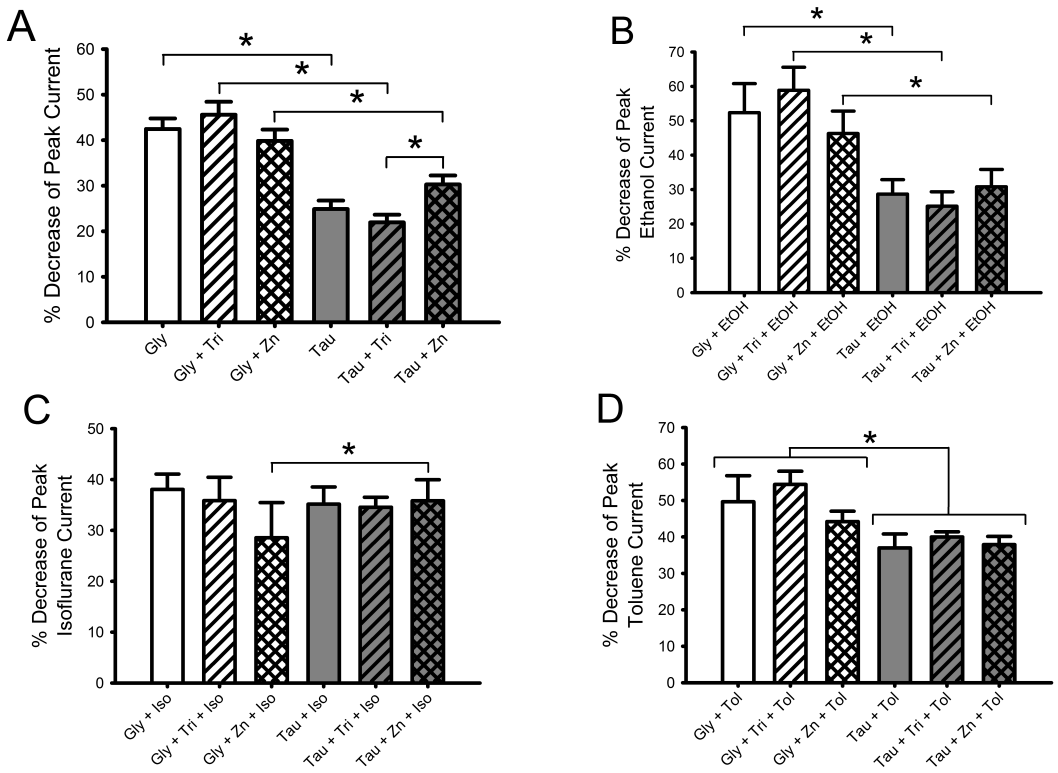

Figure 4.7 – Zn^{2+} levels do not significantly affect desensitization of glycine- or taurine-activated glycine receptors.

A) Zn^{2+} does not affect the rate of desensitization produced by maximally-effective glycine or taurine. Percent decrease in peak current observed 5 s post-peak is graphed for each agonist/Zn^{2+} level combination. Data are shown as mean + SEM of 26–35 oocytes. B) Zn^{2+} and ethanol do not affect the rate of desensitization produced by maximally-effective glycine or taurine. Percent decrease in peak current seen 5 s post-peak in the presence of 200 mM ethanol is graphed for each agonist/Zn^{2+} level combination. Data are shown as mean + SEM of 6 oocytes. C) Zn^{2+} levels have no effect on isoflurane changes in desensitization rates of taurine-activated glycine receptor currents. Percent decrease in peak current observed 5 s post-peak in the presence of 0.55 mM isoflurane is graphed for each agonist/Zn^{2+} level combination. Data are shown as mean + SEM of 6 oocytes. D) Zn^{2+} and toluene do not interact to affect desensitization rates of maximally-effective glycine and taurine. Percent decrease in peak current seen 5 s post-peak in the presence of 0.42 mM toluene is graphed for each agonist/Zn^{2+} level combination. Data are shown as mean + SEM of 5 oocytes. *, $p < 0.05$.

4.4 – Discussion

The dopaminergic projection from the ventral tegmental area (VTA) to the nAcc is critical to the perception of the rewarding properties of drugs of abuse, and ethanol's actions on the GlyR may be particularly important in these brain regions. For example, extracellular dopamine levels increase in the NAcc following ethanol (Imperato and Di Chiara, 1986) or glycine (Molander et al., 2005) administration and glycine perfusion into the NAcc of rats decreases alcohol consumption (Molander et al., 2005). Many volatile agents such as isoflurane and toluene also have abuse liability (Johnston et al., 2012; Wilson et al., 2008). Toluene also increases extracellular dopamine levels in the VTA and NAcc when perfused into the former (Riegel et al., 2007). Most studies examining the effects of these agents on GlyR functioning do so by determining the effects of single modulators in isolation. However, since zinc is ubiquitous in cerebrospinal and interstitial fluids at GlyR-potentiating levels, the effects of drugs of abuse on GlyR *in vivo* will always be seen in combination with zinc effects. In fact one could go so far as to say that studying these compounds in the absence of zinc would represent an artificial situation unlikely to be found *in vivo*. Since taurine and glycine may act as GlyR agonists in brain regions such as the NAcc, we examined the effects of combinations of allosteric modulators on GlyR activated by these agonists. Maximally-effective concentrations of taurine but not glycine were affected by zinc chelation (**Figs. 4.1, 4.2**). This is likely the result of glycine producing a very high probability of channel opening (intra-cluster $P_o \sim 1$), with maximally-effective concentrations keeping the channel open almost 100% of the time before it desensitizes, regardless of the presence of any allosteric modulator. As a partial agonist, taurine has a much lower P_o (~0.5) at

maximally-effective concentrations (Lape et al., 2008), allowing for zinc to exhibit its enhancing effects. The zinc potentiation seen after 10 min of continuous taurine perfusion could be attributable to zinc: (1) increasing P_o; (2) enhancing conductance; (3) decreasing the desensitization rate or; (4) increasing the rate of GlyR resensitization. Previous studies performed using low agonist concentrations show that zinc does increase P_o but it does not affect conductance (Laube et al., 2000). Our data (**Fig. 4.7A**) shows that zinc can also increase the desensitization rate in taurine-activated GlyR, which would tend to counteract its P_o enhancing effects. In this way, zinc acts in a very similar fashion to other GlyR allosteric modulators (Kirson et al., 2012). The decrease in responses seen when zinc is chelated by tricine suggests that sub-maximal glycine responses and all taurine responses are overestimated when not controlling for background zinc concentrations in buffer solutions.

Because zinc is ubiquitous in the CNS, the effects of any drugs of abuse or other allosteric modulators of interest on GlyR functioning require comparison in the presence and absence of potentiating concentrations of zinc. In the presence of a maximally-effective concentration of glycine, changing the zinc concentration had no effect on responses for any of the modulators tested, since 10 mM glycine has already produced a maximal response. However, effects on maximally-effective concentrations of taurine were expected and seen. If zinc and other positive modulators were acting in an additive or synergistic manner, we would expect the 100 nM zinc condition to give a higher degree of potentiation than our standard buffers, with chelation of zinc by 2.5 mM tricine giving a lower degree of potentiation than both other conditions. However we did not find this to be the case for maximally-effective concentrations of taurine with alcohol, isoflurane, or toluene.

Chelation of zinc with tricine did not change the alcohol, isoflurane, or toluene potentiation of a maximally-effective taurine concentration when compared to the effects seen in the presence of background levels of zinc (**Figs. 4.3B, 4.5A, 4.5B**). However, at sub-maximal concentrations of glycine or taurine, chelation of background zinc does decrease ethanol potentiation of GlyR responses (**Fig. 4.6B**). The most parsimonious explanation for the lack of change seen at higher levels of taurine would be that background levels of zinc during those particular experiments were low. However, the addition of 100 nM zinc to buffers, ensuring that the concentration of zinc is in the potentiating range, led to a significant reduction in the ethanol, isoflurane, and toluene potentiation of taurine-activated GlyR responses (**Figs. 4.3B, 4.5A, 4.B**). This finding cannot be explained by simple competition between modulators as zinc is not believed to bind the receptor at the same locations as alcohols, anesthetics, and inhalants (Beckstead et al., 2000; Laube et al., 2000; Lynch et al., 1998; Mihic et al., 1997; Yamakura et al., 1999). However, zinc does increase the P_o of the taurine-activated GlyR (Laube et al., 2000), in effect mimicking the glycine-bound GlyR. When this occurs and the GlyR P_o approaches 1 any other positive modulator present will as a result produce decreased percent enhancement compared to when less zinc is present.

Since the α2 subunit appears to be expressed at higher levels than α1 in higher brain regions (Jonsson et al., 2012) we studied ethanol/zinc interactions on a variety of different GlyR subtypes activated by taurine vs. glycine (**Figs. 4.3B, 4.4A–C**). The α2-containing receptors were previously shown to be less sensitive to ethanol (Mascia et al., 1996a), and zinc (Miller et al., 2005), than those that contain α1 subunits and this was also reflected in our experiments using a maximally-effective concentration of taurine. We performed these experiments in the absence and presence of the β subunit which

anchors the GlyR to gephyrin in the synapse (Kirsch and Betz, 1995). Badanich et al. (2013) found that in the orbitofrontal cortex, where α2-containing GlyR are thought to predominate (Jonsson et al., 2012), there was no effect of the glycine receptor antagonist strychnine on neuronal holding current, but strychnine did antagonize ethanol-induced changes in holding current and spike firing. The most parsimonious explanation for these findings is that there are insufficient extracellular glycine or taurine concentrations to significantly affect holding current, unless ethanol is present. It is reasonable to hypothesize that ethanol promotes the release of glycine or taurine and it may also then enhance the effects of these compounds on the GlyR, although the Badanich et al. (2013) study does not address the relative importance of each phenomenon. If taurine is the responsible agonist then our findings raise two possible complicating issues. First, like Shmieden et al. (1992), we found that, relative to glycine, taurine has very low efficacy on α2-containing GlyR, much lower than its efficacy on α1-containing GlyR. Even at saturating concentrations, taurine could at best have only modest effects on α2 GlyR function. The next issue is that ethanol weakly enhances taurine-mediated currents in α2 and α2β GlyR. These findings are difficult to reconcile with the possibility that the effects seen in the Badanich et al. (2013) study are mediated by taurine on α2-containing receptors in the orbitofrontal cortex. Further studies addressing these issues are warranted.

In summary, low concentrations of zinc potentiated GlyR responses from maximally-effective concentrations of taurine but not glycine. Chelation of zinc reduced GlyR responses produced by maximally-effective concentration of taurine but not glycine, and thus any experiments conducted in the absence of zinc chelation will tend to overestimate taurine efficacy. This would also be true when sub-maximal glycine

concentrations are used. At the low concentrations tested, zinc decreased the enhancing effect of taurine-mediated responses for all drugs of abuse tested when applied in combination with them. As taurine is likely to be an endogenous GlyR ligand in brain regions affected by these compounds, the presence of low concentrations of zinc in these regions results in GlyR responses that are not the result of a simple summation of responses to single modulators, and this needs to be taken into consideration when investigating the role of the GlyR *in vivo*. It is highly likely that previously published studies of this receptor have in reality been studying the zinc-modulated GlyR. To truly understand how allosteric modulators act at the GlyR one must examine their actions in the context of the physiological milieu at the receptor, reflecting *in vivo* conditions, as well as studying each modulator's contribution in isolation.

5.0 | SINGLE CHANNEL ANALYSIS OF ETHANOL AND ISOFLURANE ENHANCEMENT OF GLYCINE RECEPTOR FUNCTION

5.1 – Introduction

Glycine receptors (GlyR) are responsible for the majority of inhibitory neurotransmitter in the brainstem and spinal cord, but are also found in higher brain regions such as the hippocampus, nucleus accumbens (NAcc), and prefrontal cortex (van den Pol and Gorcs, 1988; Malosio et al., 1991; Lynch, 2004; Waldvogel et al., 2007; Baer et al., 2009; Jonsson et al., 2009, 2012; Lu and Ye, 2011). GlyRs are a member of the cys-loop ligand gated ion channel superfamily, and are comprised of a pentameric arrangement of subunits that form a central anion-conducting pore. Many different compounds can modulate GlyR functioning, including alcohols, volatile anesthetics, and more (Lynch, 2004; Yevenes and Zeilhofer, 2011). Some of the behavioral effects of these compounds have been shown to be mediated by GlyR, as would be expected given GlyR expression in the regions important for these effects (Yamashita et al., 2001; Molander et al., 2005, 2007; Badanich et al., 2013).

Alcohols and volatile anesthetics enhance GlyR-mediated currents in a concentration dependent manner (Mascia et al., 1996a, 1996b). At the whole cell level, this results in left shifts of the concentration response curve with no effect on currents generated by maximally-effective concentrations of glycine (Welsh et al., 2010; Kirson et

al., 2012). At the single channel level, ethanol enhancement of GlyR-mediated currents results from ethanol decreasing glycine unbinding rates with no change to open probability (P_o), thus simply increasing durations of burst activity (Eggers and Berger, 2004; Welsh et al., 2009).

The sulfonic acid taurine acts as a partial agonist of the GlyR, having ~50% the efficacy seen at activating the channel compared to glycine (Lape et al., 2008). However, taurine is the second most abundant amino acid in the brain, and taurine release has been found to activate GlyR (Dahchour et al., 1996; Mori et al., 2002; Albrecht and Schousboe, 2005; Ericson et al., 2006; Choe et al., 2012). GlyRs have been implicated in mediating the effects of multiple drugs of abuse, and interestingly, taurine-mediated GlyR activation has been found to play a role in the rewarding effects of ethanol (Molander et al., 2005, 2007; Ericson et al., 2011; Jonsson et al., 2014). Unlike glycine-mediated GlyR currents, taurine-mediated GlyR currents are enhanced at maximally-effective concentrations of taurine, at the whole cell level, by many different modulators (Kirson et al., 2012, 2013). However, little research has been done into the effects of ethanol and other drugs of abuse on the taurine-activated GlyR at the single channel level.

Here we report on studies conducted on human α1 homomeric GlyR expressed in *Xenopus* oocytes, investigating various single channel parameters for modulation of taurine-mediated GlyR activation by ethanol and the volatile anesthetic isoflurane. We examined channel conductance, open dwell times, and closed dwell times, determining that ethanol and isoflurane enhance taurine-activated GlyR by stabilizing the open state, increasing the open probability (P_o).

5.2 – Materials and Methods

Isolation, injection, and patch clamp electrophysiology of *Xenopus* oocytes were described in Chapter 2. Specific methods pertaining to the experiments in this chapter are outlined below.

Outside-out patches were pulled from the animal pole of *Xenopus* oocytes expressing α1 homomeric WT GlyRs. Prior to recording, the oocyte was placed in a high-osmolarity stripping solution to aid in manual removal of the vitelline membrane using forceps. Patch pipettes were pulled from thick-walled borosilicate glass (WPI, Sarasota, FL) using a P-97 Flaming/Brown Micropipette Puller (Sutter Instruments). Pipettes were coated with wax or with Sylgard 184 (Dow Corning, Midland, MI) just above the tips and fire-polished with an MF-830 Microforge (Narishige, Japan) to obtain a smooth tip with resistances of 5 to 15 MΩ. Outside-out patches were held at –80 mV, and recordings were made according to standard methods (Hamill et al., 1981) using an Axopatch 200B amplifier (Molecular Devices, Sunnyvale, CA). Data was digitized at 50 kHz with a Digidata 1322A (Molecular Devices), low-pass filtered at 5 kHz, and recorded on a PC hard drive using pClamp 9 software (Molecular Devices). Taurine and drug solutions were prepared in external solution + 2.5 mM tricine (to chelate free zinc) before being perfused over outside-out patches using an SF-77B Perfusion Fast Step apparatus (Warner Instruments, Hamden, CT).

Data were analyzed using the single channel analysis programs in QUB (Qin et al., 2000a, 2000b); version 1.5.0.0 was used for preprocessing, open/closed dwell time analysis, and kinetic modeling. Tracings were first baseline-corrected and clusters were selected by eye that only had one channel present. These clusters were idealized using

the segmental-k-means (SKM) algorithm (Qin et al., 2000a, 2000b). Data were initially idealized with a simple two-state C ↔ O model. Multiple exponentials were subsequently fit and added sequentially to form a star model (closed state as the center) using the maximum interval likelihood (MIL) method after imposing a deadtime resolution of 60 μS. When this model was complete, as determined by log likelihood, the data were re-idealized and used for dwell time analyses. Dwell time distributions were constructed using a log time x-axis and a square-root count/total y-axis, and fit with a mixture of exponentials components using the MIL function. Clusters were defined as being separated by closed-time durations equal to or longer than 10 ms, based on previously determined τ_{crit} values (Welsh et al., 2009). P_o values were determined using Equation 2.4. Statistical analyses were performed using SigmaPlot version 11.0 (Systat Software, San Jose, CA) utilizing appropriate statistical tests as indicated.

5.3 – Results

5.3.1 – Ethanol and isoflurane do not affect taurine-activated GlyR single channel conductance

Single channel experiments were conducted on outside-out patches pulled from *Xenopus* oocytes expressing the human homomeric α1 GlyR. Patches were exposed to 200 mM ethanol or 0.55 mM isoflurane co-applied with 100 mM taurine and compared to patches exposed to 100 mM taurine alone. This saturating concentration of taurine was chosen to maximize channel opening (Lape et al., 2008) and appropriately examine the effects of these modulators on this partial agonist. 100 mM taurine alone or in

combination with one of the modulators produced clearly defined clusters of channel activity as seen in **Fig. 5.1**. Conductance of taurine-activated GlyR was 89 ± 3.4 pS (n = 5), and although decreased slightly in the presence of modulator, conductance was not significantly affected by ethanol [$t(11) = 2.00$, $p > 0.05$] or isoflurane [$t(8) = 2.30$, $p \geq 0.05$] as seen in **Fig. 5.2**.

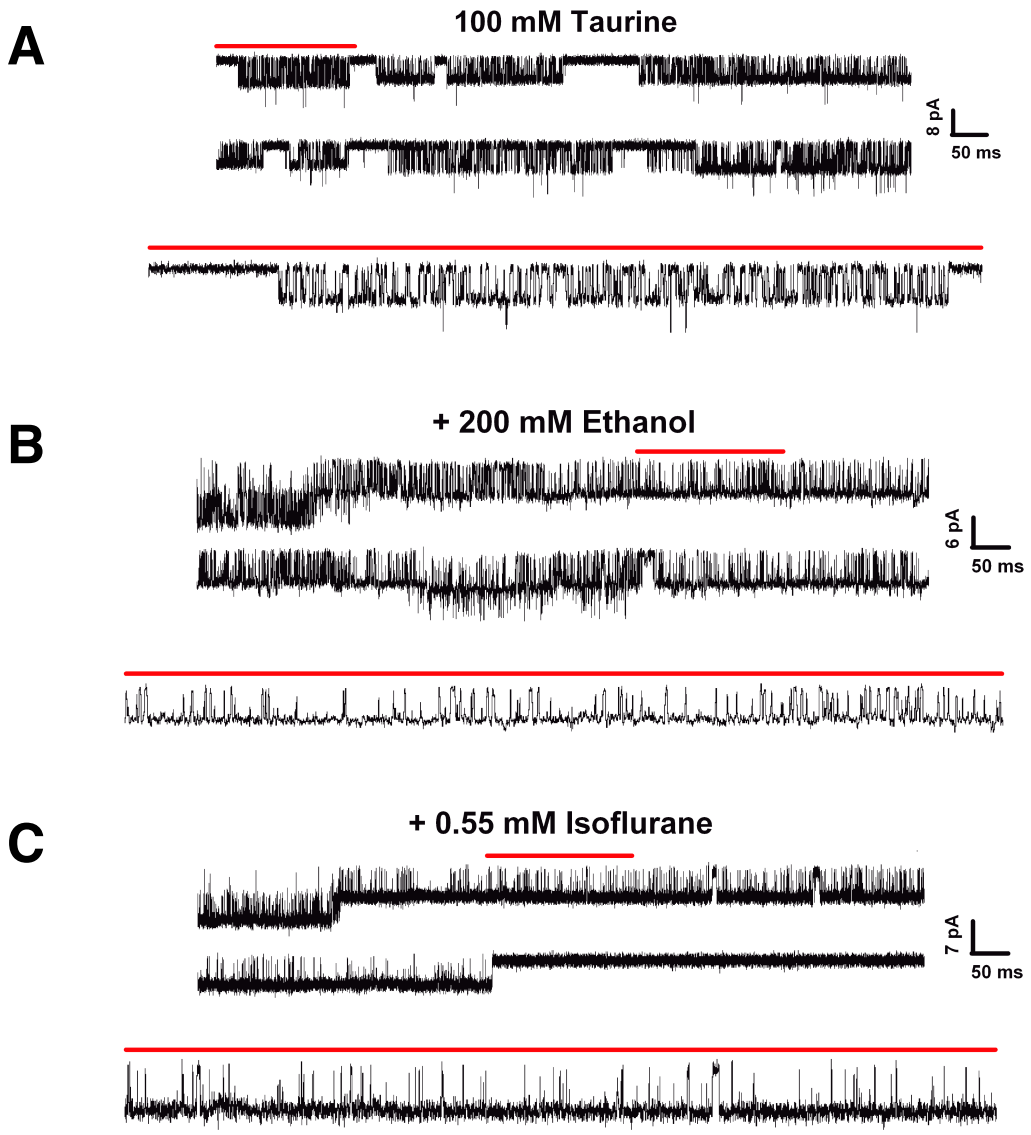

Figure 5.1 – Sample tracings of taurine-activated GlyR alone and with ethanol or isoflurane

Representative tracings show ~2 s of single channel homomeric α1 GlyR responses to 100 mM taurine (A), 100 mM taurine + 200 mM EtOH (B), or 100 mM taurine + 0.55 mM isoflurane (C). The red line above each top trace denotes the ~200 ms expanded view seen in the trace below.

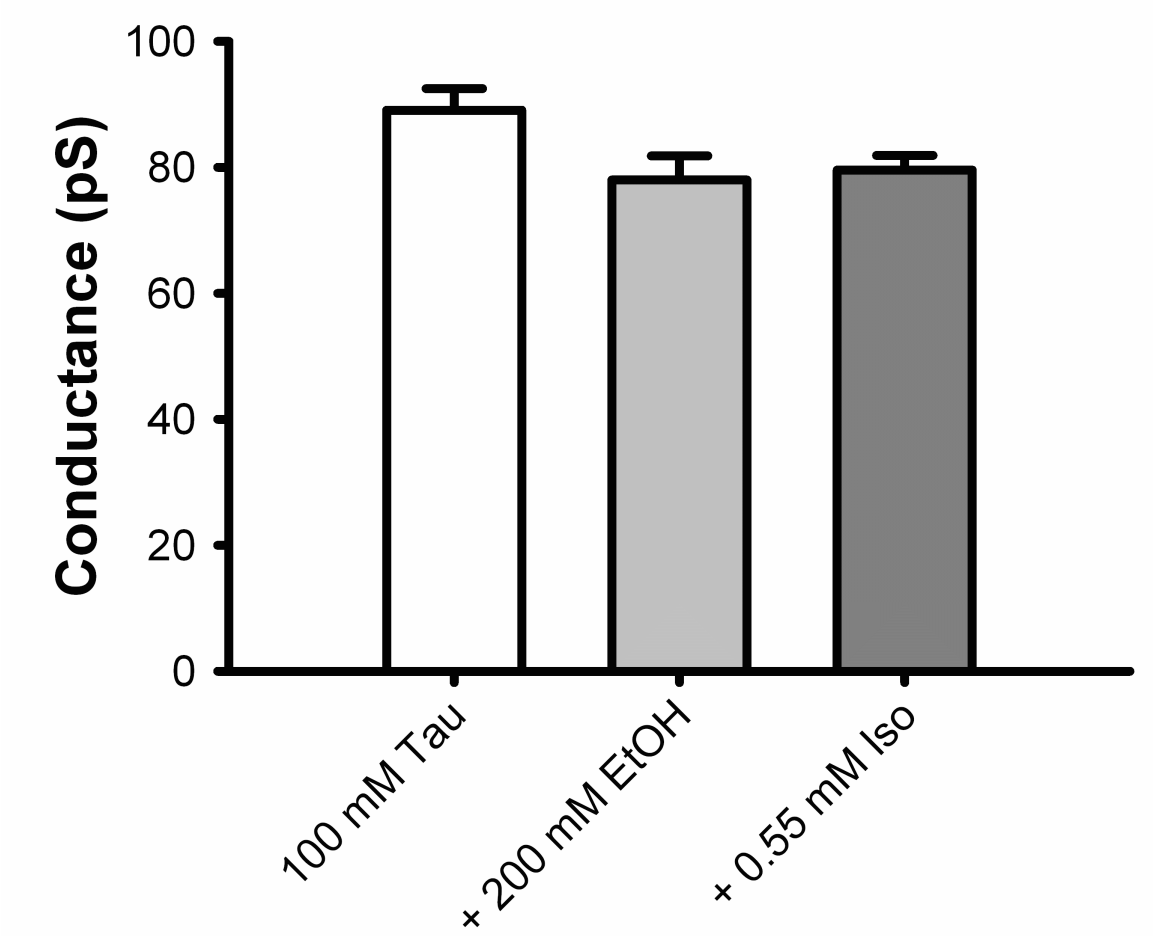

Figure 5.2 – Ethanol and isoflurane do not affect taurine-activated GlyR conductance

Conductance level (pS) is graphed for each condition. Taurine-activated GlyR conductance was 89 ± 3.4 pS as seen in the white bar. Ethanol (light grey bar) and isoflurane (dark grey bar) slightly decreased conductance to 78 ± 3.8 pS and 80 ± 2.3 pS respectively, though these decreases were not significant. Data are shown as mean + SEM of 5–8 patches.

5.3.2 – Ethanol and isoflurane increase taurine-activated GlyR mean open time without affecting mean closed time

When saturating taurine is applied alone, GlyR exhibit a mean open time of 0.90 ± 0.10 ms (n = 5). When co-applied with ethanol or isoflurane, mean open time is significantly increased to 1.46 ± 0.14 ms [$t(11) = 2.86$, $p < 0.05$] and 2.80 ± 0.78 ms [$t(8) = 2.43$, $p < 0.05$] respectively (**Fig. 5.3A**). However, neither ethanol nor isoflurane significantly affected mean closed time of taurine-activated GlyR [ethanol: $t(11) = 1.03$, $p > 0.30$; isoflurane: $t(8) = 1.53$, $p > 0.15$]. Although mean closed time of taurine-activated GlyR (0.60 ± 0.20 ms) was decreased by both ethanol (0.41 ± 0.08 ms) and isoflurane (0.29 ± 0.03 ms) as seen in **Fig. 5.3B**.

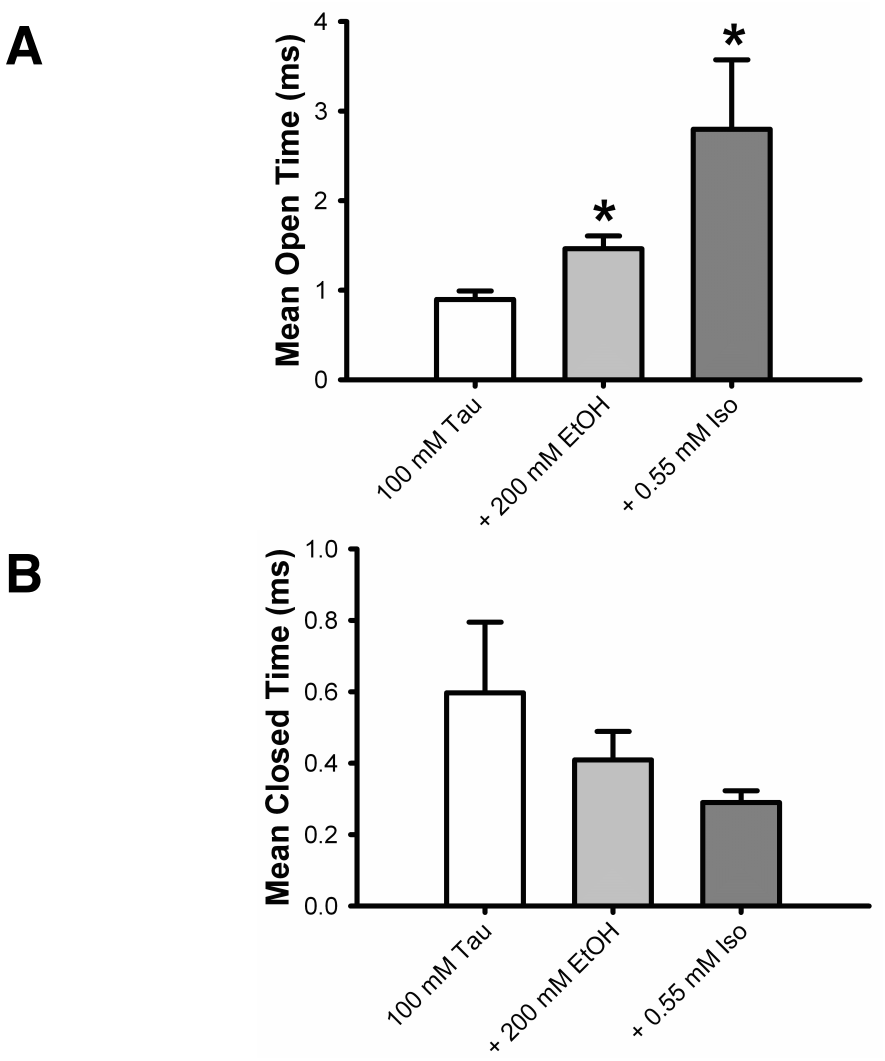

Figure 5.3 – Ethanol and isoflurane significantly increase mean open time of taurine-activated GlyR

A) Summary graph showing effects of ethanol (light grey bar) and isoflurane (dark grey bar) on mean open time of the taurine activated GlyR. Both modulators significantly increased mean open time of channels. B) Summary graph showing effects of ethanol (light grey bar) and isoflurane (dark grey bar) on mean closed time of the taurine activated GlyR. Neither modulator had a significant effect on mean closed time of channels. Data are shown as mean + SEM of 5–8 patches. *, $p < 0.05$.

5.3.3 – ETHANOL AND ISOFLURANE INCREASE THE LIKELIHOOD OF THE SECOND LONGEST OPEN TIME

Open dwell time data are adequately described using three exponential components for all conditions. Sample open dwell-time histograms from individual patches are shown in **Fig. 5.4A** for all three experimental conditions. A two-way ANOVA revealed each open lifetime is significantly different amongst the three components (τs) [$F(2,38) = 31.8$, $p < 0.001$] as expected. A Bonferroni post-hoc test found neither modulator affected the average durations of the first two open dwell-times, while the longest lived open dwell-time was changed with ethanol and isoflurane [$t(11) = 5.06$, $p < 0.001$; $t(8) = 3.11$, $p < 0.01$; respectively]. However, this difference was largely due to the error in the taurine alone data. The third open dwell-time could not be fit for all patches. Addition of modulator increased the prevalence of the third open dwell-time from 20% of taurine patches to 63% and 80% of ethanol and isoflurane patches respectively. Both ethanol (68.5 ± 5.8%) and isoflurane (68.7 ± 4.0%) significantly increased the likelihood of the second longest lived open time [Two-way ANOVA with Bonferroni post-hoc: $t(11) = 4.37$, $p < 0.001$; $t(8) = 3.95$, $p < 0.001$; respectively] from taurine (32.3 ± 6.9%), while significantly decreasing the likelihood (ethanol, 25.0 ± 7.0%; isoflurane, 20.9 ± 4.8%) of the shortest lived open time [$t(11) = 5.01$, $p < 0.001$; $t(8) = 4.96$, $p < 0.001$; respectively] when compared to taurine alone (66.6 ± 7.2%). Both modulators also increased the likelihood of the longest lived open time (ethanol, 6.5 ± 3.2%; isoflurane, 10.5 ± 4.8%) compared to taurine alone (1.2 ± 1.1%), but these increases were not significant. Summary graphs of these differences can be seen in **Fig. 5.4B,C**.

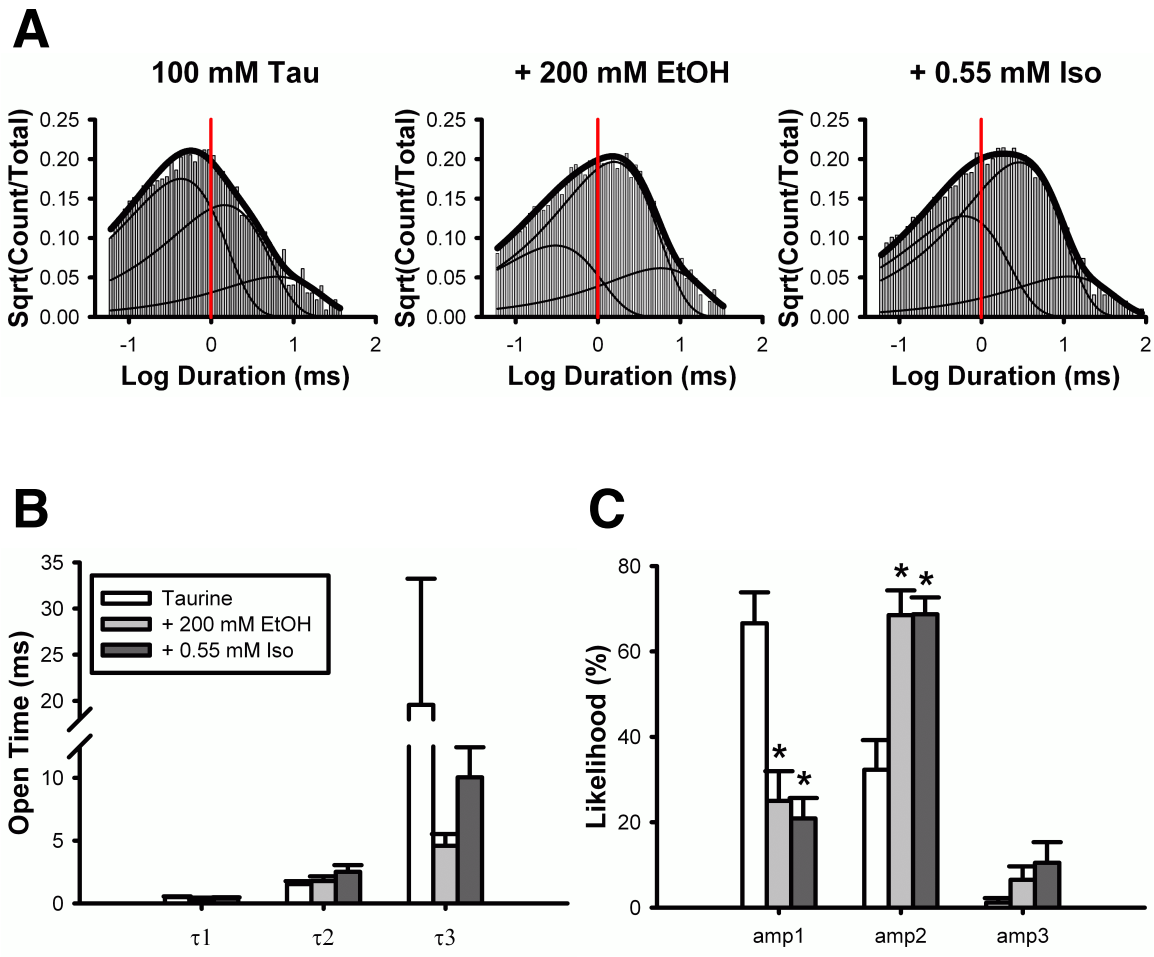

Figure 5.4 – Ethanol and isoflurane increase the likelihood of the second longest open time

A) Representative histograms demonstrating the fits for the open dwell-times. Each condition was fit using three open time components (τs). In each graph, the thinner lines describe the individual dwell-time exponential functions and the thicker line is a fit of the total data. The red line denotes 1 ms for visual aid of differences of fit. B) Neither modulator affected average duration of open dwell-times. C) Both ethanol and isoflurane increase the likelihood of the second longest open time while decreasing the likelihood of the shortest lived open time. Data are shown as mean + SEM of 5–8 patches. *, $p < 0.05$.

5.3.3 – ETHANOL AND ISOFLURANE HAVE NO EFFECT ON CHANNEL INTRACLUSTER CLOSED DWELL-TIME COMPONENTS

Intracluster closed dwell-times are adequately fit by three exponential components (τs) in all conditions tested. Sample closed dwell-time histograms for all conditions can be seen in **Fig. 5.5A**. Again as expected, there was a significant difference in the duration of the three closed dwell-time components [$F(2,42) = 91.8$, $p < 0.001$]. Neither ethanol nor isoflurane affected the duration of the closed times [$F(2,42) = 0.24$, $p > 0.75$] (**Fig. 5.5B**) nor the likelihood of any of the closed time components [$F(2,42) = 0.08$, $p > 0.90$] (**Fig. 5.5C**).

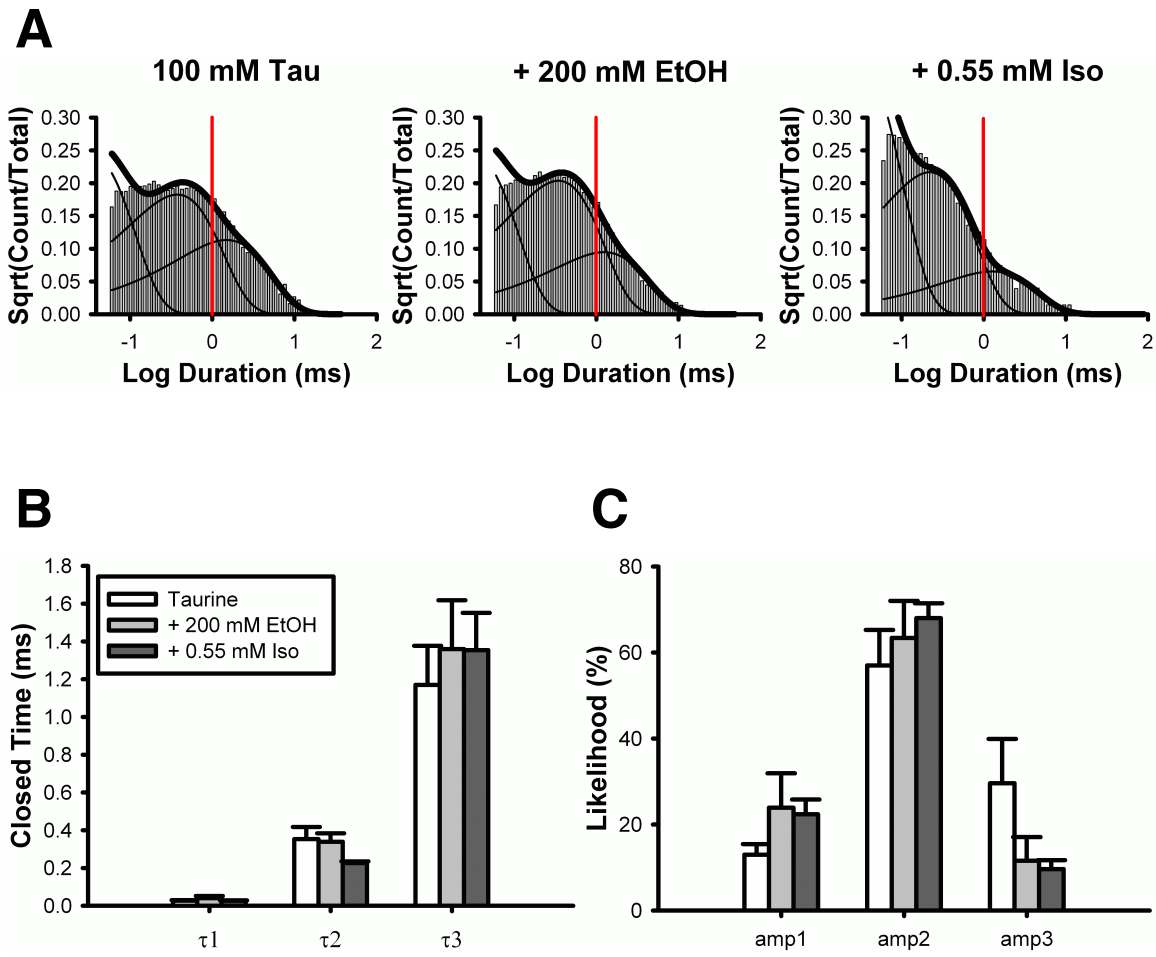

Figure 5.5 – Ethanol and isoflurane have no effect on closed dwell-time components

A) Representative histograms demonstrating the fits for the closed dwell-times. Each condition was fit using three closed time components (τs). In each graph, the thinner lines describe the individual dwell-time exponential functions and the thicker line is a fit of the total data. The red line denotes 1 ms for visual aid of fits. B) Neither modulator affected average duration of closed dwell-times. C) Neither modulator affected likelihood of the closed time components. Data are shown as mean + SEM of 5–8 patches.

5.3.3 – ETHANOL AND ISOFLURANE INCREASE INTRACLUSTER P_O

Ethanol and isoflurane increased mean open time by increasing the likelihood of longer lived open time components (**Fig. 5.3, 5.4**). However, neither modulator tested had any effects on closed time components (**Fig. 5.5**). Thus, when intracluster open probability (P_o) was calculated as a ratio of open time to total cluster time, both ethanol (0.78 ± 0.03) and isoflurane (0.89 ± 0.02) significantly increased P_o [ethanol: $t(11) = 2.37$, $p < 0.05$; isoflurane: $t(8) = 4.098$, $p < 0.01$] compared to the taurine-activated GlyR P_o (0.63 ± 0.06). This increase can be seen in **Fig. 5.6** below. These increases in P_o correspond to taurine efficacies (E) of 3.55 for ethanol and 8.09 for isoflurane, increased above the E of 1.70 for taurine alone (equation 1.4).

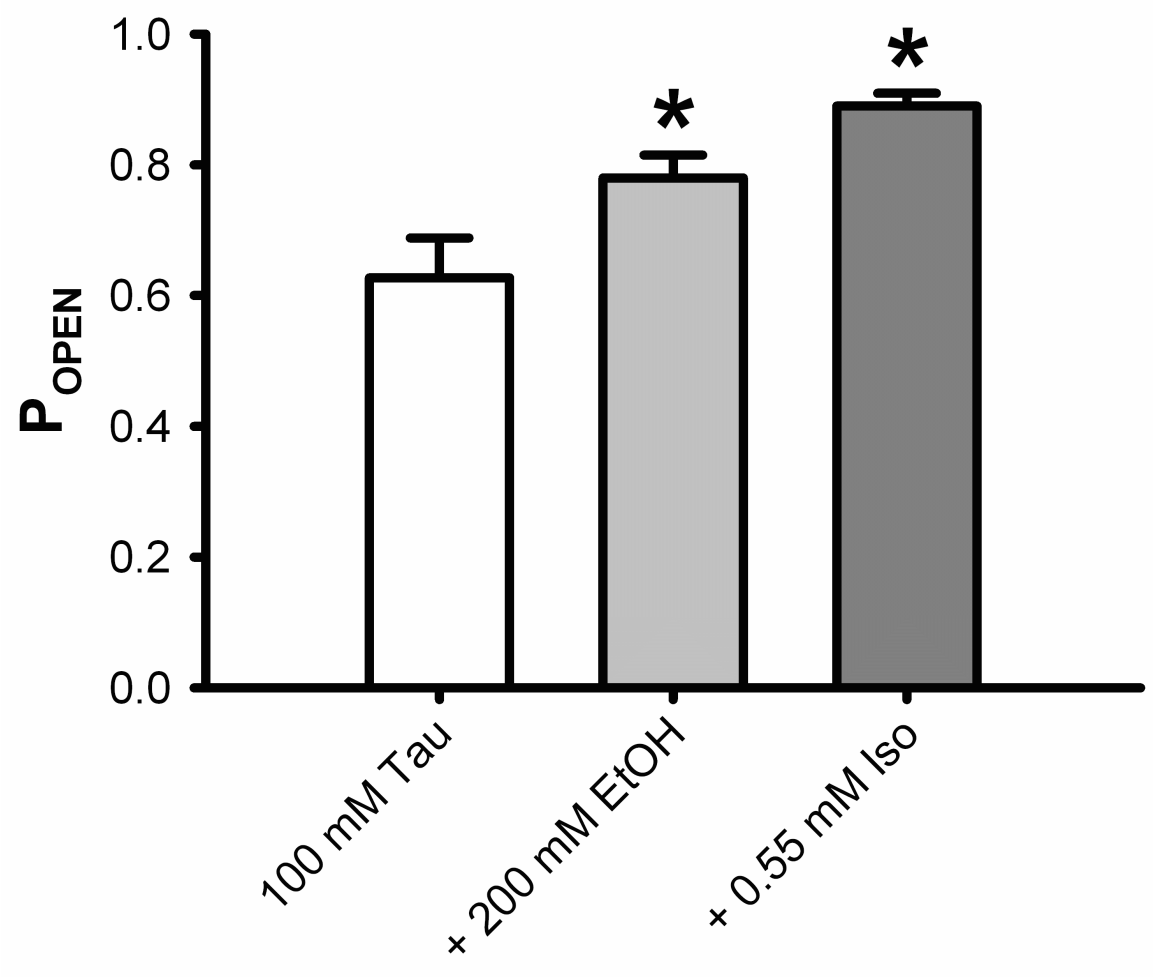

Figure 5.6 – Ethanol and isoflurane increase taurine-activated GlyR P_o

Intracluster P_o is shown for 100 mM taurine alone (white bar), and with ethanol (light grey bar) or isoflurane (dark grey bar). Both ethanol and isoflurane significantly increased intracluster P_o. Data are shown as mean + SEM. *, $p < 0.05$.

5.4 – Discussion

Ethanol and volatile anesthetics act as nervous system depressants and produce a variety of behavioral effects including memory loss, loss of consciousness at high concentrations, and have reinforcing properties through modulation of the mesolimbic dopamine system believed to be responsible for reward. In many of the brain areas responsible for these behavioral effects, functional GlyR have been found (Yamashita et al., 2001; Molander et al., 2005, 2007; Badanich et al., 2013) and taurine may act as an endogenous ligand for these GlyR (Dahchour et al., 1996; Mori et al., 2002; Ericson et al., 2006, 2011; Choe et al., 2012). Thus, here we have examined the effects of two of these compounds, ethanol and isoflurane, on the single channel properties of the GlyR when activated by taurine instead of glycine.

We have previously shown that allosteric modulators have differential effects on GlyR responses when activated by different agonists (Kirson et al., 2012, 2013). However, in these whole cell experiments we were only able to suggest the effects of these compounds at the single channel level. Here we have performed these single channel experiments and find that both ethanol and isoflurane increase GlyR open state likelihoods when activated by taurine, consistent with our previous data. Although the longest lived open state appeared to differ with modulator present, this is due to the low occurrence of this open time in the taurine alone condition. Interestingly, both of the modulators tested increased the occurrence of this longer lived state, in agreement with the rest of the data suggesting a stabilization of longer lived open times. This again shows differences in allosteric modulator effects on GlyR that are agonist dependent. In single channel investigations into the effects of ethanol on the glycine-activated GlyR, no

changes to open times were seen. Ethanol exerted its potentiating effects of GlyR currents by decreasing the rate of glycine unbinding (Eggers and Berger, 2004; Welsh et al., 2009). Thus, at the single channel level, ethanol enhancement of GlyR functioning is dependent on which agonist activates it. Interestingly, while the mechanism with which ethanol and isoflurane increase taurine activated GlyR open states is similar, the degree to which these changes occur is consistent with isoflurane being a more potent modulator at the whole cell level (Kirson et al., 2012).

It is worth considering the possible effects of isoflurane on glycine-gated GlyR at the single channel level. As this modulator has no effects on currents generated by maximally-effective concentrations of glycine (Kirson et al., 2012), it is likely isoflurane would not stabilize GlyR open states at saturating concentrations, as glycine already displays a very high P_o. However, at sub-maximal concentrations of glycine, where there is no ceiling effect of P_o, isoflurane does appear able to increase mean open time and P_o (Roberts, 2005). Then, are effects of these compounds at high concentrations of taurine important?

In examining the nature of partial agonism on the GlyR, Lape et al., (2008) examined both glycine- and taurine-activated GlyR at the single channel level with varying concentrations of agonist. Interestingly, when their data was fit to a kinetic mechanism, they found states corresponding to three bindings of agonist, be it glycine or taurine. However, taurine-mediated GlyR openings were rare at low concentrations, leading to a fit of only gating constants with at least two taurine bound. In fact, the rate constants found for transitions to the open state when only two taurine are bound were low while rates governing the transition to the closed state were exceptionally high (Lape et al., 2008). Thus, at any concentration of taurine where two molecules are bound to the

GlyR, it is far more likely another taurine will bind before the channel can open. Therefore, where the taurine-activated GlyR is concerned, only saturating concentrations of agonist are useful in studying to ensure channel opening. Glycine-activated GlyR can still open with only a single glycine bound, thus modulator effects are more difficult to interpret when comparing between glycine and taurine. For example, at a whole cell level, low concentrations of glycine elicit currents generated by an amalgam of GlyR occupied by one or more glycine molecules, while currents generated by taurine are likely exclusively from a subpopulation of fully occupied GlyR (at least three taurines bound). Additionally *in vivo* measured release of taurine can increase the extracellular concentration tenfold; at synaptic or perisynaptic regions, this can result in saturating concentrations of taurine at GlyR (Albrecht and Schousboe, 2005; Scimemi and Beato, 2009). As we used only saturating concentrations of taurine, we did not attempt to fit the data to one of the currently accepted kinetic models of GlyR activation, as we have eliminated any affinity rate constant consideration. Instead we desired to examine the effects of these compounds on a descriptive model of the data only.

In summary, we have investigated the effects of ethanol and isoflurane on the saturating taurine-activated GlyR at the single channel level, and found both modulators increase taurine efficacy at opening the GlyR. Additionally, these effects are distinct from effects on glycine-activated GlyR at the concentrations of agonist likely to be seen *in vivo*. As more evidence accumulates for the physiological role of the taurine-activated GlyR, utilizing the nature of differential GlyR modulation when taurine is the agonist will be useful for targeted approaches at drug discovery and therapy involving GlyR.

6.0 | DISRUPTION OF AN INTERSUBUNIT ELECTROSTATIC BOND IS A KEY DETERMINANT OF AGONIST EFFICACY

6.1 – Introduction

The glycine receptor (GlyR) is an anion conducting member of the cys-loop receptor superfamily of ligand-gated ion channels (LGICs). The GlyR is composed of a pentameric arrangement of subunits around the ion conducting pore. Each subunit contains a large extracellular domain, four transmembrane domains (TM), and a large intracellular domain between TM3 and TM4. In the pentameric arrangement, TM2 of each subunit lines the pore. The ligand-binding domain lies in between extracellular domains of adjacent subunits, and is comprised of loops from each side of the interface (Lynch, 2004; Grudzinska et al., 2005). Ligand binding causes a conformational change that allows loops from the extracellular domain to contact the TM regions and cause opening of the channel (Langosch et al., 1994; Rajendra et al., 1995; Lynch et al., 1997; Lynch, 2004; Lee and Sine, 2005). Analysis of the contribution of individual residues to the gating reaction in the related nicotinic acetylcholine receptor (nAChR), revealed that groupings of residues of this channel move in concert, in a conformational wave of activity from agonist binding to gating of the pore (Purohit et al., 2007).

GlyR can also be activated by the endogenous sulfonic acid taurine, which may be the endogenous ligand for extrasynaptic GlyR in some brain areas (Mori et al., 2002). Taurine acts as a partial agonist at the GlyR, having a decreased maximum response to taurine when compared to glycine (Schmieden et al., 1992; McCool and Botting, 2000; Lape et al., 2008; Welsh et al., 2010; Kirson et al., 2012). A recent study examining the

single channel characteristics of the α1β GlyR found that taurine was less efficacious at transitioning the receptor from a bound closed state to an intermediate closed state prior to the final gating step (Lape et al., 2008). Taurine reduction in transitioning to this "fllipped" state results in taurine having an efficacy of opening the channel that is ~50% that of glycine. This kinetic model places the root of partial agonism earlier than the final gating step and when considered in combination with the Φ-analysis of the conformational wave of activity from binding to gating (Purohit et al., 2007), this suggests that partial agonist efficacy may be determined early after ligand binding.

Previously we identified a charged residue, D97 in the α1 homomeric GlyR, pointing into the intersubunit interface (from the principal subunit) that is highly conserved throughout the cys-loop receptor superfamily (Beckstead et al., 2002). A charge swap mutation at this residue (D97R) results in a channel that can sporadically spontaneously open (Beckstead et al., 2002). Single channel characterization of the D97R mutant found that clusters of spontaneous activity had an open probability (Po) of 0.91, almost identical to the Po of 0.90 for glycine on wild type GlyR and the Po of 0.96 for glycine on homomeric GlyR (Lape et al., 2008; Todorovic et al., 2010). We recently found that taurine-activated D97R clusters have a Po of 0.98, transforming taurine from a partial agonist to one with high efficacy (Welsh et al., *In prep*). We previously found that spontaneous activity in this mutant is due to disruption of an intersubunit electrostatic bond with residue R119 on the adjacent (complementary) subunit, proposed to aid in keeping the receptor in the closed state (Todorovic et al., 2010). A double charge reversal mutation of these residues (D97R/R119E) repaired this electrostatic interaction and resulted in decreased spontaneous activity (Todorovic et al., 2010). However, this

R119E mutation greatly right shifted concentration response curves, leading us to question whether the R119 residue was the true bond partner for the D97 residue.

On the basis of updated computer models of the GlyR extracellular domain (Trudell J, *personal communication with Mihic SJ*), we identified a residue, R131, in the intersubunit interface as a possible alternate binding partner for D97. Thus, we investigated a charge reversal mutation of this residue, R131D, at the whole cell and single channel levels, under the hypothesis that a mutation to this residue would result in spontaneous activity of GlyR, and that taurine would have an increased efficacy on this mutant, similar to D97R.

6.2 – Materials and Methods

Isolation, injection, and patch clamp electrophysiology of *Xenopus* oocytes were described in Chapter 2. Specific methods pertaining to the experiments in this chapter are outlined below.

All chemicals were purchased from Sigma-Aldrich (St. Louis, MO). *Xenopus laevis* were obtained from Nasco (Fort Atkinson, WI) and housed at 19°C on a 12-h light/dark cycle. Portions of ovaries were removed and placed in isolation media. Forceps were used to manually remove the thecal and epithelial layers from stage V and VI oocytes. The oocyte follicular layer was removed using a 10 min incubation in 0.5 mg/ml type 1A collagenase (Sigma-Aldrich) solution. Animal poles of oocytes were injected with 30 nl of the wild type (WT) or mutant glycine α1-receptor subunit cDNA (1.5 ng/30 nl) in a modified pBK-cytomegalovirus vector (Mihic et al., 1997) by the "blind" method of Colman (1984), using a micropipette (10–15 μm tip size) attached to an electronically activated microdispenser. Oocytes were stored in the dark at 19°C in 96-well plates containing incubation media. Oocytes expressed the wild-type, R131D, and D97R/R131D GlyR within 24 h, and all electrophysiological measurements were made within 5 days of cDNA injection.

For whole cell recordings, oocytes were impaled in the animal pole with two high-resistance (0.5–10 MΩ) glass electrodes filled with 3 M KCl. Cells were voltage clamped at –70 mV using an OC-725C oocyte clamp (Warner Instruments, Hamden, CT) and perfused with MBS at a rate of 2 ml/min using a Masterflex USA peristaltic pump (Cole Parmer Instrument Co., Vernon Hills, IL) through 18-gauge polyethylene tubing. All drug solutions were prepared in MBS. Applications lasted for 15–60 s followed by 6

to 10 min washout periods to allow for complete receptor resensitization. Currents were acquired using either a Powerlab 4/30 digitizer with LabChart version 7 software (ADInstruments, Bella Vista, NSW, Australia). Peak currents were measured and used in data analysis.

Outside-out patches were pulled from the animal pole of *Xenopus* oocytes expressing WT, R131D, or D97R/R131D α1 homomeric WT GlyRs. Prior to recording, the oocyte was placed in a high-osmolarity stripping solution to aid in manual removal of the vitelline membrane using forceps. Patch pipettes were pulled from thick-walled borosilicate glass (WPI, Sarasota, FL) using a P-97 Flaming/Brown Micropipette Puller (Sutter Instruments). Pipettes were coated with wax or with Sylgard 184 (Dow Corning, Midland, MI) just above the tips and fire-polished with an MF-830 Microforge (Narishige, Japan) to obtain a smooth tip with resistances of 5 to 15 MΩ. Outside-out patches were held at –80 mV, and recordings were made according to standard methods (Hamill et al., 1981) using an Axopatch 200B amplifier (Molecular Devices, Sunnyvale, CA). Data was digitized at 50 kHz with a Digidata 1322A (Molecular Devices), low-pass filtered at 5 kHz, and recorded on a PC hard drive using pClamp 9 software (Molecular Devices). Taurine solutions were prepared in external solution + 2.5 mM tricine (to chelate free zinc) before being perfused over outside-out patches using an SF-77B Perfusion Fast Step apparatus (Warner Instruments, Hamden, CT).

Data were analyzed using the single channel analysis programs in QUB (Qin et al., 2000a, 2000b); version 1.5.0.0 was used for preprocessing, and open probability determination. Tracings were first baseline-corrected and clusters were selected by eye that only had one channel present. These clusters were idealized using the segmental-k-means (SKM) algorithm (Qin et al., 2000a, 2000b). Data were idealized with a simple

two-state C ↔ O model. Multiple exponentials were subsequently fit and added sequentially to form a star model (closed state as the center) using the maximum interval likelihood (MIL) method after imposing a deadtime resolution of 60 μS. When this model was complete, as determined by log likelihood, the data were re-idealized and used for dwell time analyses. Dwell time distributions were constructed using a log time x-axis and a square-root count/total y-axis, and fit with a mixture of exponentials components using the MIL function. Clusters were defined as being separated by closed-time durations equal to or longer than 10 ms, based on previously determined τ_{crit} values (Welsh et al., 2009). P_o values were determined using Equation 2.4.

A homology model of GlyR α1 was built by threading the GlyR primary sequence onto an x-ray crystal structure template using the Modeler module of Discovery Studio (Todorovic et al., 2010). The template we used was the prokaryotic ligand-gated ion channel homolog GLIC (PDB ID 3EAM) (Bocquet et al., 2009).

6.3 – Results

6.3.1 – R131D GlyR mutation increases taurine efficacy

The putative location of the R131 residue in relation to D97 and the previously studied R119 can be seen in **Fig. 6.1**. We have previously verified proximity of these residues using cysteine substitutions at these residues to form disulfide bonds (Todorovic, 2010). Varying concentrations of glycine and taurine were assayed on homomeric R131D α1 GlyR and used to generate concentration-response curves, as seen in **Fig. 6.2**. Unlike the R119E mutant receptor, R131D GlyR have a glycine concentration-response curve similar to that of WT receptors (Welsh et al., 2010; Kirson et al., 2012), with an EC_{50} for glycine of 0.35 ± 0.08 mM and a Hill coefficient, n_H of 1.43 ± 0.42. While taurine responses could not be fit with a concentration response curve, the graph does show that taurine responses are somewhat right shifted from glycine responses with saturating taurine concentrations generating responses at or greater than saturating glycine generated responses.

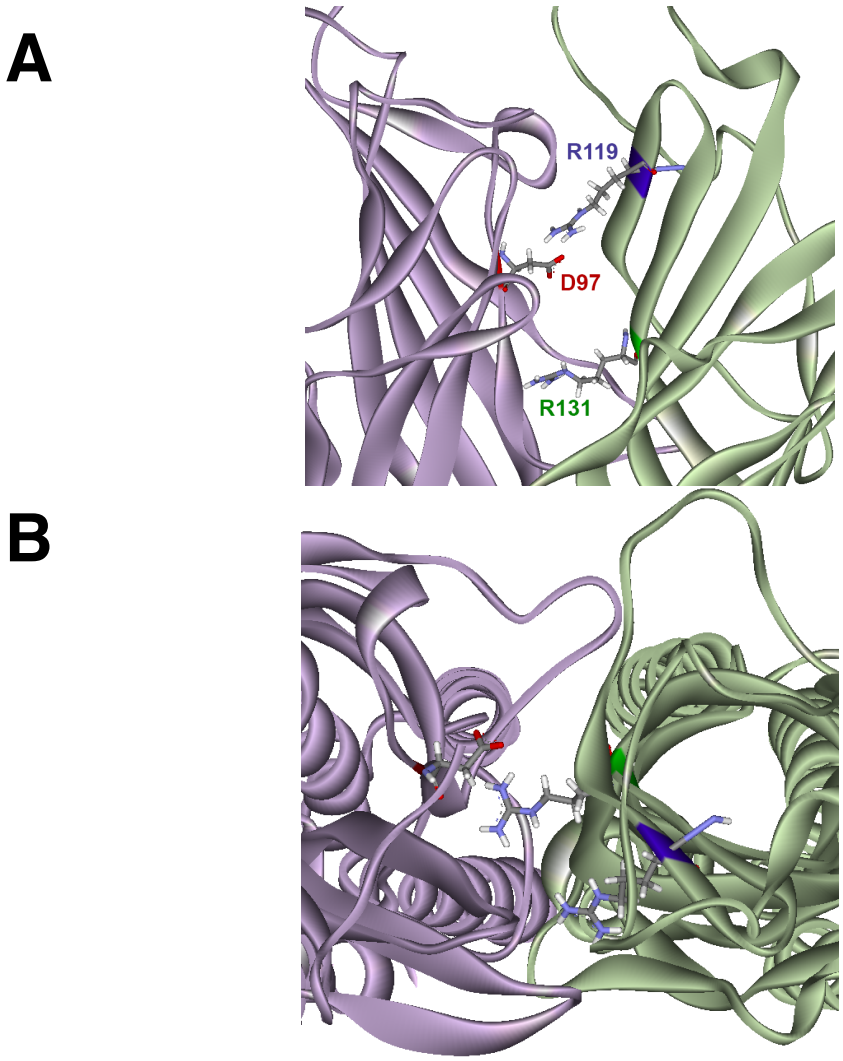

Figure 6.1 – Homology model of the α1 GlyR intersubunit interface

A) A homology model of GlyR was built as described in chapter 6.2. Here two of the five subunits of the homopentamer are shown (side view) with a ribbon structure to highlight the intersubunit interface where R131 is located in proximity to D97 and R119. The (+) and (–) interfaces of adjacent subunits are colored purple and green respectively. Amino acids D97, R131, and R119 have colored backbones of red, green, and blue respectively. Nitrogen atoms are depicted in light blue, oxygen in red, carbon in gray, and hydrogen in white. B) Top down view of the same interface as in A.

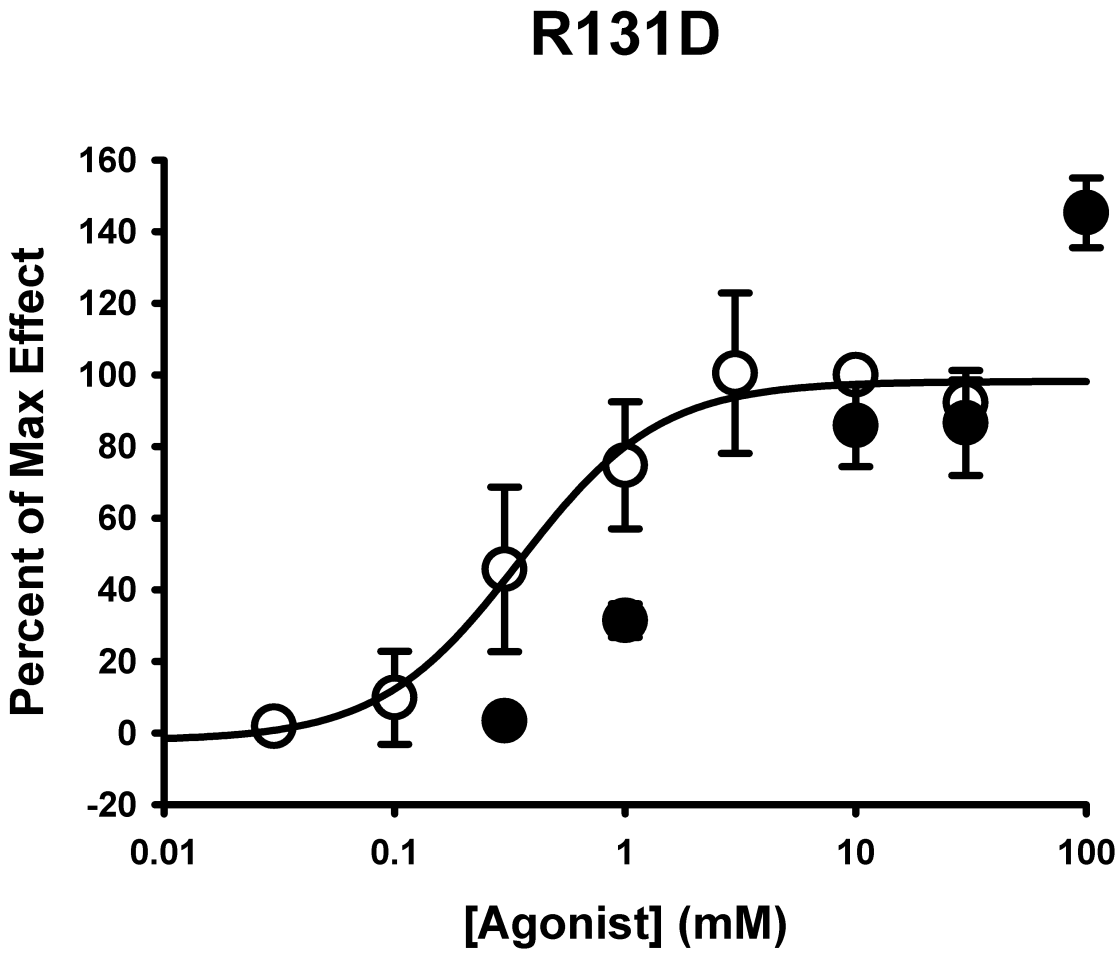

Figure 6.2 – R131D GlyR do not affect glycine currents while increasing taurine peak currents

Open symbols represent glycine-mediated responses, and filled symbols show taurine-mediated responses. Line is a logistic fit to the glycine set of data. Glycine activation of the GlyR produced an EC_{50} of 0.35 mM with a Hill coefficient (n_H) of 1.43. Data are shown as mean ± SEM of 3–8 oocytes.

6.3.2 – D97R/R131D GlyR mutation increases taurine efficacy

We next investigated the double mutant D97R/R131D GlyR. With this double mutation, the putative intersubunit electrostatic bond is repaired, which we hypothesized would decrease spontaneous activity and, unlike the D97R/R119E mutant, would retain normal glycine response behavior. We again generated concentration response curves for varying concentrations of both glycine and taurine as seen in **Fig. 6.3**. Again, similar to the R131D single mutant, the glycine concentration response curve were very similar to WT GlyR with an EC_{50} of 0.25 ± 0.05 mM and an n_H of 1.42 ± 0.39. The taurine concentration response curve had an EC_{50} of 1.59 ± 0.20 mM and an n_H of 0.91 ± 0.11. This EC_{50} is again close to previously determined taurine EC_{50} on WT GlyR (Welsh et al., 2010; Kirson et al., 2012), though the Hill coefficient is slightly decreased, indicating a modest loss of cooperatively of taurine binding. Again, as with the single R131D mutant, saturating taurine concentrations generated responses at or greater than saturating glycine generated responses.

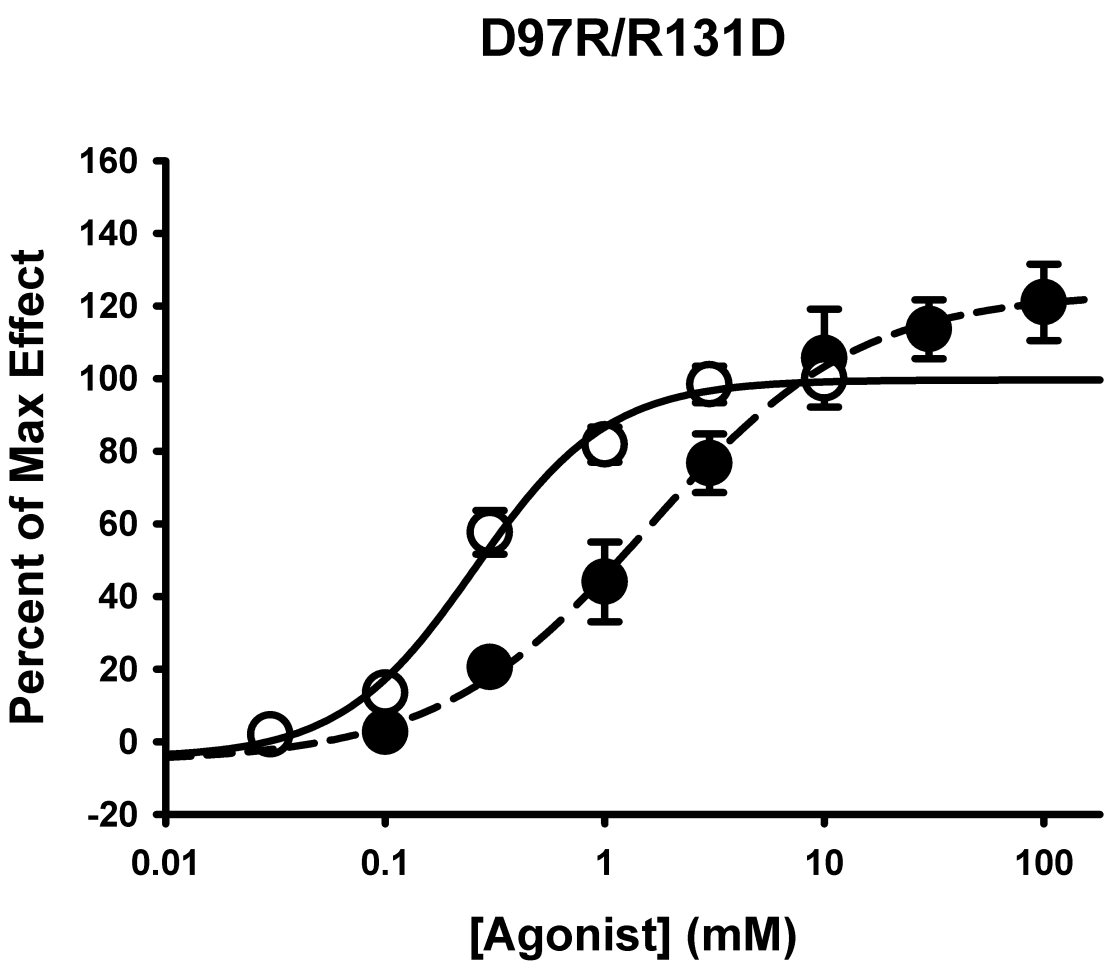

Figure 6.3 – D97R/R131D GlyR do not affect glycine currents while increasing taurine peak currents

Open symbols represent glycine-mediated responses, and filled symbols show taurine-mediated responses. Lines are a logistic fit to the glycine (solid) and taurine (dashed) sets of data. Glycine activation of the GlyR produced an EC_{50} of 0.25 mM with a Hill coefficient (n_H) of 1.42. Taurine activation of the GlyR produced an EC_{50} of 1.59 mM with a Hill coefficient (n_H) of 0.91. Data are shown as mean ± SEM of 3–9 oocytes.

6.3.3 – R131D AND D97R/R131D GLYR SINGLE CHANNEL CHARACTERIZATION

Outside out patches were pulled from *Xenopus* oocytes expressing either the R131D or D97R/R131D GlyR and exposed to 100 mM taurine. To date, clusters from only a single patch for each mutant have been obtained and analyzed, thus the following characterization will describe each patch as an example for the two mutants. An example tracing for each mutant activated by 100 mM taurine can be seen in **Fig. 6.4** below.

Recordings from both mutants were obtained first in the presence of no agonist, with only external solution being applied to the patch, in order to determine spontaneous activity of these mutants. We have previously examined spontaneous activity of these mutants on the whole cell level, noting that holding currents for R131D GlyR expressing oocytes are larger than for WT GlyR expressing oocytes or uninjected oocytes (Todorovic, 2010). However, for both the R131D and D97R/R131D patches, no spontaneous cluster activity was seen in the absence of agonist.

For both R131D and D97R/R131D mutant GlyR, taurine-activated clusters were long lived, with short and sparse closings (**Fig. 6.4**). Mean open times were 115.44 ms for taurine-activated R131D GlyR and 141.92 ms for taurine-activated D97R/R131D GlyR. Mean closed times were 0.27 ms for R131D GlyR and 0.34 ms for D97R/R131D. Intracluster P_o for taurine-activated R131D GlyR was 0.998 and was 0.997 for D97R/R131D GlyR when activated by saturating taurine. These long open times for these high P_o clusters resulted in very few closing events that made dwell time analyses unreliable, thus these analyses were not conducted. Equation 1.4 would then give efficacy values (E) of ~499 for the taurine-activated R131D GlyR, and ~332 for the taurine-activated D97R/R131D GlyR.

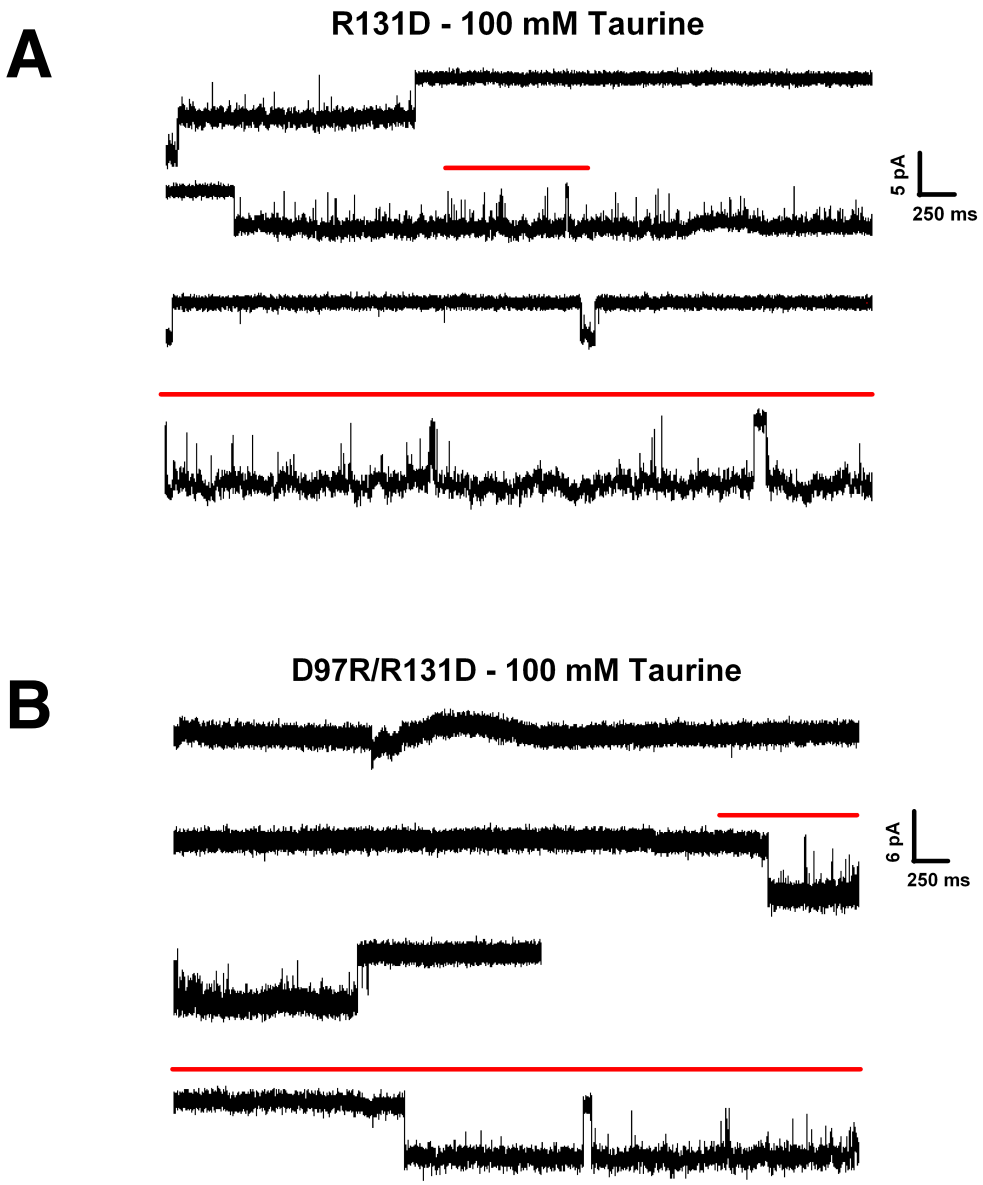

Figure 6.4 – Sample tracings of taurine-activated R131D and D97R/R131D GlyR

Representative tracings show ~12–15 s of single channel responses to 100 mM taurine for homomeric R131D α1 GlyR (A), and homomeric D97R/R131D α1 GlyR (B). The red line above each top trace denotes the ~1 s expanded view seen in the trace below.

6.3.4 – TAURINE RELATIVE EFFICACY TO GLYCINE IS DIRECTLY AFFECTED BY TEMPERATURE

Disruption of the closed conformation electrostatic bond between D97 and R131 enhances taurine efficacy. We therefore reasoned that taurine partial agonism may result from a decreased ability to break this bond relative to glycine. Thus, we hypothesized that any experimental modification that weakens this interaction would enhance taurine's ability to break this bond, and increase taurine efficacy relative to glycine. Thus we examined the effects of taurine and glycine activation of the GlyR in a variety of temperatures. **Fig. 6.5A** shows the effects of recording whole-cell currents in oocytes at temperatures ranging from 10 – 30°C using saturating concentrations of glycine or taurine. Absolute glycine currents in WT GlyR were minimally affected by temperature (38.2 ± 7.9% potentiation, comparing 10°C with 30°C), but there was a significant [$t(6) = 3.75$, $p<0.01$] increase seen in taurine's ability to open the GlyR channels under warmer conditions (265.9 ± 60.3% potentiation). Maximal taurine responses were normalized against maximal glycine responses at each temperature (**Fig. 6.5B**). Taurine's efficacy relative to glycine was clearly dependent on temperature, ranging from approximately 15% at 10°C and increasing to ~45% at 37°C.

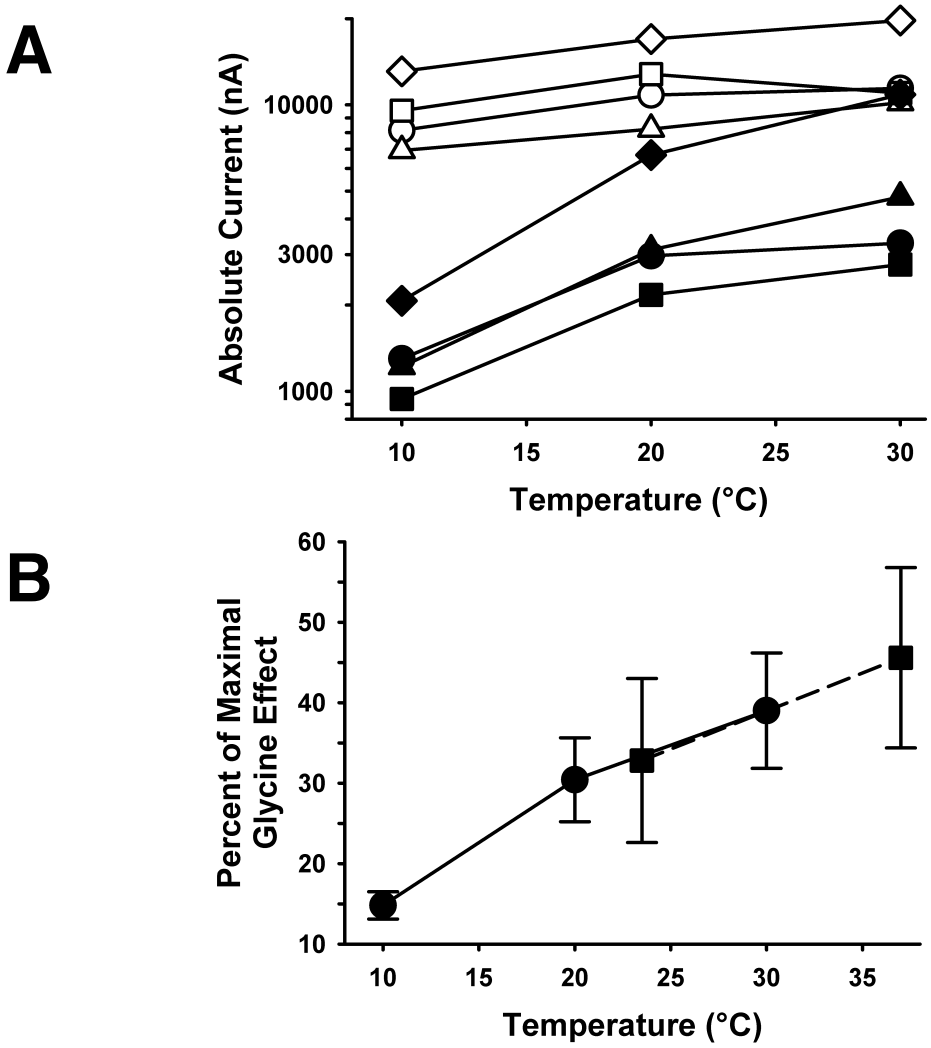

Figure 6.5 – Dependence of taurine efficacy on temperature

A) Absolute GlyR current responses to 100 mM taurine increase with temperature. Each symbol represents a different oocyte, with open symbols showing current response to 10 mM glycine and closed symbols showing current response to 100 mM taurine. B) Average responses to 100 mM taurine as a percentage of the response to 10 mM glycine increase with increasing temperature. Circles and the solid line show the results from a set of oocytes tested at 10°C, 20°C, and 30°C (n = 4 oocytes), while squares and the dashed line show results from oocytes tested at 23.5°C (room temperature) and 37°C (n = 6 oocytes.

6.4 – Discussion

In this chapter we have shown that disruption of the putative electrostatic bond between residues D97 and R131 of the α1 GlyR increases taurine efficacy. This finding is in agreement with our previous investigation of mutations at the D97R residue (Welsh et al., *In prep*). This indicates that the intersubunit interface region where binding occurs may be an important determinant of agonist efficacy. The case for an early determination of agonist efficacy would be in agreement with the findings from Lape et al. (2008) that place the mechanism of partial agonism in taurine's reduced ability, relative to glycine, to cause a transition to an additional intermediate closed state. Disruption of this electrostatic bond would essentially transition the GlyR to the "flipped" state, where glycine and taurine are similar in their efficacy at moving to the open state. However, if disruption of the D97–R131 interaction results in the flipped state, then we would expect behavior of the R131D single mutant to parallel the behavior of the D97R single mutant. Unfortunately, unlike D97R, we do not see clear single channel open clusters in the absence of agonist for R131D single channel recordings.

Interestingly, when this electrostatic bond is restored with the double mutation D97R/R131D, taurine retains high efficacy. However, in both the R131D single mutant (disruption of bond) and the D97R/R131D double mutant (restored bond) glycine-mediated responses at the whole cell level were essentially normal. An implication of this finding is that disruption of the D97–R131 interaction is not indicative of the intermediate flipped state. Restoration of the electrostatic interaction with the double mutant D97R/R131D would theoretically reduce taurine efficacy back to being a partial agonist. Perhaps then, the conserved D97 residue is stabilized in the intersubunit

interface by multiple residues from the complementary subunit. For example, R119 and R131 may both interact with D97 to hold the receptor in the closed state. Mutation of D97 would disrupt all interactions, and result in spontaneous activity and increased efficacy of partial agonists. Mutation of either R119 or R131 alone would only weaken the interactions, resulting in less spontaneous activity but increased efficacy of partial agonists. Double mutations involving D97 and one of the binding partners would artificially create the conditions of a single mutation to one of the positively charged residues, with a functional bond to reduce spontaneous activity, but a disrupted interaction with the other binding partner resulting in increased partial agonist efficacy.

Another implication of this study is that the R131 residue is not directly involved in glycine binding as concentration response curves were not changed. This finding is in stark contrast to mutations at the R119 residue, that greatly right shifted concentration response curves (Todorovic et al., 2010). However, R131 may have some effect on taurine binding. Efficacy for taurine on these mutants was extraordinarily high. Based on equation 1.3, if taurine efficacy alone was increased, EC_{50} of the taurine concentration response curve would be expected to decrease. To retain the same EC_{50} as seen for taurine-activation of the double mutant D97R/R131D, an appropriate increase in K_d would be necessary to balance the increase in E. Interestingly, the n_H was correspondingly decreased for taurine actions on this double mutant. Thus the decrease in taurine affinity in this mutant may be due to a decreased cooperativity for additional taurine molecules to bind.

Overall, the data presented here suggest that these charged residues in the intersubunit interface play a critical role not only in keeping the receptor in the closed state, but also in determining agonist efficacy.

7.0 | CONCLUSIONS AND DISCUSSION

7.1 – Overview

The collective knowledge regarding the structure and function of ion channels is continuously increasing both in scope and detail. The research presented in this dissertation provides novel insight to both the activation and modulation mechanisms of the glycine receptor (GlyR). The overall conclusions from these studies can be summarized in three main points. First, allosteric modulators differentially affect the GlyR when activated by full vs. partial agonists, such as taurine. Second, two example allosteric modulators, ethanol and isoflurane, enhance taurine-activated GlyR currents by increasing efficacy, thereby stabilizing the open state of the receptor. Third, the disruption of a single electrostatic interaction near the ligand-binding region in the extracellular domain is sufficient to increase the efficacy of partial agonists, such as taurine, implicating this region for agonist efficacy determination. Together these results increase our understanding of the relationship between GlyR activation and the modulation of the receptor by ethanol.

7.2 – Allosteric Modulation of Partial Agonist Action on the GlyR

Drugs of abuse, including alcohol, co-opt the natural brain reward system leading to addiction which can have large individual and societal implications. The mesolimbic system, believed to be responsible for reward has been studied extensively, revealing the release of dopamine into the nucleus accumbens (NAcc) to be an important signal modulated by drugs of abuse. Recently, evidence for GlyR involvement in this process has been found (Söderpalm and Ericson, 2013). GlyRs are expressed in the nucleus accumbens (Waldvogel et al., 2007), likely by medium spiny neurons (MSNs) that project to the ventral tegmental area (VTA). The MSNs are gabaergic, forming inhibitory synapses onto either the dopaminergic neurons of the VTA , that release dopamine into the NAcc, or cholinergic neurons that stimulate the dopaminergic VTA neurons. Drugs of abuse that enhance GlyR functioning cause inhibition of the MSNs, resulting in a reduction of GABA release into the VTA. The neurons of the VTA, now released from inhibition by GABA, increase firing and subsequent release of dopamine into the NAcc (Söderpalm and Ericson, 2013).

This effect has been best characterized for ethanol enhancement of GlyRs in the NAcc (Molander et al., 2005, 2007). However, one recent study has also found implications for GlyR involvement in cannabinoid and nicotine effects on dopamine release in the NAcc (Jonsson et al., 2014). An ethanol-induced taurine release into the NAcc was found to be necessary for ethanol-induced dopamine release there, thus implicating the taurine-activated GlyR for ethanol's effects on dopamine signaling (Ericson et al., 2011). Interestingly, administration of both nicotine and cocaine result in a release of taurine in the NAcc (Kashkin and De Witte, 2005; Li et al., 2012). Thus, the

taurine-activated GlyR may be of importance in regulating the rewarding effects of multiple drugs of abuse. The data in this dissertation adds to the understanding of ethanol and other drug modulation of the taurine-activated GlyR, which had not been well characterized previously.

The major finding in Chapter 3 was that alcohol, anesthetics, and inhalants enhance the efficacy of maximally-effective taurine concentrations, while having no effect on maximally-effective glycine concentrations. Enhancement of sub-maximal glycine currents by ethanol, with a lack of enhancement seen at saturating glycine concentrations, had been established previously (Mascia et al., 1996a). Interestingly, we previously found that ethanol enhancement of sub-maximal concentrations of glycine and taurine were similar (Welsh et al., 2010). Taurine, as a partial agonist on GlyR, elicits currents whose maximal peak is much less than half the peak currents elicited by saturating glycine. This difference in current peak is potential room in which an allosteric modulator might enhance taurine currents. While we saw large potentiation of taurine responses at saturating concentrations, peak current levels of taurine + modulator were never able to match peak glycine current levels. The discrepancy between these levels warrants further research. Though higher concentrations of a very potent drug like one of the anesthetics may have been able to do it, high concentrations of these compounds also run the risk of damaging oocyte integrity.

Some research into the activation of the GlyR has implicated separate activation pathways for glycine and taurine, finding residues that when mutated seemed to convert taurine from a partial agonist into an antagonist (Lynch et al., 1997; Absalom et al., 2003). A separate pathway for taurine and glycine activation might explain differences in allosteric modulation. Though mutations to the alcohol binding pocket altered glycine

and taurine modulation by alcohol, isoflurane and TCE in similar ways (**Fig. 3.10**), indicating identical pathways regarding allosteric modulation by these compounds. Other allosteric modulators may work in similar fashion. Laube et al. (2000) found that zinc, also had differential effects on taurine-activated GlyR compared to glycine-activated GlyR. Zinc may have physiological implications in GlyR modulation as it is not only released from within some synaptic vesicles, but also present throughout the CNS at concentrations known to potentiate GlyR responses (Kay, 2004; Frederickson et al., 2006a, 2006b). Examination of the effects of zinc in combination with other allosteric modulators on taurine-activated GlyR was the focus of Chapter 4.

Zinc is not only found at GlyR potentiating concentrations in the CNS, it is also found at these low levels as a contaminant throughout the environment, including all buffer solutions. At the time of conducting the research in Chapter 4, the contaminating concentration of zinc in our buffers was unable to be exactly determined, though it was found to be in the potentiating range of the GlyR (McCracken et al., 2010). Thus we used three buffers with different zinc concentrations to examine combinatorial effects with other allosteric modulators. We found that zinc, like the drug of abuse modulators, enhanced maximally-effective taurine currents with no effect on saturating glycine currents. Additionally, a potentiating concentration of zinc decreased further potentiation of maximally-effective taurine-mediated currents by ethanol, isoflurane, and toluene.

This effect was best explained by a zinc-induced increase in taurine efficacy (Laube et al., 2000) masking some of the further efficacy increase seen with the drugs of abuse. This data supports the idea that lack of allosteric modulation at saturating glycine concentrations is due simply to a ceiling effect for maximum generated currents. The combinatorial zinc and drugs of abuse experiments also indicated that contaminating

levels of zinc in our buffers were low, as potentiation of taurine-activated GlyR by drugs of abuse was similar to potentiation seen when all zinc was chelated by tricine. Subsequent to this study, contaminating zinc concentrations in buffer were determined by inductively-coupled plasma mass spectrometry (ICP-MS) and found to be ~45 nM (Cornelison and Mihic, 2014).

7.3 – Mechanisms of Ethanol and Isoflurane Enhancement of Taurine-Activated GlyR

Ethanol is the most commonly used drug in society, but the biological mechanisms underlying the behavioral changes seen with alcohol use are still not well understood. Ethanol is a "dirty" drug in that it has numerous molecular targets. Many of these targets are known including proteins such as ion channels, enzymes, etc. While the contribution of ethanol's effects on each target to the general effects of ethanol are not fully identified, even the mechanism by which ethanol exerts its effects on individual ion channels has not been fully characterized. There is a wealth of evidence investigating the effects of ethanol on GlyR at the cellular level and system level, but the mechanisms by which ethanol exerts its effects on a single GlyR are few.

This gap in knowledge is mirrored for anesthetics like isoflurane. The mechanisms by which anesthetics cause general anesthesia is poorly understood, with many conflicting theories to how these compounds act. Like ethanol, anesthetics have many targets including ion channels. Structural information regarding anesthetic binding to cys-loop receptors has been recently found with crystal structures of GLIC bound by propofol and desflurane (Nury et al., 2011). However, even knowing the binding location

of an anesthetic does not illuminate the effects it has once bound to the ion channel. The data in this dissertation directly address the mechanism of ethanol's and isoflurane's enhancement of taurine-activated GlyR function.

The allosteric modulator enhancement of GlyR currents elicited by maximally-effective taurine concentrations seen in Chapters 3 and 4 could have been explained by multiple mechanisms on single GlyR, which were tested in Chapter 5. First, a decrease in the rate of desensitization could cause an increase in peak current. However, as seen in Chapter 3, ethanol did not affect desensitization rates and isoflurane increased desensitization rates, which as a solitary effect would result in decreased peak currents. In the experiments from Chapter 5, we used saturating concentrations of taurine to elicit a maximum effect from GlyR. However this also has an added effect of eliminating the unbound closed state from consideration. When this high concentration is continuously applied, receptors can only be in one of three bound states: closed, open, or desensitized. When taurine binds the receptor, and the channel opens beginning a cluster of activity, the channel flickers between the bound open and closed states. This cluster of activity comes to an end with receptor desensitization. Were a taurine molecule to unbind and the GlyR resensitize to a closed state, there is so much agonist around that taurine would bind almost instantaneously and begin another cluster of activity. Thus any intercluster closed times are actually desensitized times. While it is conceivable to measure these intercluster desensitized times and perform analyses similar to dwell time analyses, in practice measuring these desensitized times becomes very difficult. The number of channels in a patch becomes an issue of great importance. While we may assume all GlyR in a patch are the same and analyze all single opening clusters as example behavior, a second channel resensitizing and beginning a cluster of activity in the middle of the first

channel's desensitization period is problematic. Additionally, consistently high patch integrity would be needed for these experiments. If only a few desensitized periods per patch are found before patch death, analysis would be very difficult. Especially if each desensitized period is long lived giving a single sample of a long time constant. Still, though difficult, experiments such as this are needed to better understand desensitization of GlyR and any effects of allosteric modulators on this process.

An increase in channel conductance could also explain enhancement of max taurine currents. We found that neither ethanol nor isoflurane had a significant effect on conductance level. No allosteric modulator found so far has caused a change to GlyR conductance. Generally structural changes to the pore itself are needed to drastically change conductance states, such as changing subunit composition or mutations to pore residues (Lynch, 2004). Additionally, if either drug were somehow changing conductance at the pore, it is likely it would have the same effect on the glycine-activated GlyR as changes to the pore seem to affect both agonists equally (Lynch, 2004).

The final possibility for seeing enhancement of max taurine currents is stabilization of the open state. This effect is the main mechanism of action we found for both ethanol and isoflurane. Both drugs increase the likelihood of longer lived open states, increasing efficacy and thus the P_o of the taurine-activated GlyR. This finding provides the first direct evidence we are aware of for differential effects of an allosteric modulator on the GlyR based on agonist. While zinc potentiation of saturating taurine currents was found at the single channel level to be due to zinc enhancement of taurine P_o, zinc showed this same enhancement of glycine P_o (Laube et al., 2000). We have previously examined the effects of ethanol on sub-maximal glycine activation of single GlyR, finding no effects on glycine efficacy (Welsh et al., 2009), even though there is no

ceiling effect as seen with saturating glycine. Thus, the mechanism of ethanol enhancement of the taurine-activated GlyR is separate from the mechanism of glycine-activated GlyR enhancement, and in light of the possible role of taurine-activated GlyR in the rewarding effects of ethanol (Ericson et al., 2011), these differences must be considered when examining the effects of ethanol.

7.4 – Partial Agonist Efficacy of the GlyR

A central goal of single channel electrophysiology has been to separate the phenomena of binding and gating. Mutational studies often give some evidence of specific residue and region contributions to each process. However, it is difficult to predict all possible changes to the three dimensional structure caused by a single point mutation. Inability to obtain direct structural information for all channels, like the GlyR, aids in this difficulty. Thus partial agonists serve as an interesting tool to examine differences in channel kinetics without a primary structural change to the ion channel. For the cys-loop receptors, the flip model of partial agonism seems to fit well for both GlyR and nAChR partial agonists (Lape et al., 2008). If the structural basis of the flipped to open transition is believed to be the final gating step involving movement of the TM domains to open the channel, then the closed to flipped transition occurs somewhere within the ligand-binding domain during the conformational changes that convey the binding signal to the TM domains.

We have now identified multiple residues (Chapter 6) near the ligand-binding domain that are important for holding the channel in the closed state as well as affecting agonist efficacy. It is of note that mutations to the R131 residue greatly affected taurine

efficacy while seemingly having no effect on glycine-activation at the whole cell level. Single channel studies of these R131 mutants using glycine are underway, and it will be interesting to see if glycine efficacy is greatly increased with a corresponding decrease in affinity, like taurine, as EC_{50}s remain unchanged compared to WT GlyR. If not, this would be good evidence for differential GlyR activation pathways for glycine and taurine. This notion is supported by the temperature effects on taurine efficacy relative to glycine. While changing temperature of the environment will change intrinsic energy of the GlyR, resulting in changes to flexibility of the structure and speed of movement, these changes would normally be assumed to be agonist independent.

7.5 – Clinical Implications

This dissertation has provided research into the effects of allosteric modulators on partial agonists of the GlyR, as well as research into the nature of partial agonism at the GlyR. It is worth noting then how the knowledge gained in this dissertation may be put to practical use. There are three realms involving human health which the research in this dissertation may pertain to: Addiction, pain, and the startle disease hyperekplexia.

It has previously been noted in this dissertation that GlyR in the nucleus accumbens has been implicated as having an endogenous role in the rewarding effects of ethanol (Molander et al., 2005, 2007), and that specifically, ethanol modulation of taurine activation of the GlyR may be responsible for the reward signal of increased dopamine release into the NAcc (Ericson et al., 2011). GlyR have been implicated in the dopamine elevating effects of cannabinoids and nicotine, and nicotine and other drugs of abuse alter taurine levels in the NAcc (Kashkin and De Witte, 2005; Li et al., 2012; Bu et al., 2013;

Jonsson et al., 2014). Thus it is worth considering whether taurine may be the endogenous player for these GlyR. Taurine and GlyR effects are not limited to the NAcc. Functional GlyR are also expressed in the hippocampus, a brain area important for memory, and the prefrontal cortex, a brain area important for complex cognitive processes like decision making (Malosio et al., 1991; Baer et al., 2009; Keck and White, 2009; Lu and Ye, 2011). These regions are thus important for other effects of drugs of abuse such as impaired decision making and memory loss, and GlyR have been implicated in ethanol effects in one of these regions (Badanich et al., 2013). Taurine levels are also altered following administration of drugs of abuse in these areas (Dahchour and De Witte, 2003; Bu et al., 2013). Thus it is possible that changes to taurine-activated GlyR functioning may be involved in the effects of multiple drugs of abuse. Then the taurine-activated GlyR may be an important site of intervention into the effects of drugs of abuse and addiction. The research shown in this dissertation makes clear that the taurine-activated GlyR has functional differences from the glycine-activated GlyR, thus targeting of GlyR in general may be insufficient, as taurine specific changes are warranted. There is some evidence that extrasynaptic homomeric α2 GlyR may be more involved in these processes than synaptic β containing GlyR (Jonsson et al., 2012). However, though taurine efficacy relative to glycine is lower in α2 containing receptors, modulator enhancement of saturating taurine concentrations is still seen in these receptors (**Fig. 4.4**).

In the spinal cord, GlyR play are important in the role of regulating pain-signaling pathways. Nociceptors that detect noxious stimuli in the periphery send signals to the dorsal horn of the spinal cord and then towards higher brain regions. If this circuit becomes sensitized due to decreased glycine release or decreased GlyR sensitivity,

persistent neuropathic pain may occur. For example, the major inflammation related pain pathway involves the release of prostaglandins that activate a signal cascade ending in inhibition of α3 containing GlyR, resulting in a disinhibition of dorsal horn neurons; a mechanism that has been implicated in pain sensitization (Ahmadi et al., 2002; Zeilhofer, 2005). Thus, α3 containing GlyR are a promising target for analgesia. Taurine efficacy relative to glycine on α3 containing GlyR is much lower than for α1 GlyR (Chen et al., 2009). However, taurine administration has anti-nociceptive effects for multiple models of neuropathic pain, acting on GlyR (Terada et al., 2011). Even at this low efficacy on α3 GlyR, taurine has a noted effect in the treatment of pain, and it is likely that allosteric modulator enhancement of taurine-mediated responses would be present for α3 containing GlyR as it was for both α1 and α2 containing GlyR. Thus selective potentiation of the taurine-activated GlyR similar to the results seen in this dissertation may be useful in treating neuropathic pain.

Hyperekplexia is a hereditary disease where the startle response to unexpected stimuli is greatly exaggerated. This disorder is caused by an ever increasing number of mutations or deletions to GlyR, that all result in decreased GlyR functioning (Bode and Lynch, 2014). Recently, one hyperekplexia related GlyR mutation, W170S in the α1 subunit, was found to selectively remove zinc potentiation of GlyR, while agonist sensitivity to glycine, β-alanine, and taurine remained normal (Zhou et al., 2013). As zinc is found at GlyR potentiating levels in the nervous system, this mutation causes hyperekplexia by a loss of allosteric modulation which results in a decreased GlyR current *in vivo*. The research in this dissertation into the effects of zinc in combination with other allosteric modulators suggests that taurine-activated GlyR currents in this mutant could be potentiated with another allosteric modulator to counteract the deficiency

in zinc potentiation. Thus, allosteric modulation of taurine-activated GlyR may be useful in developing treatment for some forms of hyperekplexia.

7.6 – Future Directions

The research presented in this dissertation has added to our understanding of GlyR partial agonism and how these signals are modulated by various allosteric modulators. However, there are many questions that arise from this research that should be investigated in future studies. Below, is a brief outline of possibilities for follow-up studies.

1. We have used taurine exclusively as an example of a partial agonist. Although taurine is of particular interest due to its biological prevalence and role in GlyR activation, we have seen that differences in agonists are not simply due to efficacy changes. Thus it would be useful to examine how allosteric modulation affects other partial agonist action on the GlyR, using compounds such as β-alanine (higher efficacy than taurine), β-ABA or β-AIBA (both lower efficacy than taurine).

2. We only tested allosteric modulators of two different mechanisms; drugs of abuse that bind in the alcohol/anesthetic binding pocket and the divalent cation zinc. Investigation of other classes of allosteric modulators with different mechanisms of action, such as neurosteroids, would add greatly to the understanding of allosteric modulation of partial agonists at the GlyR. Additionally, we only used positive allosteric modulators in our studies. Negative allosteric modulators of physiological

relevance on the GlyR, like caffeine, would expand understanding of modulation of partial agonism of GlyR as well.

3. In our single channel analysis, we did not fit any specific kinetic mechanism preferring to remain descriptive of changes with allosteric modulators. At our high concentrations of taurine, we excluded binding effects thus only examining changes in efficacy on a descriptive model of the data. It would be of use to examine a full range of concentrations of taurine and glycine with allosteric modulators in single channel analysis of the GlyR. This full data set would allow us to determine not only efficacy changes but also affinity changes, and could be fit simultaneously to a kinetic mechanism to further elucidate differences in binding and gating with allosteric modulator.

4. As previously mentioned, rigorous characterization of desensitization of the glycine- and taurine-activated GlyR with and without allosteric modulators is necessary at the whole cell and single channel levels. However, there are many problems associated with these types of experiments as described in Chapter 7.3. Advanced techniques or advances in structural identification may be necessary to accomplish these goals, but this remains a major question in understanding GlyR.

5. Further single channel analysis of the charged residues in the intersubunit interface are necessary. For example, would a double mutation to R119 and R131 result in a spontaneously active GlyR similar to D97R, and would taurine have an increased efficacy on this mutant? This particular double mutation may not be

tractable as R119 mutations greatly right shift concentration response curves, but D97R behavior should be mirrored by some combination of residues on the complementary side of the interface if this electrostatic interaction is truly key to keeping the receptor in the closed state. A related question is to attempt to identify residues that are important for keeping the receptor in the open state. Likely there are some in the TM regions where the gating action happens, but do these residues important for closing bind to alternative partners after a conformational change to the open state? If so, could that interaction be strengthened, resulting in a tonically active receptor? Such a receptor would be very useful in studying channel activation and structural changes as a result of binding, as well as desensitization assuming the mutation did not affect this state.

6. The agonist efficacy increasing effects of R131 mutations could be investigated further. In particular, it is interesting to consider the implications of decrease to the Hill coefficient for taurine. This decrease would traditionally be associated with a loss of cooperativity in taurine binding. Could this decrease be linked to high taurine efficacy at opening the channel? This could mean that unlike the WT GlyR, a single taurine molecule might be able to open the channel. A double mutation could be created with one of the previously mentioned residues that eliminates taurine agonism and R131D to increase efficacy at opening the channel. Mixed ratios of these double mutants and WT GlyR subunits could result in receptors that have only one or two taurine binding sites. An investigation of whether one or two taurine molecules are enough to open this channel would be interesting.

7. In an attempt to expand the scope of the work in this dissertation, the experimental ideas should be utilized at levels beyond the single channel and single cell. Investigating the effects of allosteric modulators on taurine-activated GlyR can be accomplished first in slice recordings to understand effects on circuits of neurons, then in *in vivo* experiments to attempt to link potentiation of taurine-activated GlyR to specific behaviors. This would be particularly useful in the mesolimbic system where perturbation of taurine-activated GlyR may influence the rewarding effects of drugs of abuse.

References

Absalom NL, Lewis TM, Kaplan W, Pierce KD, Schofield PR (2003) Role of charged residues in coupling ligand binding and channel activation in the extracellular domain of the glycine receptor. *J Biol Chem* 278: 50151–50157.

Ahmadi S, Lippross S, Neuhuber WL, Zeilhofer HU (2002) PGE_2 selectively blocks inhibitory glycinergic neurotransmission onto rat superficial dorsal horn neurons. *Nat Neurosci* 5: 34–40.

Albrecht J, Schousboe A (2005) Taurine interaction with neurotransmitter receptors in the CNS: an update. *Neurochem Res* 30: 1615–1621.

Araki T, Yamano M, Murakami T, Wanaka A, Betz H, Tohyama M (1988) Localization of glycine receptors in the rat central nervous system: an immunocytochemical analysis using monoclonal antibody. *Neuroscience* 25: 613–624.

Badanich KA, Mulholland PJ, Beckley JT, Trantham-Davidson H, Woodward JJ, (2013) Ethanol reduces neuronal excitability of lateral orbitofrontal cortex neurons via a glycine receptor dependent mechanism. Neuropsychopharmacology 38: 1176–1188.

Baer K, Waldvogel HJ, Faull RL, Rees MI (2009) Localization of glycine receptors in the human forebrain, brainstem, and cervical spinal cord: an immunohistochemical review. *Front Mol Neurosci* 2: 25.

Bale AS, Smothers CT, Woodward JJ (2002) Inhibition of neuronal nicotinic acetylcholine receptors by the abused solvent, toluene. *Br J Pharmacol* 137: 375–383.

Banay-Schwartz M, Palkovits M, Lajtha A (1993) Heterogeneous distribution of functionally important amino acids in brain areas of adult and aging humans. *Neurochem Res* 18: 417–423.

Beato M, Groot-Kormelink PJ, Colquhoun D, Sivilotti LG (2002) Openings of the rat recombinant alpha 1 homomeric glycine receptor as a function of the number of agonist molecules bound. *J Gen Physiol* 119: 443–466.

Beato M, Groot-Kormelink PJ, Colquhoun D, Sivilotti LG (2004) The activation mechanism of alpha1 homomeric glycine receptors. *J Neurosci* 24: 895–906.

Becker CM, Hoch W, Betz H (1988) Glycine receptor heterogeneity in rat spinal cord during postnatal development. *EMBO J* 7: 3717–3726.

Becker K, Breitinger HG, Humeny A, Meinck HM, Dietz B, Aksu F, Becker CM (2008) The novel hyperekplexia allele GLRA1(S267N) affects the ethanol site of the glycine receptor. *Eur J Hum Genet* 16: 223-228.

Beckstead MJ, Weiner JL, Eger EI 2nd, Gong DH, Mihic SJ (2000) Glycine and gamma-aminobutyric acid$_A$ receptor function is enhanced by inhaled drugs of abuse. *Mol Pharmacol* 57: 1199–1205.

Beckstead MJ, Phelan R, Mihic SJ (2001) Antagonism of inhalant and volatile anesthetic enhancement of glycine receptor function. *J Biol Chem* 276: 24959–24964.

Beckstead MJ, Phelan R, Trudell JR, Bianchini MJ, Mihic SJ (2002) Anesthetic and ethanol effects on spontaneously opening glycine receptor channels. *J Neurochem* 82: 1343–1351.

Belachew S, Malgrange B, Rigo JM, Rogister B, Leprince P, Hans G, Nguyen L, Moonen G (2000) Glycine triggers an intracellular calcium influx in oligodendrocyte progenitor cells which is mediated by the activation of both the ionotropic glycine receptor and Na^+-dependent transporters. *Eur J Neurosci* 12: 1924–1930.

Birinyi A, Parker D, Antal M, Shupliakov O (2001) Zinc colocalizes with GABA and glycine in synapses in the lamprey spinal cord. *J Comp Neurol* 433: 208–221.

Bocquet N, Nury H, Baaden M, Le Poupon C, Changeux JP, Delarue M, Corringer PJ (2009) *Nature* 457: 111-114.

Bode A, Lynch JW (2014) The impact of human hyperekplexia mutations on glycine receptor structure and function. *Mol Brain* 7: 2.

Bormann J, Hamill OP, Sakmann B (1987) Mechanism of anion permeation through channels gated by glycine and γ-aminobutyric acid in mouse cultured spinal neurones. *J Physiol* 385: 243–286.

Bormann J, Rundström N, Betz H, Langosch D (1993) Residues within transmembrane segment M2 determine chloride conductance of glycine receptor homo- and hetero-oligomers. *EMBO J* 12: 3729–3737.

Bowen SE, Batis JC, Paez-Martinez N, Cruz SL (2006) The last decade of solvent research in animal models of abuse: mechanistic and behavioral studies. *Neurotoxicol Teratol* 28: 636–647.

Brejc K, van Dijk WJ, Klaassen RV, Schuurmans M, van Der Oost J, Smit AB, Sixma TK (2001) Crystal structure of an ACh-binding protein reveals the ligand-binding domain of nicotinic receptors. *Nature* 411: 269–276.

Bu Q, Lv L, Yan G, Deng P, Wang Y, Zhou J, Yang Y, Li Y, Cen X (2013) NMR-based metabonomic in hippocampus, nucleus accumbens and prefrontal cortex of methamphetamine-sensitized rats. *Neurotoxicology* 36: 17–23.

Burzomato V, Beato M, Groot-Kormelink PJ, Colquhoun D, Sivilotti LG (2004) Single-channel behavior of heteromeric α1β glycine receptors: an attempt to detect a conformational change before the channel opens. *J Neurosci* 24: 10924–10940.

Butler AS, Lindesay SA, Dover TJ, Kennedy MD, Patchell VB, Levine BA, Hope AG, Barnes NM (2009) Importance of the C-terminus of the human 5-HT3A receptor subunit. *Neuropharmacol* 56: 292–302.

Chau PL (2010) New insights into the molecular mechanisms of general anaesthetics. Br *J Pharmacol* 161: 288–307.

Chen X, Webb TI, Lynch JW (2009) The M4 transmembrane segment contributes to agonist efficacy differences between alpha1 and alpha3 glycine receptors. *Mol Membr Biol* 26: 321–332.

Cheng G, Kendig JJ (2002) Pre- and postsynaptic volatile anaesthetic actions on glycinergic transmission to spinal cord motor neurons. *Br J Pharmacol* 136: 673–684.

Choe KY, Olson JE, Bourque CW (2012) Taurine release by astrocytes modulates osmosensitive glycine receptor tone and excitability in the adult supraoptic nucleus. *J Neurosci* 32: 12518–12527.

Colman A (1984) Expression of exogenous DNA in *Xenopus* oocytes, in *Transcription and Translation: A Practical Approach* (Hames BD, Higgins SJ eds) pp 49–69, Oxford Press, Washington, DC.

Colquhoun D, Hawkes AG (1977) Relaxation and fluctuations of membrane currents that flow through drug-operated channels. *Proc R Soc Lond B Biol Sci* 199: 231–262.

Colquhoun D (1998) Binding, gating, affinity, and efficacy: the interpretation of structure-activity relationships for agonists and of the effects of mutating receptors. *Br J Pharmacol* 125: 924–947.

Colquhoun D (2006) Agonist-activated ion channels. *Br J Pharmacol* 147: S17–S26.

Coombs JS, Eccles JC, Fatt P (1955) The specific ionic conductances and the ionic movements across the motoneuronal membrane that produce the inhibitory post-synaptic potential. *J Physiol* 130: 326–373.

Cornelison GL, Mihic SJ (2014) Contaminating levels of zinc found in commonly-used labware and buffers affect glycine receptor currents. *Brain Res Bull* 100: 1–5.

Corringer PJ, Bertrand S, Galzi JL, Devillers-Thierry A, Changeux JP, Bertrand D (1999) Mutational analysis of the charge selectivity filter of the $\alpha 7$ nicotinic acetylcholine receptor. *Neuron* 22: 831–843.

Dahchour A, Quertemont E, De Witte P (1996) Taurine increases in the nucleus accumbens microdialysate after acute ethanol administration to naïve and chronically alcoholised rats. *Brain Res* 735: 9–19.

Dahchour A, De Witte P (2003) Excitatory and inhibitory amino acid changes during repeated episodes of ethanol withdrawal: an *in vivo* microdialysis study. *Eur J Pharmacol* 459: 171–178.

Davidoff RA, Shank RP, Graham LT, Aprison MH, Werman R (1967) Association of glycine with spinal interneurones. *Nature* 214: 680–681.

Del Re AM, Dopico AM, Woodward JJ (2006) Effects of the abused inhalant toluene on ethanol-sensitive potassium channels expressed in oocytes. *Brain Res* 1087: 75–82.

Dieudonne S (1995) Glycinergic synaptic currents in Golgi cells of the rat cerebellum. *Proc Natl Acad Sci USA* 92: 1441–1445.

Downie DL, Hall AC, Lieb WR, Franks NP (1996) Effects of inhalational general anaesthetics on native glycine receptors in rat medullary neurons and recombinant glycine receptors in *Xenopus* oocytes. *Br J Pharmacol* 118: 493–502.

Dumoulin A, Rostaing P, Bedet C, Lévi S, Isambert MF, Henry JP, Triller A, Gasnier B (1999) Presence of the vesicular inhibitory amino acid transporter in GABAergic and glycinergic synaptic terminal boutons. *J Cell Sci* 112: 811–823.

Duret G, Van Renterghem C, Weng Y, Prevost M, Moraga-Cid G, Huon C, Sonner JM, Corringer PJ (2011) Functional prokaryotic-eukaryotic chimera from the pentameric ligand-gated ion channel family. *Proc Natl Acad Sci USA* 108: 12143–12148.

Dutertre S, Drwal M, Laube B, Betz H (2012) Probing the pharmacological properties of distinct subunit interfaces within heteromeric glycine receptors reveals a functional ββ agonist-binding site. *J Neurochem* 122: 38–47.

Eger EI 2nd, Saidman LJ, Brandstater B (1965) Minimum alveolar anesthetic concentration: a standard of anesthetic potency. *Anesthesiology* 26: 756–763.

Eggers ED, Berger AJ (2004) Mechanisms for the modulation of native glycine receptor channels by ethanol. *J Neurophysiol* 91: 2685–2695.

Ericson M, Molander A, Stomberg R, Söderpalm B (2006) Taurine elevates dopamine levels in the rat nucleus accumbens: antagonism by strychnine. *Eur J Neurosci* 23: 3225–3229.

Ericson M, Chau P, Clarke RB, Adermark L, Söderpalm B (2011) Rising taurine and ethanol concentrations in nucleus accumbens interact to produce dopamine release after ethanol administration. *Addict Biol* 16: 377–385.

Evans EB, Balster RL (1991) CNS depressant effects of volatile organic solvents. *Neurosci Biobehav Rev* 15: 233–241.

Fatima-Shad K, Barry PH (1993) Anion permeation in GABA- and glycine-gated channels of mammalian cultured hippocampal neurons. *Proc R Soc Lond B Biol Sci* 253: 69–75.

Ferragamo MJ, Golding NL, Oertel D (1998) Synaptic inputs to stellate cells in the ventral cochlear nucleus. *J Neurophysiol* 79: 51–63.

Franks NP, Lieb WR (1982) Molecular mechanisms of general anaesthesia. *Nature* 300: 487–493.

Franks NP, Lieb WR (1984) Do general anaesthetics act by competitive binding to specific receptors? *Nature* 310: 599–601.

Franks NP, Lieb WR (1997) Inhibitory synapses: anaesthetics set their sites on ion channels. *Nature* 389: 334–335.

Franks NP (2008) General anaesthesia: from molecular targets to neuronal pathways of sleep and arousal. *Nat Rev Neurosci* 9: 370–386.

Frederickson CJ (1989) Neurobiology of zinc and zinc-containing neurons. *Int Rev Neurobiol* 31: 145–238.

Frederickson CJ, Giblin LJ, Balaji RV, Masalha R, Frederickson CJ, Zeng Y, Lopez EV, Koh JY, Chorin U, Besser L, Hershfinkel M, Li Y, Thompson RB, Krezel A (2006a) Synaptic release of zinc from brain slices: factors governing release, imaging, and accurate calculation of concentration. *J Neurosci Methods* 154: 19–29.

Frederickson CJ, Giblin LJ, Krezel A, McAdoo DJ, Mueller RN, Zeng Y, Balaji RV, Masalha R, Thompson RB, Fierke CA, Sarvey JM, de Valdenebro M, Prough DS, Zornow MH (2006b) Concentrations of extracellular free zinc (pZn)e in the central nervous system during simple anesthetization, ischemia and reperfusion. *Exp Neurol* 198: 285–293.

Galzi JL, Devillers-Thiery A, Hussy N, Bertrand S, Changeux JP, Bertrand D (1992) Mutations in the channel domain of a neuronal nicotinic receptor convert ion selectivity from cationic to anionic. *Nature* 359: 500–505.

Gardner P, Ogden DC, Colquhoun D (1984) Conductances of single ion channels opened by nicotinic agonists are indistinguishable. *Nature* 309: 160–162.

Grosman C, Zhou M, Auerbach A (2000) Mapping the conformational wave of acetylcholine receptor channel gating. *Nature* 403: 773–776.

Grudzinska J, Schemm R, Haeger S, Nicke A, Schmalzing G, Betz H, Laube B (2005) The β subunit determines the ligand binding properties of synaptic glycine receptors. *Neuron* 45: 727–739.

Gunthorpe MJ, Lummis SC (2001) Conversion of the ion selectivity of the 5-HT_{3a} receptor from cationic to anionic reveals a conserved feature of the ligand-gated ion channel superfamily. *J Biol Chem* 276: 10977–10983.

Hamill OP, Marty A, Neher E, Sakmann B, Sigworth FJ (1981) Improved patch-clamp techniques for high-resolution current recording from cells and cell-free membrane patches. *Pflugers Arch* 391: 85–100.

Hamill OP, Bormann J, Sakmann B (1983) Activation of multiple-conductance state chloride channels in spinal neurones by glycine and GABA. *Nature* 305: 805–808.

Harvey RJ, Thomas P, James CH, Wilderspin A, Smart TG (1999) Identification of an inhibitory Zn^{2+} binding site on the human glycine receptor alpha1 subunit. *J Physiol* 520: 53–64.

Hibbs RE, Gouaux E (2011) Principles of activation and permeation in an anion-selective Cys-loop receptor. *Nature* 474: 54–60.

Hilf RJ, Dutzler R (2008) X-ray structure of a prokaryotic pentameric ligand-gated ion channel. *Nature* 452: 375–379.

Imperato A, Di Chiara G (1986) Preferential stimulation of dopamine release in the nucleus accumbens of freely moving rats by ethanol. *J Pharmacol Exp Ther* 239: 219–228.

Johnston LD, O'Malley PM, Bachman JG, Schulenberg JE, (2012) Monitoring the Future National Survey Results on Drug Use, 1975–2011. In: Secondary School Students, vol. I. Institute for Social Research, The University of Michigan, Ann Arbor.

Johnston LD, O'Malley PM, Bachman JG, Schulenberg JE (2013) Monitoring the Future national survey results on drug use, 1975–2012: Volume 1, secondary school students. Ann Arbor: Institute for Social Research, The University of Michigan.

Johnston LD, O'Malley PM, Bachman JG, Schulenberg JE (2013) Monitoring the Future national survey results on drug use, 1975–2012: Volume 2, college students and adults ages 19–50. Ann Arbor: Institute for Social Research, The University of Michigan.

Jonsson S, Kerekes N, Hyytiä P, Ericson M, Söderpalm B, (2009) Glycine receptor expression in the forebrain of male AA/ANA rats. *Brain Res* 1305: S27–S36.

Jonsson S, Morud J, Pickering C, Adermark L, Ericson M, Söderpalm B, (2012) Changes in glycine receptor subunit expression in forebrain regions of the Wistar rat over development. *Brain Res* 1446: 12–21.

Jonsson S, Adermark L, Ericson M, Söderpalm B (2014) The involvement of accumbal glycine receptors in the dopamine-elevating effects of addictive drugs. *Neuropharmacol* 82: 69–75.

Jursky F, Tamura S, Tamura A, Mandiyan S, Nelson H, Nelson N (1994) Structure, function and brain localization of neurotransmitter transporters. *J Exp Biol* 196: 283–295.

Kash TL, Jenkins A, Kelley JC, Trudell JR, Harrison NL (2003) Coupling of agonist binding to channel gating in the $GABA_A$ receptor. *Nature* 421: 272–275.

Kashkin VA, De Witte P (2005) Nicotine increases microdialysate brain amino acid concentrations and induces conditioned place preference. *Eur Neuropsychopharmacol* 15: 625–632.

Kay AR, (2004) Detecting and minimizing zinc contamination in physiological solutions. *BMC Physiol* 4: 4.

Keck T, White JA (2009) Glycinergic inhibition in the hippocampus. *Rev Neurosci* 20: 13–22.

Kelley SP, Dunlop JI, Kirkness EF, Lambert JJ, Peters JA (2003) A cytoplasmic region determines single-channel conductance in 5-HT_3 receptors. *Nature* 424: 321–324.

Kirsch J, Betz H (1995) The postsynaptic localization of the glycine receptor-associated protein gephyrin is regulated by the cytoskeleton. *J Neurosci* 15: 4148–4156.

Kirson D, Todorovic J, Mihic SJ (2012) Positive allosteric modulators differentially affect full versus partial agonist activation of the glycine receptor. *J Pharmacol Exp Ther* 342: 61–70.

Kirson D, Cornelison GL, Philpo AE, Todorovic J, Mihic SJ (2013) Physiological concentrations of zinc reduce taurine-activated GlyR responses to drugs of abuse. *Neuropharmacol* 75: 286–294.

Langosch D, Thomas L, Betz H (1988) Conserved quaternary structure of ligand-gated ion channels: the postsynaptic glycine receptor is a pentamer. *Proc Natl Acad Sci USA* 85: 7394–7398.

Langosch D, Laube B, Rundstrom N, Schmieden V, Bormann J, Betz H (1994) Decreased agonist affinity and chloride conductance of mutant glycine receptors associated with human hereditary hyperekplexia. *EMBO J* 13: 4223–4228.

Lape R, Colquhoun D, Sivilotti LG (2008) On the nature of partial agonism in the nicotinic receptor superfamily. *Nature* 454: 722–727.

Laube B, Kuhse J, Rundström N, Kirsch J, Schmieden V, Betz H (1995) Modulation by zinc ions of native rat and recombinant human inhibitory glycine receptors. *J Physiol* 483: 613–619.

Laube B, Kuhse J, Betz H (2000) Kinetic and mutational analysis of Zn^{2+} modulation of recombinant human inhibitory glycine receptors. *J Physiol* 522: 215–230.

Lee WY, Sine SM (2005) Principal pathway coupling agonist binding to channel gating in nicotinic receptors. *Nature* 438: 243–247.

Legendre P (2001) The gylcinergic inhibitory synapse. *Cell Mol Life Sci* 58: 760–793.

Lewis TM, Sivilotti LG, Colquhoun D, Gardiner RM, Schoepfer R, Rees M (1998) Properties of human glycine receptors containing the hyperekplexia mutation α1(K276E), expressed in *Xenopus* oocytes. *J Physiol* 507: 25–40.

Lewis TM, Schofield PR, McClellan AM (2003) Kinetic determinants of agonist action at the recombinant human glycine receptor. *J Physiol* 549: 361–374.

Li Y, Yan GY, Zhou JQ, Bu Q, Deng PC, Yang YZ, Lv L, Deng Y, Zhao JX, Shao X, Zhu RM, Huang YN, Zhao YL, Cen XB (2012) 1H NMR-based metabonomics in brain nucleus accumbens and striatum following repeated cocaine treatment in rats. *Neuroscience* 218: 196–205.

Lim R, Alvarez FJ, Walmsley B (2000) GABA mediates presynaptic inhibition at glycinergic synapses in a rat auditory brainstem nucleus. *J Physiol* 525: 447–459.

Lu Y, Ye JH (2011) Glycine-activated chloride currents of neurons freshly isolated from the prefrontal cortex of young rats. *Brain Res* 1393: 17–22.

Lubman DI, Yücel M, Lawrence AJ (2008) Inhalant abuse among adolescents: neurobiological considerations. *Br J Pharmacol* 154: 316–326.

Lynch JW, Rajendra S, Pierce KD, Handford CA, Barry PH, Schofield PR (1997) Identification of intracellular and extracellular domains mediating signal transduction in the inhibitory glycine receptor chloride channel. *EMBO J* 16: 110–120.

Lynch JW, Jacques P, Pierce KD, Schofield PR (1998) Zinc potentiation of the glycine receptor chloride channel is mediated by allosteric pathways. *J Neurochem* 71: 2159–2168.

Lynch JW (2004) Molecular structure and function of the glycine receptor chloride channel. *Physiol Rev* 84: 1051–1095.

Malosio ML, Marqueze-Pouey B, Kuhse J, Betz H (1991) Widespread expression of glycine receptor subunit mRNAs in the adult and developing rat brain. *EMBO J* 10: 2401–2409.

Mascia MP, Mihic SJ, Valenzuela CF, Schofield PR, Harris RA (1996a) A single amino acid determines differences in ethanol actions on strychnine-sensitive glycine receptors. *Mol Pharmacol* 50: 402–406.

Mascia MP, Machu TK, Harris RA (1996b) Enhancement of homomeric glycine receptor function by long-chain alcohols and anaesthetics. *Br J Pharmacol* 119: 1331–1336.

Mascia MP, Trudell JR, Harris RA (2000) Specific binding sites for alcohols and anesthetics on ligand-gated ion channels. *Proc Natl Acad Sci USA* 97: 9305–9310.

McCool BA, Botting SK (2000) Characterization of strychnine-sensitive glycine receptors in acutely isolated adult rat basolateral amygdala neurons. *Brain Res* 859: 341–351.

McCracken LM, Trudell JR, Goldstein BE, Harris RA, Mihic SJ (2010) Zinc enhances ethanol modulation of the alpha1 glycine receptor. *Neuropharmacol* 58: 676–681.

McGovern PE, Zhang J, Tang J, Zhang Z, Hall GR, Moreau RA, Nuñez A, Butrym ED, Richards MP, Wang CS, Cheng G, Zhao Z, Wang C (2004) Fermented beverages of pre- and proto-historic China. *Proc Natl Acad Sci USA* 101: 17593–17598.

Mihic SJ, McQuilkin SJ, Eger EI 2nd, Ionescu P, Harris RA (1994) Potentiation of gamma-aminobutyric acid type A receptor-mediated chloride currents by novel halogenated compounds correlates with their abilities to induce general anesthesia. *Mol Pharmacol* 46: 851–857.

Mihic SJ, Ye Q, Wick MJ, Koltchine VV, Krasowski MD, Finn SE, Mascia MP, Valenzuela CF, Hanson KK, Greenblatt EP, Harris RA, Harrison NL (1997) Sites of alcohol and volatile anaesthetic action on GABA(A) and glycine receptors. *Nature* 389: 385–389.

Mihic SJ (1999) Acute effects of ethanol on $GABA_A$ and glycine receptor function. *Neurochem Int* 35: 115–123.

Miller PS, Da Silva HM, Smart TG (2005) Molecular basis for zinc potentiation at strychnine-sensitive glycine receptors. *J Biol Chem* 280: 37877–37884.

Miyazawa A, Fujiyoshi Y, Stowell M, Unwin N (1999) Nicotinic acetylcholine receptor at 4.6 Å resolution: transverse tunnels in the channel wall. *J Mol Biol* 288: 765–786.

Miyazawa A, Fujiyoshi Y, Unwin N (2003) Structure and gating mechanism of the acetylcholine receptor pore. *Nature* 424: 949–955.

Molander A, Löf E, Stomberg R, Ericson M, Söderpalm B (2005) Involvement of accumbal glycine receptors in the regulation of voluntary ethanol intake in the rat. *Alcohol Clin Exp Res* 29: 38–45.

Molander A, Lidö HH, Löf E, Ericson M, Söderpalm B (2007) The glycine reuptake inhibitor Org 25935 decreases ethanol intake and preference in male wistar rats. *Alcohol Alcohol* 42: 11–18.

Mokdad AH, Marks JS, Stroup DF, Gerberding JL (2004) Actual causes of death in the United States, 2000. *JAMA* 291: 1238–1245.

Mori M, Gähwiler BH, Gerber U (2002) Beta-alanine and taurine as endogenous agonists at glycine receptors in rat hippocampus in vitro. *J Physiol* 539: 191–200.

Neher E, Sakmann B (1976) Single-channel currents recorded from membrane of denervated frog muscle fibres. *Nature* 260: 799–802.

Nevin ST, Cromer BA, Haddrill JL, Morton CJ, Parker MW, Lynch JW (2003) Insights into the structural basis for zinc inhibition of the glycine receptor. *J Biol Chem* 278: 28985–28992.

Nury H, Van Renterghem C, Weng Y, Tran A, Baaden M, Dufresne V, Changeux JP, Sonner JM, Delarue M, Corringer PJ (2011) X-ray structures of general anaesthetics bound to a pentameric ligand-gated ion channel. *Nature* 469: 428–431.

Palkovits M, Elekes I, Láng T, Patthy A (1986) Taurine levels in discrete brain nuclei of rats. *J Neurochem* 47: 1333–1335.

Pallotta BS (1991) Single ion channel's view of classical receptor theory. *FASEB J* 5: 2035–2043.

Plested AJ, Groot-Kormelink PJ, Colquhoun D, Sivilotti LG (2007) Single-channel study of the spasmodic mutation α1A52S in recombinant rat glycine receptors. *J Physiol* 581: 51–73.

Poyatos I, Ponce J, Aragón C, Giménez C, Zafra F (1997) The glycine transporter GLYT2 is a reliable marker for glycine immunoreactive neurons. *Brain Res Mol Brain Res* 49: 63–70.

Pringle MJ, Brown KB, Miller KW (1981) Can the lipid theories of anesthesia account for the cutoff in anesthetic potency in homologous series of alcohols? *Mol Pharmacol* 19: 49–55.

Purohit P, Mitra A, Auerbach A (2007) A stepwise mechanism for acetylcholine receptor channel gating. *Nature* 446: 930–933.

Qin F, Auerbach A, Sachs F (2000a) A direct optimization approach to hidden Markov modeling for single channel kinetics. *Biophys J* 79: 1915–1927.

Qin F, Auerbach A, Sachs F (2000b) Hidden Markov modeling for single channel kinetics with filtering and correlated noise. *Biophys J* 79: 1928–1944.

Rajendra S, Lynch JW, Pierce KD, French CR, Barry PH, Schofield PR (1994) Startle disease mutations reduce the agonist sensitivity of the human inhibitory glycine receptor. *J Biol Chem* 269: 18739–18742.

Rajendra S, Vandenberg RJ, Pierce KD, Cunningham AM, French PW, Barry PH, Schofield PR (1995) The unique extracellular disulfide loop of the glycine receptor is a principal ligand binding element. *EMBO J* 14: 2987–2998.

Rajendra S, Lynch JW, Schofield PR (1997) The glycine receptor. *Pharmacol Ther* 73: 121–146.

Riegel AC, Zapata A, Shippenberg TS, French ED (2007) The abused inhalant toluene increases dopamine release in the nucleus accumbens by directly stimulating ventral tegmental area neurons. Neuropsychopharmacology 32: 1558–1569.

Roberts MT (2005) Molecular mechanisms of alcohol and volatile anesthetic modulation of glycine receptor function. The University of Texas at Austin

Roberts MT, Phelan R, Erlichman BS, Pillai RN, Ma L, Lopreato GF, Mihic SJ (2006) Occupancy of a single anesthetic binding pocket is sufficient to enhance glycine receptor function. *J Biol Chem* 281: 3305–3311.

Rodríguez-Navarro JA, Gonzalo-Gobernado R, Herranz AS, Gonzlez-Vigueras JM, Solís JM (2009) High potassium induces taurine release by osmosensitive and osmoresistant mechanisms in the rat hippocampus *in vivo*. *J Neurosci Res* 87: 208–217.

Rundstrom N, Schmieden V, Betz H, Bormann J, Langosch D (1994) Cyanotriphenylborate: subtype-specific blocker of glycine receptor chloride channels. *Proc Natl Acad Sci USA* 91: 8950–8954.

Ryan SG, Dixon MJ, Nigro MA, Kelts KA, Markand ON, Terry JC, Shiang R, Wasmuth JJ, O'Connell P (1992) Genetic and radiation hybrid mapping of the hyperekplexia region on chromosome 5q. *Am J Hum Genet* 51: 1334–1343.

Sauguet L, Shahsavar A, Poitevin F, Huon C, Menny A, Nemecz A, Haouz A, Changeux JP, Corringer PJ, Delarue M (2014) Crystal structures of a pentameric ligand-gated ion channel provide a mechanism for activation. *Proc Natl Acad Sci USA* 111: 966–971.

Saul B, Schmieden V, Kling C, Mulhardt C, Gass P, Kuhse J, Becker CM (1994) Point mutation of glycine receptor α1 subunit in the spasmodic mouse affects agonist responses. *FEBS Lett* 350: 71–76.

Schmieden V, Kuhse J, Betz H (1992) Agonist pharmacology of neonatal and adult glycine receptor alpha subunits: identification of amino acid residues involved in taurine activation. *EMBO J* 11: 2025–2032.

Schmieden V, Kuhse J, Betz H (1993) Mutation of glycine receptor subunit creates beta-alanine receptor responsive to GABA. *Science* 262: 256–258.

Schofield CM, Jenkins A, Harrison NL (2003) A highly conserved aspartic acid residue in the signature disulfide loop of the α_1 subunit is a determinant of gating in the glycine receptor. *J Biol Chem* 278: 34079–34083.

Scimemi A, Beato M (2009) Determining the neurotransmitter concentration profile at active synapses. *Mol Neurobiol* 40: 289–306.

Shan Q, Haddrill JL, Lynch JW (2001) Ivermectin, an unconventional agonist of the glycine receptor chloride channel. *J Biol Chem* 276: 12556–12564.

Shibanoki S, Kogure M, Sugahara M, Ishikawa K (1993) Effect of systemic administration of *N*-methyl-D-aspartic acid on extracellular taurine level measured by microdialysis in the hippocampal CA1 field and striatum of rats. *J Neurochem* 61: 1698–1704.

Söderpalm B, Ericson M (2013) Neurocircuitry involved in the development of alcohol addiction: the dopamine system and its access points. *Curr Top Behav Neurosci* 13: 127–161.

Smith SM, McBurney RN (1989) Caesium ions: a glycine-activated channel agonist in rat spinal cord neurones grown in cell culture. *Br J Pharmacol* 96: 940–948.

Spike RC, Watt C, Zafra F, Todd AJ (1997) An ultrastructural study of the glycine transporter GLYT2 and its association with glycine in the superficial laminae of the rat spinal dorsal horn. *Neuroscience* 77: 543–551.

Stein V, Nicoll RA (2003) GABA generates excitement. *Neuron* 87: 375–378.

Terada T, Hara K, Haranishi Y, Sata T (2011) Antinociceptive effect of intrathecal administration of taurine in rat models of neuropathic pain. *Can J Anaesth* 58: 630–637.

Tipps ME, Lawshe JE, Ellington AD, Mihic SJ (2010) Identification of novel specific allosteric modulators of the glycine receptor using phage display. *J Biol Chem* 285: 22840–22845.

Todorovic J (2010) Critical elements contributing to the control of glycine receptor activation and allosteric modulation. The University of Texas at Austin.

Todorovic J, Welsh BT, Bertaccini EJ, Trudell JR, Mihic SJ (2010) Disruption of an intersubunit electrostatic bond is a critical step in glycine receptor activation. *Proc Natl Acad Sci USA* 107: 7987–7992.

Twyman RE, MacDonald RL (1991) Kinetic properties of they glycine receptor main- and sub-conductance states of mouse spinal cord neurones in culture. *J Physiol* 435: 303–331.

Unwin N (2005) Refined structure of the nicotinic acetylcholine receptor at 4 Å resolution. *J Mol Biol* 346: 967–989.

Vandenberg RJ, French CR, Barry PH, Shine J, Schofield PR (1992a) Antagonism of ligand-gated ion channel receptors: two domains of the glycine receptor α subunit form the strychnine-binding site. *Proc Natl Acad Sci USA* 89: 1765–1769.

Vandenberg RJ, Handford CA, Schofield PR (1992b) Distinct agonist- and antagonist-binding sites on the glycine receptor. *Neuron* 9: 491–496.

van den Pol AN, Gorcs T (1988) Glycine and glycine receptor immunoreactivity in brain and spinal cord. *J Neurosci* 8: 472–492.

Waldvogel HJ, Baer K, Allen KL, Rees MI, Faull RLM (2007) Glycine receptors in the striatum, globus pallidus, and substantia nigra of the human brain: an immunohistochemical study. *J Comp Neurol* 502: 1012–1029.

Wang F, Xiao C, Ye JH (2005) Taurine activates excitatory non-synaptic glycine receptors on dopamine neurones in ventral tegmental area of young rats. *J Physiol* 565: 503–516.

Welsh BT, Goldstein BE, Mihic SJ (2009) Single-channel analysis of ethanol enhancement of glycine receptor function. *J Pharmacol Exp Ther* 330: 198–205.

Welsh BT, Kirson D, Allen HM, Mihic SJ (2010) Ethanol enhances taurine-activated glycine receptor function. *Alcohol Clin Exp Res* 34: 1634–1639.

Welsh BT, Kirson D, Allen HM, Todorovic, J, Bayly MD, Mihic SJ (2014) An inter-subunit electrostatic bond determines agonist efficacy at the glycine receptor. *In prep*.

Werman R, Davidoff RA, Aprison MH (1967) Inhibition of motoneurones by iontophoresis by glycine. *Nature* 214: 681–683.

Wilson JE, Kiselanova N, Stevens Q, Lutz R, Mandler T, Tran ZV, Wischmeyer PE (2008) A survey of inhalational anaesthetic abuse in anaesthesia training programmes. *Anaesthesia* 63: 616–620.

Yamakura T, Mihic SJ, Harris RA (1999) Amino acid volume and hydropathy of a transmembrane site determine glycine and anesthetic sensitivity of glycine receptors. *J Biol Chem* 274: 23006–23012.

Yamashita M, Ueno T, Akaike N, Ikemoto Y (2001) Modulation of miniature inhibitory postsynaptic currents by isoflurane in rat dissociated neurons with glycinergic synaptic boutons. *Eur J Pharmacol* 431: 269–276.

Ye Q, Koltchine VV, Mihic SJ, Mascia MP, Wick MJ, Finn SE, Harrison NL, Harris RA (1998) Enhancement of glycine receptor function by ethanol is inversely

correlated with molecular volume at position alpha267. *J Biol Chem* 273: 3314–3319.

Yevenes GE, Zeilhofer HU (2011) Allosteric modulation of glycine receptors. *Br J Pharmacol* 164: 224–236.

Zafra F, Aragón C, Olivares L, Danbolt NC, Giménez C, Storm-Mathisen JB (1995a) Glycine transporters are differentially expressed among CNS cells. *J Neurosci* 15: 3952–3969.

Zafra F, Gomeza J, Olivares L, Aragón C, Giménez C (1995b) Regional distribution and developmental variation of the glycine transporters GLYT1 and GLYT2 in the rat CNS. *Eur J Neurosci* 7: 1342–1352.

Zeilhofer HU (2005) The glycinergic control of spinal pain processing. *Cell Mol Life Sci* 62: 2027–2035.

Zhang HX, Lyons-Warren A, Thio LL (2009) The glycine transport inhibitor sarcosine is an inhibitory glycine receptor agonist. *Neuropharmacol* 57: 551–555.

Zhou N, Wang CH, Zhang S, Wu DC (2013) The GLRA1 missense mutation W170S associates lack of Zn^{2+} potentiation with human hyperekplexia. *J Neurosci* 33: 17675–17681.

Vita

Dean Kirson was born on Long Island, NY, and grew up in Albuquerque, NM. He attended the University of New Mexico from 1998 to 2003 where he graduated with a Bachelor of Science degree in Biochemistry and a Bachelor of Science degree in Psychology. In 2006 he moved to Austin, TX to begin graduate school at the University of Texas at Austin in the Institute for Neuroscience.

Permanent email: dkirson@utexas.edu

This dissertation was typed by the author.